INSTITUTO SUPERIOR DE ENGENHARIA DE LISBOA
Departamento de Engenharia Mecânica

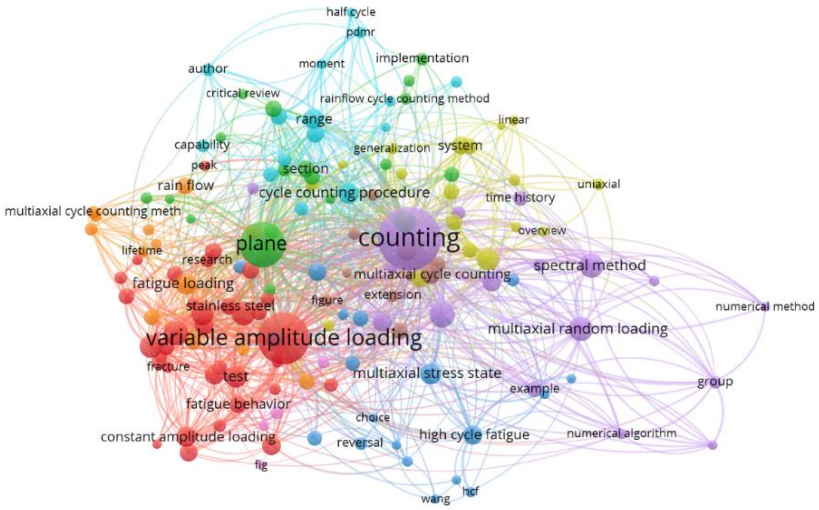

A Critical Review on Damage Accumulation in Multiaxial Fatigue Models

RUI MANUEL RESENDES ROQUE
(Licenciado em Engenharia Mecânica)

Trabalho Final de Mestrado para obtenção do grau de Mestre
em Engenharia Mecânica

Orientador:
Doutor Vítor Manuel Rodrigues Anes

Júri:
Presidente: Doutora Maria Amélia Ramos Loja
Vogais: Doutor Rui Fernando dos Santos Pereira Martins
Doutor Vítor Manuel Rodrigues Anes

Setembro de 2023

INSTITUTO SUPERIOR DE ENGENHARIA DE LISBOA
Departamento de Engenharia Mecânica

A Critical Review on Damage Accumulation in Multiaxial Fatigue Models

RUI MANUEL RESENDES ROQUE
(Licenciado em Engenharia Mecânica)

Trabalho Final de Mestrado para obtenção do grau de Mestre
em Engenharia Mecânica

Orientador:
Doutor Vítor Manuel Rodrigues Anes

Júri:
Presidente: Doutora Maria Amélia Ramos Loja
Vogais: Doutor Rui Fernando dos Santos Pereira Martins
Doutor Vítor Manuel Rodrigues Anes

Setembro de 2023

Acknowledgments

First and foremost, I would like to thank the Almighty God for the gift of life. I would also like to add my gratitude to my supervisor Dr. Vítor Anes for guaranteeing my success throughout this whole period. I am grateful for his availability and assistance at all times, for he helped me find the guidance needed to always deliver what was needed of myself.

Moreover, I wish to extend my gratitude to all the faculty that had taught me during my time at Instituto Superior de Engenharia de Lisboa. I believe without them and the things I learned from each and every one, this dissertation would not have have been accomplished.

To my family, especially my parents, I dedicate all the hard work put in throughout all these past 5 years, for without all of you at my side I would not be where I am today. This is truly the end of a journey, and I can't wait to start another alongside you all over again.

Lastly, to everyone who encouraged me to never give up, to chase after what I feel is rightfully mine and never ever look back. I truly hope this marks the beginning of something I've always dreamed of becoming.

Abstract

Fracture and fatigue are common causes of failure in mechanical components of structures, needing a comprehensive understanding of the underlying physical mechanisms by mechanical design engineers. An area that requires further investigation is the impact of loading type on the fatigue strength of materials. Proportional and nonproportional loads lead to different fatigue lives, even when subjected to the same loading amplitudes. Even within proportional loads, the fatigue life can vary depending on the ratio between shear and normal stresses. Numerous models have been proposed in the literature to address these concerns, but a universally applicable model for estimating fatigue strength considering loading effects is yet to be developed.

This dissertation presents a thorough literature review focusing on multiaxial fatigue, covering topics such as the phenomenological characterization of fatigue, critical plane models, cycle counting methods, fatigue damage monitoring and bibliographic data. During the review, a modified equivalent strain amplitude (MESA) model, raised pertinent questions that are addressed in subsequent chapters.

A case study was conducted that utilizes multiaxial fatigue data of the high strength steel 42CrMo4, which was obtained from literature sources. The analysis was made to include plane orientations ranging from -90° to 90° while evaluating ten multiaxial loading paths. The research hypothesis aimed to evaluate the effectiveness of a proposed critical plane model in determining the crack initiation plane and estimating the fatigue life of variable amplitude loading paths, without relying on cycle counting methods. In order to simplify the demonstration of this method, alternative critical plane models were employed to assess their efficiency in determining these parameters.

The obtained results revealed that the MESA critical plane model is indeed effective in successfully estimating fatigue life under multiaxial fatigue loading paths while others cannot without the use of additional cycle counting methods. Nevertheless, the MESA critical plane model exhibited unsatisfactory results when assessing the crack initiation plane in comparison to other critical plane models like SWT, Fatemi-Socie, Brown-Miller, and Liu. The estimations of these models for the crack initiation plane showed relatively strong consistency, except for the MESA model.

Furthermore, a bibliographic analysis was included with the purpose of better illustrating the current state of the engineering field that researches multiaxial fatigue and damage accumulation approaches. A study on scientific papers published since the 2000's until now is conducted by outlining the output and growth trend of said publications in the selected research areas, the most influential countries and journals and by establishing the connection between internationalization and multiaxial fatigue and damage accumulation.

Findings regarding this analysis indicate a significant growth in the research field, with a substantial increase in the number of published documents each year. The People's Republic of China emerges as the leading contributor with 1434 publications across all the mentioned subjects, closely followed by the USA and Germany. Furthermore, it is noteworthy that nearly half of the countries worldwide are actively involved in researching these subjects, demonstrating a diverse range of nationalities contributing to the field. Interestingly, Portugal ranks among the top 15 countries in all selected keyword categories, highlighting its involvement and contribution in the research.

Keywords: Fatigue Life, Multiaxial Fatigue, Critical Plane, Equivalent Strain Amplitude, Damage Parameter, Bibliographic Analysis.

Resumo

Durante o decorrer do século XX, diversas tragédias ocorreram devido a falhas em componentes mecânicos submetidos a níveis de tensão imprevistos, gerando grande preocupação na comunidade global. Estes eventos catastróficos estimularam a exploração e o avanço de novas tecnologias de forma a garantir um desempenho ótimo e a durabilidade adequada dos componentes mecânicos ao longo da sua vida útil. É essencial destacar que as falhas em componentes mecânicos resultam não só em acidentes como também afetam os prejuízos económicos das empresas e países, potenciais danos ambientais e, em muitos casos, até mesmo perdas humanas. É, portanto, essencial que os engenheiros responsáveis compreendam o comportamento dos componentes mecânicos sob tensões constantes ou cíclicas. Uma compreensão profunda das propriedades mecânicas dos materiais capacita os engenheiros e outros especialistas a avaliar precisamente se um componente específico ou sistema requer substituição ou apenas manutenção.

Apesar dos avanços criados no desenvolvimento da teoria da mecânica da fratura, existe ainda uma grande necessidade de ferramentas aprimoradas e confiáveis que possam ser aplicadas em cenários onde as ferramentas existentes apresentam limitações. O objetivo deve ser aperfeiçoar a coleção de dados sobre acumulação de danos em diferentes condições de carga e correlacionar essas informações com monitorização da integridade estrutural. Atualmente, descrever e interpretar com precisão os dados obtidos por sensores em relação à acumulação de danos ainda é um desafio. Considerando este aspeto, há uma necessidade de abordar cenários da vida real que componentes e estruturas enfrentam, incluindo tensões multiaxiais com condições de carga variáveis e aleatórias.

A fratura e a fadiga são frequentemente responsáveis por falhas em componentes mecânicos de estruturas, exigindo que os engenheiros de projeto mecânico tenham uma compreensão abrangente dos mecanismos físicos subjacentes. Uma área que necessita de investigação adicional é o impacto do tipo de carregamento na resistência à fadiga dos materiais. Cargas proporcionais e não proporcionais levam a diferentes vidas à fadiga, mesmo quando sujeitas às mesmas amplitudes de carregamento. Mesmo no caso da aplicação de cargas proporcionais, a vida à fadiga pode variar dependendo da relação entre tensões de corte e normais. Vários modelos são propostos na literatura de modo a

poder abordar essas preocupações, contudo um modelo universalmente aplicável para estimar a resistência à fadiga considerando os efeitos do carregamento aplicado ainda precisa ser desenvolvido.

Esta dissertação apresenta uma revisão bibliográfica abrangente focada na fadiga multiaxial, abordando tópicos como a caracterização fenomenológica da fadiga, modelos de plano crítico, métodos de contagem de ciclos, monitorização de danos por fadiga e dados bibliográficos. Durante a realização da revisão literária, um modelo de plano crítico modificado de amplitude de deformação equivalente (MESA) levantou questões pertinentes que são abordadas nos capítulos subsequentes.

Foi realizado um caso de estudo que utiliza dados de fadiga multiaxial do aço de alta resistência 42CrMo4, obtidos de fontes literárias. A análise foi feita em dez trajetórias multiaxiais de carregamento, onde para cada modelo do plano critico se fez a avaliação do respetivo parâmetro de dano em planos de diferentes orientações, variando de -90° a 90°. A hipótese de pesquisa visava avaliar a eficácia do modelo do plano crítico MESA na determinação do plano de iniciação de fenda e na estimativa da vida à fadiga de caminhos de carregamento de amplitude variável, sem depender de métodos de contagem de ciclos. Para facilitar a ilustração desse método, outros modelos de plano crítico foram incluídos para comparar sua eficácia na determinação desses parâmetros.

Os resultados obtidos revelaram que o modelo de plano crítico MESA é de facto eficaz na estimativa da vida à fadiga em trajetórias multiaxiais de amplitude variável, enquanto outros modelos não o são sem o uso de métodos adicionais de contagem de ciclos. A mitigação de técnicas de contagem de ciclos, leva a considerar o dano acumulado e ignorar a trajetória de carregamento e os modelos tradicionais, ocorrendo uma estimativa incorreta de vida infinita à fadiga em vez da vida finita esperada, evidenciada na maioria dos casos. No entanto, o modelo de plano crítico MESA apresentou resultados insatisfatórios ao avaliar o plano de iniciação de fenda em comparação com outros modelos de plano crítico, como SWT, Fatemi-Socie, Brown-Miller e Liu. As estimativas desses modelos para o plano de iniciação de fenda mostraram uma consistência relativamente forte, exceto para o modelo MESA. Tendo em conta os resultados alcançados, o modelo MESA pode ser considerado adequado para uso prático no design mecânico e no desenvolvimento de componentes mecânicos cruciais, permitindo uma estimativa precisa da vida útil à fadiga e facilita uma determinação mais precisa do fator de segurança necessário para a operação do componente. Devido às

variações na trajetória de carga, diferentes resultados de vida à fadiga são determinados, enfatizando o quão insuficiente é considerar apenas a amplitude na fadiga multiaxial.

Adicionalmente, uma análise bibliográfica foi incluída com o objetivo de ilustrar melhor o estado atual da pesquisa em fadiga multiaxial e métodos de acumulação de dano. Neste sentido, realizou-se um estudo sobre artigos científicos publicados desde os anos 2000 até o presente, delineando a produção e tendência de crescimento dessas publicações nas áreas de pesquisa selecionadas, os países e jornais mais influentes e estabelece-se a conexão entre internacionalização e o tópico da fadiga multiaxial e acumulação de dano.

Para realizar a análise bibliográfica de forma adequada, optou-se por utilizar o software *Publish and Perish*, especializado em cruzar informações bibliográficas de várias bases de dados. Entre essas bases de dados, destacam-se fontes reputáveis como o *Scopus, Web of Science, Crossref, PubMed* e o *Google Scholar*. Optou-se pela escolha do *Google Scholar* devido às suas principais vantagens, como ser gratuito e acessível à maioria das pessoas no mundo. Com o intuito de dar forma e estruturação aos dados extraídos, utilizou-se adicionalmente o software VOSviewer. Com o auxílio do VOSviewer, foi possível apresentar os dados retratados visualmente e quantitativamente. Dados agrupados na forma de mapas foram criados na análise de coautoria, coocorrência de palavras-chave, citações, co-citacções e acoplamento bibliográfico. Estes mapas têm a particularidade de poderem ser manipulados de diversas formas e ainda filtrados de acordo com o utilizador, caracterizando individualmente cada um.

Os resultados desta análise indicam um crescimento significativo no campo de pesquisa, com um aumento substancial no número de documentos publicados em cada ano até ao presente. A República Popular da China destaca-se como o principal contribuinte, com 1434 publicações em todas as áreas mencionadas, seguida pelos Estados Unidos da América e a Alemanha. Além disso, é digno de notar que quase metade dos países em todo o mundo está ativamente envolvida na pesquisa desses temas, demonstrando uma diversidade de nacionalidades contribuintes para o campo. Curiosamente, Portugal está entre os 15 países no topo em todas as categorias que incluem as palavras-chave selecionadas, sedimentando o seu envolvimento e contribuição para a pesquisa neste campo.

Finalmente, são salientadas certas limitações das análises realizadas, ambas do caso de estudo e da análise bibliográfica, como também são incluídas possíveis melhorias às mesmas com o intuito de aumentar o seu rigor.

Palavras-chave: Fadiga Multiaxial, Parâmetro de Dano, Plano Crítico, Amplitude de Deformação Equivalente, Vida à Fadiga, Análise Bibliográfica.

Table of Contents

List of Figures

List of Tables

Nomenclature

Abbreviations

GNP	Gross National Product
ASTM	American Society for Testing and Materials
S-N	Stress-Life
FEA	Finite Element Analysis
SSF	Stress Scale Factor
VCC	Virtual Cycle Counting
WG	Wang and Brown
ESA	Equivalent Strain Amplitude
MESA	Modified Equivalent Strain Amplitude
SWT	Smith Watson and Topper
F-Socie	Fatemi-Socie
SAR	Stress Amplitude Ratio

Symbology

$\sigma_{\theta,local}$	local stress
$\sigma_{x,global}$	global stress component in x direction
$\sigma_{y,global}$	global stress component in y direction
$\tau_{xy,global}$	global shear stress
$\tau_{\theta,local}$	local shear stress
σ_{max}	maximum normal stress
σ_{min}	minimum normal stress
$\Delta\sigma$	normal stress range
$\Delta\tau$	shear stress range
σ_m	normal mean stress
σ_a	normal stress amplitude
R	stress ratio
A	amplitude ratio
ε_{eq}	equivalent strain

ε_x, ε_y and ε_z	normal strain components in x, y, and z directions
γ_{xy}, γ_{yz} and γ_{xz}	shear strain components, in xy, yx, and xz directions
ν	effective Poisson ratio
ν^e	elastic Poison coefficient in Wang and Brown method
ν^p	plastic Poison coefficient in Wang and Brown method
ε^e	elastic strain coefficient in Wang and Brown method
ε^p	plastic strain coefficient in Wang and Brown method
ε_{eq}^{rel}	relative equivalent strain
ε_1, ε_2, ε_3	principal strains
ε_n	normal strain
$\Delta\varepsilon_n$	normal strain range
$\Delta\gamma_{\max}$	maximum shear strain range
D	total damage
n_i	number of cycles
S	normal strain coefficient
$\sigma_f^{'}$	axial fatigue strength coefficient
$\varepsilon_f^{'}$	axial fatigue ductility coefficient
b	axial fatigue strength exponent
c	axial fatigue ductility exponent
N_f	number of cycles to failure
E	Young's modulus
G	shear modulus
$\sigma_{n,med}$	normal mean stress
$\sigma_{n,\max}$	maximum normal stress
σ_y	yield stress
k	material constant
$\tau_f^{'}$	shear fatigue strength coefficient
$\gamma_f^{'}$	shear fatigue ductility coefficient
b_γ	shear fatigue strength exponent

c_γ	shear fatigue ductility exponent
ε_a	maximum strain amplitude
ΔW	work
ΔW^e	elastic work
ΔW^p	plastic work
ΔW_I	axial work
ΔW_{II}	shear work
$\sqrt{3}\tau$	shear component of von Mises criterion
τ_{tresca}	equivalent shear stress of Tresca yield criterion
λ	stress amplitude ratio
k^τ_{eq}	equivalent stress correction factor
$\Delta\gamma^{cr}_{eq}$	equivalent shear strain amplitude on the critical plane
k_τ	shear stress correction factor
k_σ	normal stress correction factor
ε^*_n	maximum shear strain range on the critical plane
γ'_f	shear fatigue ductility coefficient
b'	shear fatigue strength exponent
c'	shear fatigue ductility exponent
$\sigma^*_{n,max}$	maximum normal stress during normal strain excursion

1 . Introduction

Over the past two centuries, there have been significant technological improvements in engineering field. A notable example is the ability to travel through continents faster than ever before with the use of airplanes compared to a century ago. The progress in transportation industry, which is a critical part of the global economy and trade, is crucial because many products and services rely entirely on it. To deliver these products and services in competent and cost-efficient manner, it is important for the transportation industry to strive for its optimization. Engineers play a vital role in achieving efficiency by guaranteeing the reliability and functionality of every component.

A need becomes apparent when manufacturing in the transportation industry with the selection of materials. Used to manufacture a car, a train, an airplane or any other means of transportation, a large list of materials can be selected based on numerous different factors relating environmental conditions, service restrictions, standard load amounts it can withstand and so on. A new product is developed when there is a need to be satisfied. In the engineering field, the development of a product is comprised of firstly defining its requirements, function, specifications and finally an expectancy of life.

Before the manufacturing stage, the product must go through the design phase consisting of a validation process. Designing a product is an iterative process being that all the individual parts are compared to their requirements as a whole allowing potential changes to be made in the design process if necessary.

Notably, one major consideration to have is the occurrence of plastic deformation and its consequences eventually leading to failure due to loading conditions. In fact, design features may lead to the increase likelihood of failure. An example of this is sharp edges which are known to be hotspots of high stress concentrations and in order to minimize them, they are often replaced with chamfers or round curved edges resulting in a higher life cycle for the component.

When a part is manufactured, it is intended for it to carry out a specific function for a certain duration, after which it can be repaired or replaced. Nevertheless, a significant number of components fail before reaching their anticipated lifespan, and such

failures can result in numerous unfavourable outcomes like damage to other parts, monetary losses, the surroundings and even loss of human lives.

Technology is no doubt the biggest improving mechanism that engineers nowadays use to implement new and more efficient components. When it comes to addressing the economical aspect, deformation and fracture are both considered to be detrimental to numerous industries, such as the automotive and aircraft sectors. In reality, nearly 4% of the gross national product (GNP) accounts for financial costs regarding studying the prevention of failure [1].

During the 20th century many accidents were determined to be caused by fatigue failure. Today it is estimated that nearly 90% of failures occurred in mechanical components are due to fatigue [2]. For example, in 1984 a study conducted on airplane accidents that had occurred since 1927. According to the investigators, in a total of 1855 recorded airplane accidents, 1466 were determined to have been caused by fatigue failure of individual or assembled components. Tragically these accidents resulted in 1861 fatalities all together, however the number of incidents regarding mechanical fatigue as a cause of failure is likely to be much higher as accidents without fatalities were not taken into account [3]

The history involving fatigue failure has prompted the scientific community to further conduct studies that determine the underlying causes of such accidents. This, in turn, led to the re-examination of fracture mechanics theory introduced by Erwin [4], which greatly contributed to its better understanding. Fracture mechanics theory assumes that a crack is already present in a material, which will grow over time until it is deemed critical. The aim of this theory is to forecast the applied load at which the crack growth rate will increase until it reaches a critical size. An engineer’s job lies in estimating or measuring the pre-existing cracks and calculating their respective stress intensity factor, which is then correlated with the material's fracture toughness. By identifying the initial crack in a material, engineers can monitor its behaviour until it reaches a critical point.

Better understanding premature failure of structures or components is crucial to assist design engineers in early design stages by avoiding factors that may increase the likelihood of component failure. Furthermore, understanding failure mechanisms can help maintenance technicians identify signs of fatigue failure before it happens.

1.1 Motivation

Even with all the developments made in fracture mechanics theory, a need remains to help create better and dependable tools that can be utilized in engineering applications where existing tools have shortcomings. The aim must be to better gather data about damage accumulation under different loading conditions to then correlate this information with structural health monitoring. Till now it is still to precisely describe and interpret the data obtained through sensors when talking about damage accumulation.

With this in mind, a challenge arises of wanting to address the real-life experiences that components and structures deal with such as multiaxial stresses with variable loading and random loading conditions. Also evident is the fact that still today, the cumulative damage models available remain very crude or basic and that in turn makes the existing cycle counting techniques unable to fully identify cycles from complex loadings. This fact leads to an inevitable low reliability shown in real life applications. Furthermore, most of the techniques regarding cycle counting are based on the Rainflow method which means its associated drawbacks carry over to several of Rainflow-based techniques.

Considering the importance of fracture studies and its various intricacies, the research inquiry has been formulated as follows: What is the current understanding of multiaxial fatigue phenomenon and damage accumulation methods, and how have both been explored in the last two decades? The primary objective of this study is to uncover and present a coherent overview of the existing research trends on the interrelationships between multiaxial fatigue and damage accumulation models, while also highlighting potential directions for future investigations. To accomplish this aim, a bibliometric analysis was conducted, which provides a systematic and comprehensive examination of the academic literature in this field. Bibliometric analysis is a valuable methodology for capturing a broad perspective on a large volume of scientific literature, enabling the evaluation of research trends and collaboration patterns among authors, journals, and countries. By integrating the key findings from the fields of multiaxial fatigue and damage accumulation, this dissertation contributes to the literature by exploring their interrelation. The data presented in this study offers an overview of the research advancements made in the domains of multiaxial fatigue and damage accumulation, providing researchers and professionals with valuable insights into influential authors, journals, countries, and research topics.

1.2 Objectives

Making the focus of better understanding phenomena associated with multiaxial fatigue and damage accumulation, the present dissertation aims to achieve the following objectives:

- Conduct a review of existing literature on multiaxial fatigue in order to comprehend the current knowledge and available models for handling multiaxial stress states.
- Tackle the absence of bibliographic investigations performed related to multiaxial fatigue and damage accumulation and provide a clear summary of content available.
- Understand the MESA methodology in order to generate a damage map for various different orientations.
- Suggest potential improvements to further enhance the outcome of the methodology used.

1.3 Thesis outline

This dissertation is divided into five chapters, as follow:

The first chapter includes an overview of the significance of multiaxial fatigue in various industries, emphasizing the importance of gaining a deeper understanding of fatigue and its implications for businesses, the industry, and areas like product innovation. The chapter concludes by outlining the motivation, objectives, and structure of the dissertation.

Chapter 2 dives in a lengthy literature review that delves into the development of fatigue failure theory. The fundamental aspects of fatigue and cycle loading are explained, along with a discussion on various uniaxial and multiaxial cycle counting methods, along with their limitations. Additionally, this chapter provides an overview of critical plane models relevant to this dissertation and introduces the MESA approach. The section also includes an exploration of the Miner rule, a linear cumulative damage rule, and the Morrow rule, a nonlinear cumulative damage rule, to further draw differences between their uses.

In chapter 3, a bibliographic analysis is conducted to further understand the impact of the studied subject throughout the last twenty-three years. A set of keywords are utilized to uncover and present a coherent overview of the existing research trends on their interrelationships. Topics like the output and growth of publications, the most cited and influential publications and journals, which country currently has the majority of authorship, which authors are co-cited the most, and the most commonly used keywords are addressed to paint a clear image of the state of research conducted in the fatigue community.

Chapter 4 has the objective of examining the influence of assessing fatigue life estimations on different planes and identifying the crack initiation plane through a case study employing the MESA model for various orientations. Additionally, this study examines and contrasts the results with various other critical plane models, aiming to obtain a thorough comprehension of their respective effectiveness. Experimental data concerning the critical planes of high strength steel 42CrMo4 was acquired from literature sources, and the MESA approach was applied to ascertain the crack initiation plane from different orientations while also providing relative fatigue life estimations.

The final chapter, Chapter 5, consists of the presentation of conclusions and future prospects. The chapter begins by summarizing the key findings derived from the bibliographic analysis conducted in chapter 3 and continues by doing the same for the MESA approach study that was done in chapter 4. Additionally, it highlights areas that require further exploration and development to enhance the comprehension of the MESA approach and validate the proposed methodology while also highlighting the most relevant aspects of the analysed bibliography. The chapter emphasizes the importance of future research endeavours in advancing the understanding and application of the MESA approach.

2 . Literature Review

2.1 Overview of the History of Fatigue

The term "fatigue" has its origin in the Latin word "fatigare" which means "to tire" or "to wear out". The idea behind it is that a material will eventually tire just as a living being will so when a material weakens due to a certain amount of fatigue, and it is not replaced it will eventually fracture/fail. According to the American Society for Testing and Materials (ASTM) [5], fatigue is defined as "the process of gradual reduction of the strength of a material subjected to cyclic loading." In other words, fatigue is a type of failure that occurs in a material due to repeated loading and unloading, resulting in a gradual reduction in its strength and eventual failure.

As the industrial revolution propelled the advancement of various sectors, one would stand out as of detrimental for the time, transportation. The rapid spread of railways originated in Britain rapidly expanded throughout the world [6]. By developing faster trains, it meant having metal components work under higher stresses while simultaneously being subjected to an unprecedented number of repeated cycles. It would be a few years after that the first major accident occurred near Versailles, where nearly 200 deaths were reported [7].

FIGURE 2.1 RAILWAY AXLE ACCIDENT OCCURRED IN VERSAILLES, 1842 [8]

Due to this tragic accident, many engineers turned focus to possible fatigue failure in the design phase. This hypothesis led August Wholer [9] to perform many laboratory fatigue tests under repeated stresses to axle-like components. The results obtained from the experiments demonstrated that a component may not fail when subjected to a single or particular load whereas if the same amount were to be applied in a cycle the complete

failure would occur, thus given the name of the “father” of systematic failure testing. With the establishment of the S-N approach for fatigue life and the concept of fatigue limit, Wholer’s work would lay the groundwork for further focus on the areas of stress concentration in fatigue.

In the early 20th century, significant progress was made in comprehending fatigue as a material issue. Ewing and Humfrey [10] conducted an experiment in 1903, using a microscope to examine fatigue failure and determine the fatigue limit. Their microscopic analysis led to the conclusion that fatigue crack initiation in a material occurs as tiny cracks along slip-lines and slip-bands.

In 1910, Basquin [11] introduced an exponential power law that relied on the Wohler S-N approach. This proposed power law was established on the correlation between the region's alternating stress and the number of cycles to failure, as a log-log linear correlation.

For the first half of the 20^{th} century the majority of studies were considering stress-based models whilst neglecting the aspect of plastic deformation that would prove very meaningful later on. In addition, components can experience variable changing amplitudes instead of constant and multiaxial loading and not uniaxial loading.

Several critical plane models have been developed to address multiaxial loading conditions, including both in-phase and out-of-phase loading. Extensive studies spanning the past 50 years have explored critical plane models, focusing on those that consider planes with the greatest damage [12]. The critical plane approach is versatile and can be applied to both proportional and nonproportional loading while possibly being categorized as stress-based models (for high cycle fatigue), strain-based models (for high and low cycle fatigue), and energy-based models.

To account for changes in amplitude, multiple cycle counting techniques were developed in the 60s with the example of rain flow method being the most often used. Today, when it comes to qualifying the total damage, a component suffers a cumulative damage created by Palmgren-Miner is still widely used today.

Still, with many theories developed along with the introduction of FEA (Finite element analysis) software, fatigue analysis became much more reliable. However, it

doesn’t shy away from the fact that out of all the multiaxial models now available there is not one who can account for all the factors involved in fatigue failures.

Although significant improvement has been made in the field, it is evident there is even more to learn about the fatigue process that encompasses all of the prior subjects referenced. It could come in the form of improving the existing models or even with the creation of completely new ones.

2.2 Phenomenological fatigue behaviour

Fracture mechanics theory defines a particular condition where a crack present in the material is considered to be stable. As a result, the material can operate safely under these circumstances. Engineers can leverage this information to design components and systems that can withstand the applied load without experiencing fractures. In doing so, understanding the safe operating conditions of a material is deemed critical for engineers to develop safe and reliable structures.

During cyclic loading, a material experiences repeated stresses that cause microstructure modifications, also known as fatigue. These modifications may not be visible to the naked eye and can continue to grow with each loading cycle, eventually leading to macroscopic cracks and failure of the material.

Thus, the fatigue process can be described has having four distinct stages, and they are as follows:

I. Crack nucleation
II. Short crack growth period of propagation
III. Long crack growth period of propagation
IV. Fracture (rupture)

Materials themselves aren’t one hundred percent absent of flaws and often contain defects that ultimately result in stress concentrations such as geometric discontinuities, porosities, or inclusions. A graphical representation of how the fatigue process occurs is illustrated in Figure 2.2 showing the crack nucleation beginning to form in areas of high stress concentration, particularly in slip bands. The following loading and unloading of the material results in crack growth. This next stage in the fatigue process is divided into two stages. Stage I involves fatigue crack nucleation and short crack propagation across a finite length of a few grains at 45° on the local maximum shear stress plane, where the

grain size, slip characteristics, orientation, and stress level all have a significant impact on the crack tip plasticity, as the material microstructure is similar in size to the crack tip. In stage II, the cyclic loading and unloading of the material causes the crack to propagate perpendicular to the applied load until it reaches a certain level. Unlike stage I, the characteristics of long crack growth in this stage are less influenced by the microstructure, as the crack tip size is larger than the material microstructure [13].

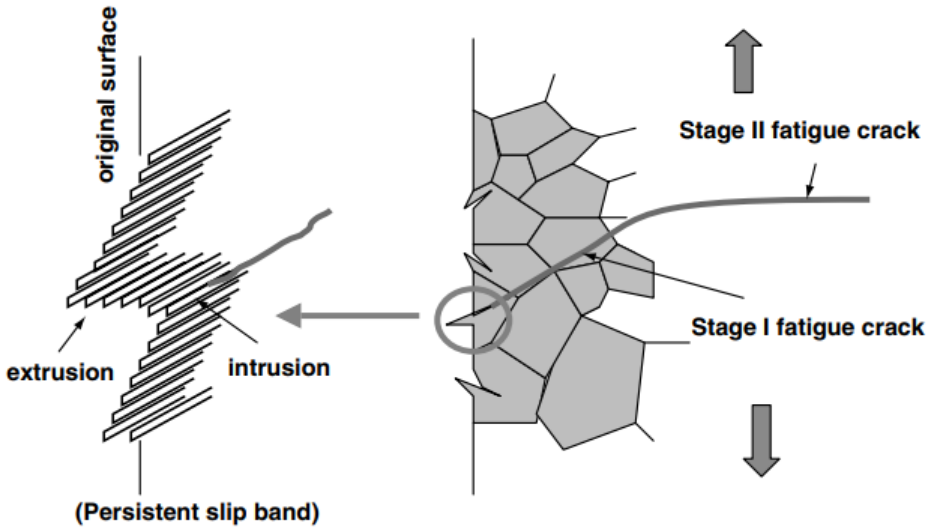

FIGURE 2.2 FATIGUE PROCESS UNDER TENSILE LOADING [13]

It is also relevant to differentiate the crack nucleation stage and crack growth stage in the fatigue process. This is due to surface conditions such as roughness that cause a significant impact on the nucleation stage but may have little to no effect during the growth period. In fact, the corrosive environment also has a different effect on the nucleation phase compared to the growth phase [14].

2.3 Proportional and nonproportional loading

In uniaxial loading, it is known that a material's response to damage varies depending on the way it is solicited. A cyclic axial loading will cause different damage than that caused by pure torsional loading. When studying the behaviour of a component subjected to multiaxial loading, it is expected that the combination of forces in more than one axis will produce varied results depending on the combination of forces applied.

A component subjected to a multiaxial loading, as the name suggests, involves the application of forces in more than one axis, such as alternating tension and torsion loading. This implies that the component can be subjected to both axial and shear stresses.

Additionally, multiaxial loadings can be divided into two categories: proportional and non-proportional.

Considering the biaxial loading depicted in Figure 2.3, where the axial stress and shear stress, after decomposition of the loading, are both represented by an in-phase sinusoidal curve. By examining the situations illustrated in points A, B, and C on the Mohr circle, it reveals that the principal stress axis maintains the same orientation throughout all three loading points, and this behaviour remains for the entire loading. This exact behaviour is defined as proportional loading.

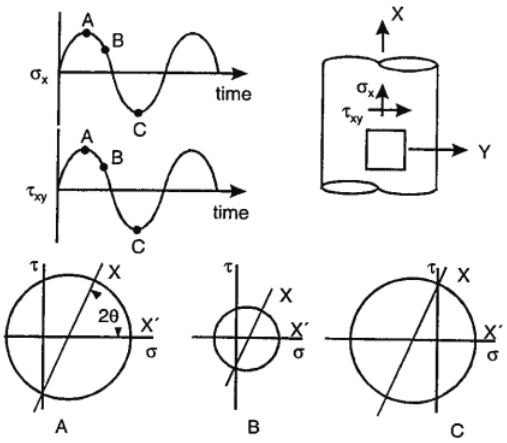

FIGURE 2.3 PROPORTIONAL MULTIAXIAL LOADING OF A SHAFT [15]

Let us consider a biaxial loading scenario again, but with a constant axial stress applied to the component over time, as shown in Figure 2.4. At each instant during the loading, the orientation of the principal stress axis changes relatively to the component axis. This change in axis orientation is visible through the representation of Mohr's circle during each instant of loading, labelled with the letters A to E.

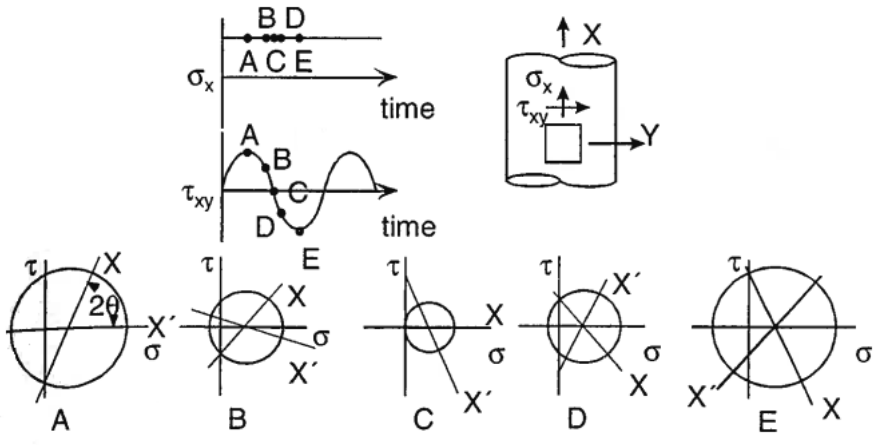

FIGURE 2.4 NONPROPORTIONAL MULTIAXIAL LOADING OF A SHAFT [15]

Identifying a non-proportional load can be easily determined by examining the loading trajectory on the von Mises stress space. If the loading trajectory is represented by one straight-line segment and the segment, or its directional extension, crosses the origin, then the load is proportional. If this particular characteristic is not observed, then the load is non-proportional. Figure 2.5 shows several examples of loading trajectories on the von Mises strain plane, of which three loads are proportional (cases a, b, and c) and the remaining loads are non-proportional.

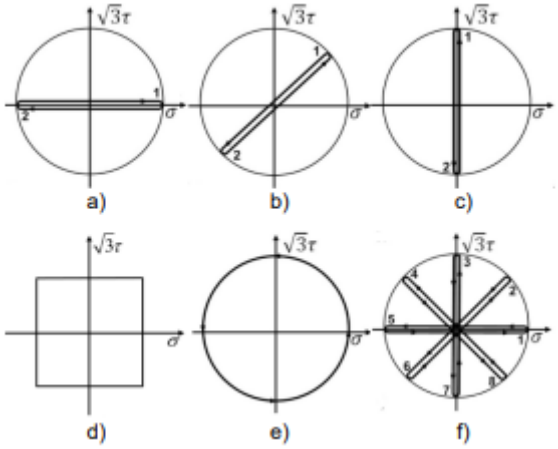

FIGURE 2.5 PROPORTIONAL LOADING TRAJECTORIES (A, B AND C) AND NONPROPORTIONAL LOADING TRAJECTORIES (D, E AND F) [16]

Illustrated in Figure 2.5, case f) for example, shows that multiple sequential proportional "sub-loads" (branches) are performed. However, as the principal stress axes rotate from branch to branch of the loading block, the loading is deemed non-proportional.

This distinction between proportionality and non-proportionality in cyclic loading is important because the fatigue behaviour of the component will differ depending on the

type of loading applied. In a proportional loading, the resulting force will act on a single plane or direction. However, in a loading where the loads are out of phase, i.e., a non-proportional loading, the resulting forces will act on multiple planes and activate multiple slip planes, increasing the damage done to the component. This is why non-proportional loadings are generally more detrimental to fatigue life than proportional loadings [15].

In studying the response of a component when subjected to non-proportional loading, a number of problems arise. The additional hardening (dependent on the type of material) must be considered. Also, in complex loadings with variable stress amplitudes, a specific method must be used to count the cycles contained in a loading block. Moreover, the interpretation of the damage parameter is also difficult given that existing models aren't precise enough when used in complex loadings [15,17].

2.3.1 Cyclic Strain hardening

Regardless of whether the fatigue loading applied to the component is uniaxial or multiaxial and whether it has a variable stress amplitude or not, if it is cyclic, it can lead to a phenomenon known as cyclic hardening. This phenomenon occurs when a metallic component is subjected to cyclic stress above the yield stress, which is defined as the stress that, when applied to a sample, causes a plastic (permanent) strain of 0.2% of its nominal length. The plasticity induced in the material as a result of applying stress beyond the elastic limit will, in some materials, lead to a new elastic limit stress caused by material hardening. In a strain-controlled fatigue test, this increase in yield stress requires a higher stress level, closer to the material's ultimate strength, to achieve a certain amount of strain, resulting in a reduction in the material's fatigue life [18].

Like cyclic stresses above the elastic limit, cyclic stresses below the elastic limit can also cause a phenomenon called cyclic softening, where the elastic limit decreases. This can also be detrimental to the material's life [18]. Moreover, in non-proportional multiaxial fatigue loading, cyclic hardening can occur regardless of whether the material's yield stress is reached or not.

In this type of loading, the variation in the orientation of the principal stress axes will activate several intersecting slip planes, causing localized plasticity in the material and, consequently, changes in its mechanical properties [19]. This effect varies depending on the material's crystal structure, so the degree of hardening may differ from material to

material. This material dependent variation is attributed to the material's stacking energy [20].

The influence of this additional hardening phenomenon, which occurs in phased loading, is illustrated in Figure 2.6, which shows two hysteresis curves illustrating the relationship between normal stress and normal strain on the plane of maximum normal strain.

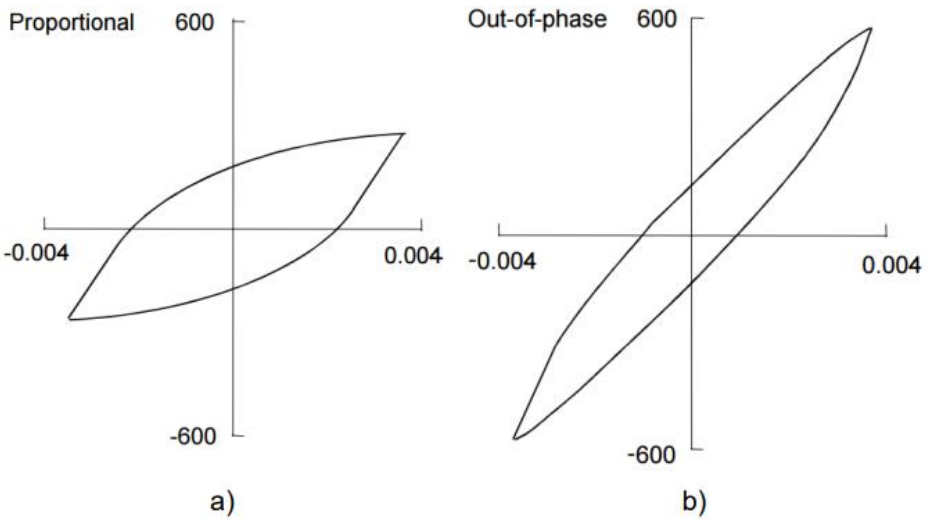

FIGURE 2.6 CYCLIC STRAIN HARDENING PHENOMENON IN A) PROPORTIONAL LOADING AND B) OUT-OF-PHASE LOADING AT 90° [15]

Both tests, proportional on the left and non-proportional on the right, were conducted under strain control for the same range of strain. Figure 2.6 also shows the fatigue life of the specimen for each type of loading [15]. For the same range of strains, which controls the test, the range of normal stress in the 90° non-proportional loading (Figure 2.6 - case b)) is double that observed in the hysteresis curve of the proportional loading (Figure 2.6- case a)). In other words, to achieve the desired level of deformation, twice the force had to be applied to the specimen in the non-proportional loading. This is precisely due to the additional cyclic hardening observed in the non-proportional loading. The remaining stress growth is due to the increase in the level of load required for the non-proportional loading to reach the magnitude of strain observed in the proportional loading [21]. As a consequence of this increase in stresses, the fatigue life of the specimen is strongly affected, being about 20 times lower for the non-proportional loading compared to the proportional loading. It is also observed from the analysis of the curves that the plastic deformation is lower in the non-proportional loading, which emphasizes the role of stresses in fatigue damage [15].

The additional cyclic hardening phenomenon resulting from non-proportional loading will vary from material to material, and it's possible that a non-proportional loading may even cause less damage to the material than a proportional loading [21].

2.4 Variable stress amplitude loading

One of the techniques used to graphically represent a biaxial load involves plotting this load on the von Mises stress space to obtain the load path. However, this load path may represent various load sequences, each of which could result in a different type of damage done to the material. Cases a) and b) in Figure 2.7 depict two biaxial loads as a function of time.

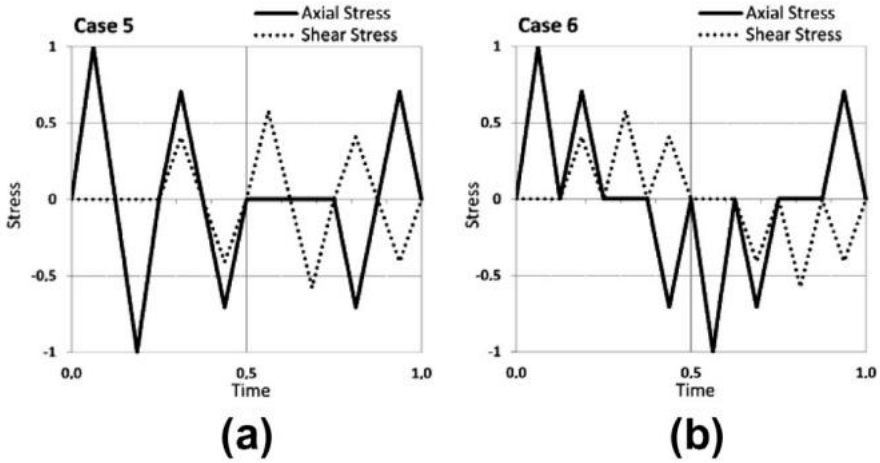

FIGURE 2.7 BIAXIAL LOADING OVER TIME: A) FULL REVERSALS AND B) SEMI-REVERSALS [22]

In the first sequence, depicted in Figure 2.7a), only complete reversals are applied at both the axial stress and shear stress levels, whereas in the corresponding load shown in Figure 2.7b), only semi-reversals are applied. When these two loads are plotted on the von Mises stress plane, the load path, which is identical to the one illustrated previously in Figure 2.5f), will be the same for both loads.

Although these two depicted loads, along with others, have different characteristics, they exhibit an identical graphical representation on the von Mises stress space. However, their fatigue lives will vary. This indicates that the order and completeness of reversals applied during loading have an impact on the fatigue life. Literature records provide evidence of this material behaviour. Specifically, in Figure 2.7, the specimens tested with a loading sequence comprising only tension/compression and torsion semi-reversals (Figure 2.7b) experienced a significantly lower number of cycles compared to the sequence with complete reversals (Figure 2.7a). Moreover, the latter

sequence was applied at lower stress levels than the former. This demonstrates that the loading sequence involving semi-reversals is more detrimental in terms of damage compared to the other loading sequence [22].

Further, Xia and Yao [23], who evaluated various damage accumulation models for a series of loads consisting of different combinations of loading blocks sequenced randomly, also found differences in fatigue lives with different sequences of the same type of loading blocks. They attributed this difference to the effect of the applied loading sequence.

2.4.1 Influence of mean stress

A component experiencing operational or practical loading conditions may be subject to loading comprised of mean stresses that can influence the component's fatigue life. The presence of a positive mean stress (tension) in the loading will decrease the fatigue life, while a negative mean stress (compression) will be favourable for the material's life expectancy [24]. In the case of mean shear stresses, Shamsaei et.al [25] concluded that they would only have an influence on loads where the maximum shear stress was greater than the shear yield stress. Meanwhile, Wang and Miller [26] suggest that the mean shear stress influences the transition from regime 1 (propagation threshold) to regime 2 (stable propagation), as well as the crack propagation rate.

2.5 Critical plane models

The use of critical plane models is founded on empirical observations of the initiation and progression of cracks under loading conditions. Variables like stress state, material type, and strain magnitude play a role in determining whether fatigue life will be primarily influenced by the growth of cracks along tensile or shear planes.

There are three categories of critical plane models: stress-based, strain-based, and energy-based. Strain-based models are appropriate for low cycle fatigue applications, while stress-based models are used for high cycle fatigue applications. Energy-based models [27] are divided into three groups, depending on their application. For high cycle fatigue, the criteria based on elastic stress energy are appropriate, for low cycle fatigue, criteria based on elastic strain energy are suitable, and for applications where both low and high cycle fatigue are present, the criteria based on the sum of elastic strain and stress energy are used.

The critical plane method is not only used to estimate the fatigue life of a component but also to identify the plane or planes where fatigue cracks are likely to occur. In this approach, the plane with the highest amount of damage is considered as the critical plane. The critical plane method is widely used for multiaxial loading conditions. Most importantly, for a critical plane model to be considered as effective, it should be able to reasonably predict the fatigue life of a component and also identify the primary failure plane.

2.5.1 Local and global stresses

In stress-based critical plane models, the damage parameter is calculated based on the local stress in each plane in a given orientation. The Mohr circle is used as a graphical method to transform the state of stress and to obtain the stresses in these planes. The main goal of the critical plane models is to determine the plane or orientation that has the highest value for the damage parameter. Equations (2.1) and (2.2) are utilized to identify the plane that experiences the most damage, as shown in Figure 2.8. These equations are based on global and normal stress components.

$$\sigma_{\theta,local}(t)=\frac{\sigma_{x,global}(t)+\sigma_{y,global}(t)}{2}+\frac{\sigma_{x,global}(t)-\sigma_{y,global}(t)}{2}\cos(2\theta)+\tau_{xy,global}\sin(2\theta) \quad (2.1)$$

$$\tau_{\theta,local}(t)=\frac{\sigma_{x,global}(t)-\sigma_{y,global}(t)}{2}\sin(2\theta)-\tau_{xy,global}\cos(2\theta) \quad (2.2)$$

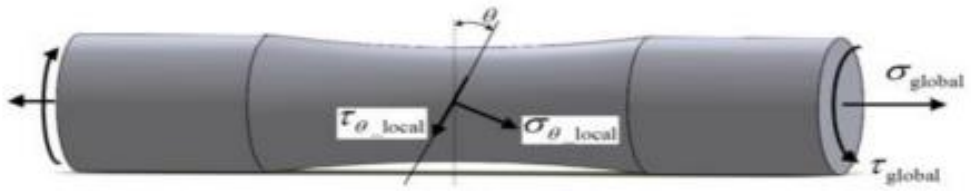

FIGURE 2.8 GLOBAL AND LOCAL STRESSES SITUATED ON A SAMPLE [28]

2.5.2 Findley

Based on observations the initial orientation of fatigue cracks in steel and aluminium specimens, Findley [29] analysed the influence of normal stress acting on the plane of maximum shear stress. The author suggests that the normal stress has a linear influence on the alternating shear stress in the projection plane. The same proposes that failure will not occur if it is found that the normal stress is below a certain threshold value, represented in Equation 2.3.

$$\left(\frac{\Delta\tau}{2} + k \cdot \sigma_{n,\,max}\right)_{max} \leq f \tag{2.3}$$

For each projection plane, a cyclic loading can be deconstructed into two cyclic components: one of shear and one of normal stress. By fixing the maximum value of the normal stress in each plane and the corresponding amplitude of projected shear stress in that plane, the value of Equation 2.4 is determined. This process is repeated for all planes θ until determining the critical plane θ that maximizes the model's parameter f.

$$f = max_{\theta}\left(\frac{\Delta\tau}{2} + k \cdot \sigma_{n,\,max}\right) \tag{2.4}$$

Here, $\frac{\Delta\tau}{2}$ represents the amplitude of shear stress on the plane θ, $\sigma_{n,max}$ is the maximum normal stress on the plane θ, and k is a material constant.

The constant k is determined based on experimental results, specifically through conducting fatigue tests on pure alternating torsion and pure alternating bending. The parameter k can be determined using Equation 2.5.

$$\frac{\sigma_{a,\,R=-1}}{\tau_{a,\,R=-1}} = \frac{2}{1 + \frac{k}{1+\sqrt{k^2}}} \tag{2.5}$$

Here, $\sigma_{a,R=-1}$ represents the fatigue limit stress under pure bending conditions, and $\tau_{a,R=-1}$ corresponds to the fatigue limit stress under pure shear conditions.

To determine the fatigue life, Nf, using the Findley model, Equation 2.6 is applied.

$$max_{\theta}\left(\frac{\Delta\tau}{2}+k\cdot\sigma_{n,\,max}\right)=\tau_f{}^{*}N_f{}^{b} \tag{2.6}$$

Here, b represents the fatigue strength exponent, and $\tau_f{}^{*}$ is calculated using the following equation:

$$\tau_f{}^{*}=\tau_f{}^{'}\cdot\sqrt{1+k^2} \tag{2.7}$$

Equation 2.7 involves $\tau_f{}'$, the fatigue strength coefficient under torsion, which can be calculated using $\frac{\sigma_f{}'}{\sqrt{3}}$, where $\sigma_f{}'$ represents the fatigue strength coefficient.

2.5.3 Brown-Miller

In their study, Brown and Miller [15] performed a tension-torsion test where they applied a constant shear strain of 0.03. Figure 2.9 shows the results they obtained from their experiment. They concluded that two strain parameters should be taken into account when explaining a fatigue process: cyclic shear and normal strain acting on the plane of maximum shear.

Brown and Miller [30] suggested a method for multiaxial fatigue analysis that is rooted in the examination of the mechanics of fatigue crack propagation, and therefore has a tangible explanation. The formula for fatigue failure in this approach is represented by a non-linear equation consisting of strain parameters, which is illustrated in Equation 2.8.

$$\frac{\varepsilon_1-\varepsilon_3}{2}=f\left[\frac{\varepsilon_1+\varepsilon_3}{2}\right],\ with\ \ \varepsilon_1\geq\varepsilon_2\geq\varepsilon_3 \tag{2.8}$$

$$\varepsilon_n=\frac{\varepsilon_1+\varepsilon_3}{2} \tag{2.9}$$

$$\frac{\gamma}{2}=\frac{\varepsilon_1-\varepsilon_3}{2} \tag{2.10}$$

The critical plane refers to the plane that exhibits the highest level of shear strain. Nonetheless, the non-linear equation described here is applicable solely under conditions of proportional loading, where the principal strain components are presumed to be constant.

Brown and Miller discovered that it is possible to have identical shear strain with two distinct loading conditions. To account for this, they classified cracks into two categories, which are depicted in Figure 2.9. In Case A, as shown in Figure 2.9, the crack progresses parallel to the material surface, as seen in torsional loading situations. In contrast, for Case B cracks, which arise under biaxial tension conditions, the shear stress causes the crack to propagate through the material thickness rather than along the surface. The angle at which a type B crack intersects the surface is 45 degrees. Under tension loading, both Case A and Case B cracks exhibit identical shear stress and can demonstrate both modes of cracking. However, under biaxial loading conditions (tension-torsion), only Case A cracks are observed.

Both cracks can be expressed by the following Equations 2.11 and 2.12.

Crack case A:

$$\left(\frac{\Delta\gamma}{g}\right)^{j}+\left(\frac{\varepsilon_n}{h}\right)^{j}=1 \tag{2.11}$$

Crack case B:

$$\frac{\Delta\gamma}{2}=constant \tag{2.12}$$

In Equation 2.11, both g and h are constants determined experimentally, and the exponent j differs in its material characteristics, taking the value of 1 for brittle materials and 2 for ductile materials. In Equation 2.13, $\frac{\Delta\gamma_{max}}{2}$ represents the maximum shear strain amplitude, $\Delta\varepsilon_n$ is the normal strain applied on the plane of maximum shear and S is the normal strain coefficient.

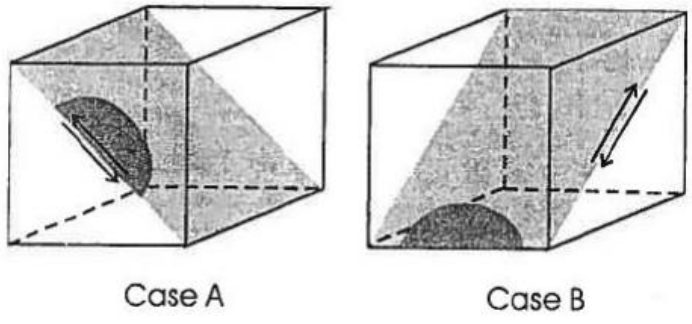

FIGURE 2.9 CASE A AND B TYPE CRACKS [26]

Subsequently, Kandil, Miller and Brown [31] suggested a simplified formula, presented in Equation 2.13, applicable to crack A type, which also considers the influence of mean stress.

$$\frac{\Delta\gamma_{max}}{2} + S\Delta\varepsilon_n = (1.3 + 0.7S)\frac{\sigma_f' - 2\sigma_{n,med}}{E}(2N_f)^b + (1.5 + 0.5S)\varepsilon_f'(2N_f)^c \quad (2.13)$$

The equation above incorporates the effects of mean stress by applying Morrow's mean stress method on the right side. The *S* value is specific to each material and can be determined through tension or torsional experiments. Figure 2.10 illustrates the variation in S value with increasing number of cycles.

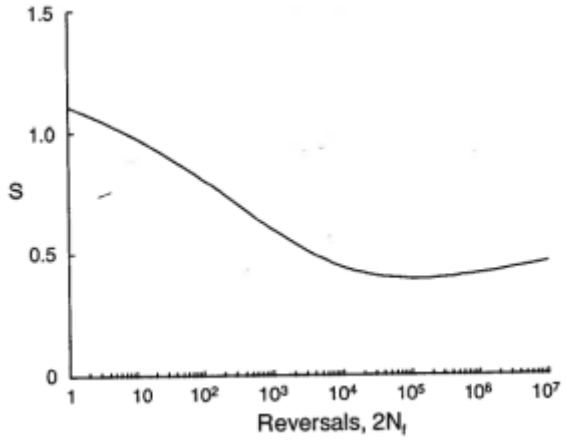

FIGURE 2.10 VARIATION OF THE NORMAL STRAIN COEFFICIENT ALONG THE NUMBER OF CYCLES [15]

The maximum shear strain will determine the critical plane, which can be estimated through Equation 2.14.

$$\left(\frac{\Delta\gamma_{max}}{2} + S\Delta\varepsilon_n\right)_{max} \quad (2.14)$$

2.5.4 Fatemi and Socie

Fatemi-Socie developed a critical plane method based on the approach of Brown-Miller. However, as the Brown-Miller method is expressed in terms of strain and does not consider the impact of cyclic hardening, some researchers believe that this is why out-of-phase loading leads to more damage than in-phase loading [32,33]. To address the impact of cyclic hardening caused by the rotation of principal axes under nonproportional loading, Fatemi-Socie suggested a modification to the Brown-Miller approach. In this

modification, the strain term was replaced with a normal stress [34]. Figure 2.11 depicts the physical significance of this model.

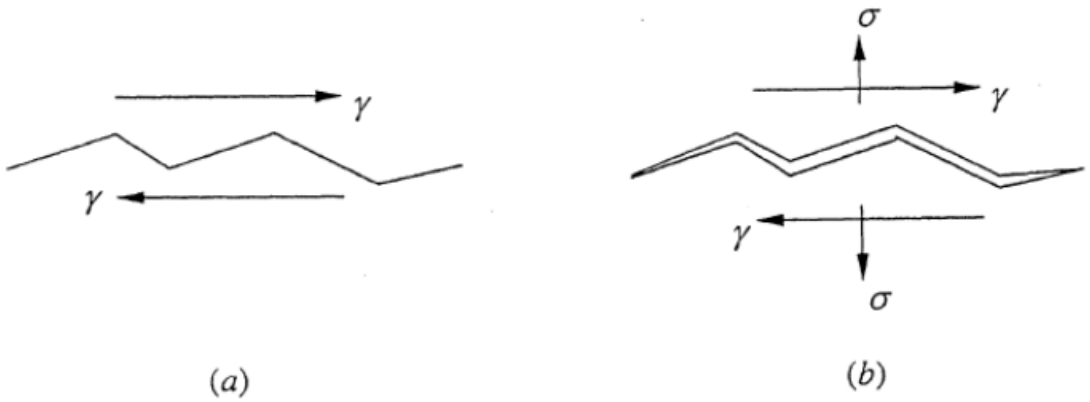

FIGURE 2.11 PHYSICAL PROGRESSION ASSESSMENT OF FATEMI-SOCIE MODEL: (A) SHEAR LOADING OF A CRACK AND (B) EFFECT OF TENSILE STRESS ON THE SHEAR CRACK [9]

Equation 2.15 reveals that the primary factors in the Fatemi-Socie approach are the maximum amplitude of shear strain and the maximum normal stress acting on the maximum shear plane amplitude. As cracks typically have an irregular shape, increasing the crack during shear loading creates frictional forces between the crack surfaces, which impede crack growth and ultimately result in a longer fatigue life (as illustrated in Figure 2.11a). Conversely, as seen in Figure 2.11b), applied tensile stress separates the two crack surfaces, reducing frictional forces and fatigue life.

$$\frac{\Delta\gamma_{max}}{2}\left(1+k\frac{\sigma_{n,max}}{\sigma_y}\right) \tag{2.15}$$

Socie and Shield [35] conducted a series of biaxial experiments using Inconel 718 specimens to evaluate the impact of maximum normal stress. The tests were conducted at room temperature, with the specimens subjected to both tension-torsion strain control. The results demonstrated that, in cases where the material experienced Mode II type of failure, the maximum shear strain amplitude plane was always identified. The experiments also revealed that the fatigue life, the preferred maximum shear plane, and the distribution of cracks were influenced by the mean stress value, although the mean stress did not affect the direction of crack propagation nor the mode of material failure.

The Fatemi-Socie critical plane approach is best suited for materials that fail under Mode II. Unlike the Brown-Miller approach, it can be utilized to evaluate the impact of

mean stress and the effects of nonproportional hardening. Concerning fatigue life, the Fatemi-Socie approach can be represented by Equation 2.16:

$$\frac{\Delta\gamma_{max}}{2}\left(1+k\frac{\sigma_{n,max}}{\sigma_y}\right)=\frac{\tau'_f}{G}\left(2N_f\right)^{b_\gamma}+\gamma'_f\left(2N_f\right)^{c_\gamma} \tag{2.16}$$

The equation for the Fatemi-Socie approach, as given by Equation 2.16, consists of several parameters and exponents. These include $\frac{\Delta\gamma_{max}}{2}$, which represents the maximum shear strain amplitude, $\sigma_{n,max}$, which is the maximum normal stress acting on the maximum shear plane amplitude, σ_y, the yield stress, k, a material constant that is determined through testing, τ'_f, the shear fatigue strength coefficient, G, the shear modulus, N_f, the number of cycles to failure, γ'_f, the shear fatigue ductility coefficient, and b_γ and c_γ, which represent the shear fatigue strength exponent and shear fatigue ductility exponent, respectively. These parameters and exponents can be determined through tension and torsion tests. Figure 2.12 shows the variation of the *K* coefficient with the number of cycles, and based on this figure, the *K* parameter can be estimated depending on known the number of cycles.

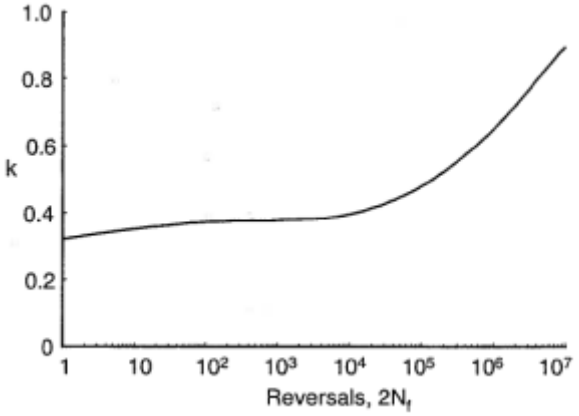

FIGURE 2.12 VARIATION OF K COEFFICIENT WITH NUMBER OF CYCLES [15]

When dealing with out-of-phase multiaxial loading, the critical plane can be established by employing Equation 2.17, which determines the plane with the maximum constant value.

$$\left[\frac{\Delta\gamma_{max}}{2}\left(1+k\frac{\sigma_{n,max}}{\sigma_y}\right)\right]_{max} \tag{2.17}$$

2.5.5 Smith, Watson and Topper (SWT)

Smith, Watson and Topper [36] developed a model in 1970 that can be utilized in both proportional and nonproportional loading situations. This approach was designed to account for materials that fail under the maximum tensile stress or strain.

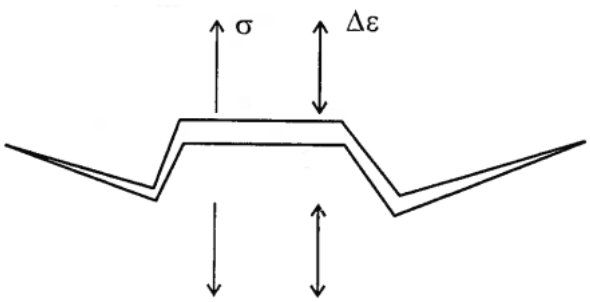

FIGURE 2.13 PHYSICAL PHENOMENON BEHIND SWT PARAMETER [15]

The SWT model, proposed by Smith, Watson, and Topper in 1970, is useful for both proportional and nonproportional loading conditions for materials that fail under maximum tensile stress or strain. When dealing with uniaxial loading, this model accounts for the impact of mean stress. For multiaxial loading, the SWT model combines the maximum stress and principal strain range to determine the governing parameter. As illustrated in Figure 2.13, if microcracks develop in mode I, the driving force is the stress that opens those microcracks in the principal strain plane. The expressions for the SWT parameter can be derived by manipulating Morrow's expressions, multiplying both sides of the Equations 2.18 and 2.19 and adapting the result for multiaxial loading, as shown in Equation 2.20.

$$\varepsilon_a = \frac{\sigma'_f}{E}\left(2N_f\right)^b + \varepsilon'_f\left(2N_f\right)^c \tag{2.18}$$

$$\sigma_a = \sigma'_f\left(2N_f\right)^b \tag{2.19}$$

$$\sigma_{max}\frac{\Delta\varepsilon_1}{2} = \frac{\sigma'^{\,2}_f}{E}\left(2N_f\right)^{2b} + \sigma'_f\varepsilon'_f\left(2N_f\right)^{b+c} \tag{2.20}$$

The previous equations represent the parameters used in the SWT model: σ_{max} represents the maximum tensile stress on the plane of principal strain, ε_a represents the maximum strain amplitude, σ'_f is the axial fatigue strength coefficient, E is the Young's

modulus, Nf represents the number of cycles to failure, ε'_f represents the axial fatigue ductility coefficient, and b and c represent the axial fatigue strength exponent and axial fatigue ductility exponent respectively.

The use of the maximum stress term in this model makes it appropriate to consider mean stresses in both multiaxial and nonproportional loading conditions [15]. With respect to the critical plane, the SWT parameter is determined based on the plane with the maximum principal strain range, which is calculated using Equation 2.21.

$$\left(\sigma_{max}\frac{\Delta\varepsilon_1}{2}\right)_{max} \tag{2.21}$$

2.5.6 K. Liu

Liu [37] proposes a model based on virtual strain energy (VSE) that is unique in that it accounts for both mode I (opening) and mode II (shearing) failures. In this model, the virtual strain energy for each plane is composed of both plastic and elastic work, as shown in Equation 2.22. The elastic work is represented by the shaded area in Figure 2.14, which can be calculated by adding both of these areas. On the other hand, the plastic work can be obtained by multiplying the change in stress ($\Delta\sigma$) with the change in plastic strain ($\Delta\varepsilon p$).

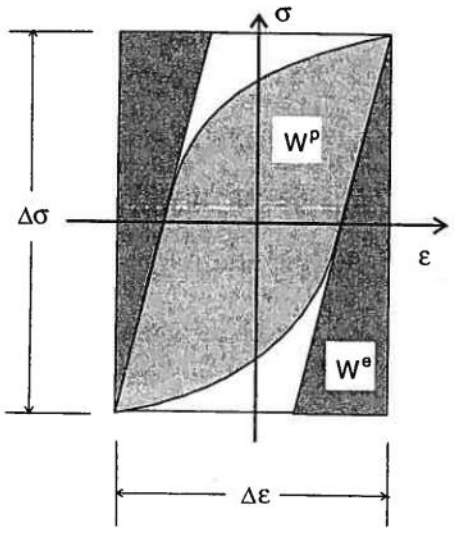

FIGURE 2.14 ELASTIC AND PLASTIC STRAIN ENERGY REPRESENTATION [15]

$$\Delta W = \Delta W^e + \Delta W^p \cong \Delta\sigma \cdot \Delta\varepsilon \tag{2.22}$$

The calculation of ΔW is obtained through Equation 2.23 by utilizing the strain-life equations.

$$\Delta W = \frac{4\sigma_f^{'2}}{E}\left(2N_f\right)^{2b} + 4\sigma_f^{'}\varepsilon_f'\left(2N_f\right)^{b+c} \tag{2.23}$$

To assess failure in a multiaxial loading scenario, the virtual strain energy method takes into account two types of failure: tensile failure (ΔWI) and shear failure (ΔWII). In the case of shear failure, both type A and type B cracks are considered, as in the Brown-Miller approach. The VSE parameter for tension-torsion loading can be calculated using Equation 2.24.

$$\Delta W = \Delta W_I + \Delta W_{II} \tag{2.24}$$

The Liu model is classified as a critical plane model because it defines work quantities for a specific plane in the material [15]. It is expected that failure in this model will occur in the plane with the highest VSE quantity. On the other hand, the axial work, ΔWI, is calculated by multiplying the ranges of normal strain and stress on the plane with the maximum value, and then adding the amount of shear present, as shown in Equation 2.25.

$$\Delta W_I = \left(\Delta\sigma\cdot\Delta\varepsilon\right)_{max} + \left(\Delta\tau\cdot\Delta\gamma\right) \tag{2.25}$$

To determine fatigue life, Equation 2.26 is used.

$$\Delta W_I = \frac{4\sigma_f^{'2}}{E}\left(2N_f\right)^{2b} + 4\sigma_f^{'}\varepsilon_f'\left(2N_f\right)^{b+c} \tag{2.26}$$

Similar to the calculation of ΔWI, the estimation of the shear work ΔWII involves multiplying the ranges of normal shear stress and shear strain on the plane of its maximum value, and then adding it to the axial work on that plane. This is expressed in Equation 2.27.

$$\Delta W_{II} = \left(\Delta\sigma\cdot\Delta\varepsilon\right) + \left(\Delta\tau\cdot\Delta\gamma\right)_{max} \tag{2.27}$$

To estimate the fatigue life, the Equation 2.28 is employed.

$$\Delta W_{II} = \frac{4\tau_f^{'2}}{G}\left(2N_f\right)^{2b_\gamma} + 4\tau_f^{'}\gamma_f'\left(2N_f\right)^{b_\gamma+c_\gamma} \tag{2.28}$$

Equation 2.28, used for fatigue life estimation involves several parameters such as normal shear stress ($\Delta\tau$), shear strain ($\Delta\gamma$), normal stress ($\Delta\sigma$), normal strain ($\Delta\varepsilon$), shear modulus (G), shear fatigue strength coefficient (τ'_f), number of cycles to failure (Nf), shear fatigue ductility coefficient (γ'_f), and shear fatigue strength exponent (b_γ) and ductility exponent (c_γ). In case of a tensile failure mode, there is only one critical plane, but for a shear failure mode, there are two critical planes for each type of crack, which are separated by 90 degrees. When subjected to uniaxial loading conditions, the axial and the bending shear work are equal $(\Delta W_{II,A} = \Delta W_{II,B})$. However, in case of tension or a combination of tension and torsion, $\Delta W_{II,A}$ is greater than $\Delta W_{II,B}$. For tension-compression loading, $\Delta W_{II,B}$ dominates. The parameter that dominates among all three parameters ΔW_I, $\Delta W_{II,A}$ and $\Delta W_{II,B}$ depends on the type of loading, material, and temperature chosen.

2.5.7 L. Xue (MESA)

L. Xue et. Al [38] proposed a new strain energy-based model in 2020, attributed to generalized fatigue damage parameters. In order to overcome deficiencies due plastic strains a fatigue damage parameter was created in the form of equivalent strain amplitude (ESA) on the critical plane:

$$ESA = k^{\tau}_{eq} \frac{\Delta\gamma^{cr}_{eq}}{2} \tag{2.29}$$

Where k^{τ}_{eq} represents the equivalent stress correction factor and $\frac{\Delta\gamma^{cr}_{eq}}{2}$ is the equivalent shear strain amplitude on the critical plane which is defined as the material plane experiencing the maximum shear strain range instead of the maximum damage. The factors k_τ and k_σ, which correct for shear stress and normal stress, respectively, are defined based on the shear strain amplitude and normal strain amplitude on the critical plane, defined by Equations (2.30) and (2.31):

$$k_\tau = \frac{\tau_{max}}{\tau'_f} \tag{2.30}$$

$$k_\sigma = \frac{\sigma_{n,max}}{\sigma'_f} \tag{2.31}$$

With $k^{\tau}{}_{eq}$ being described as Equation 2.32 by von Mises criterion.

$$k^{\tau}{}_{eq} = k_{\tau} + \frac{k_{\sigma}}{\sqrt{3}} = \frac{\tau_{max}}{\tau'_f} + \frac{\sigma_{n,max}}{\sqrt{3}\sigma'_f} \tag{2.32}$$

Since the ESA damage parameter is dependent on the shear work and the maximum normal stress on the plane with maximum shear strain range is zero for pure shear fatigue, the correlation between the equivalent stress correction factor $k^{\tau}{}_{eq}$ and the number of cycles to failure N_f can be established.

$$k^{\tau}{}_{eq} = \frac{\tau_{max}}{\tau'_f} + \frac{\sigma_{n,max}}{\sqrt{3}\sigma'_f} = \left(2N_f\right)^{b'} \tag{2.33}$$

By correlating investigations [39,40], a multiaxial fatigue damage model expressed in terms of the equivalent amplitude of shear strain and using the von-Misses criterion on the plane that experiences the maximum shear strain range is proposed:

$$\frac{\Delta\gamma^{cr}_{eq}}{2} = \sqrt{3\varepsilon_n^{*2} + \left(\frac{\Delta\gamma_{max}}{2}\right)^2} = \frac{\tau'_f}{G}\left(2N_f\right)^{b'} + \gamma'_f\left(2N_f\right)^{c'} \tag{2.34}$$

Equation 2.34 includes the normal strain excursion between adjacent turning points of the maximum shear strain range on the critical plane represented by ε_n^*, the maximum shear strain amplitude on the critical plane represented by $\frac{\Delta\gamma max}{2}$, the shear fatigue ductility coefficient represented by γ'_f, and the shear fatigue strength exponent and ductility exponent represented by b' and c', respectively.

By replacing the equivalent stress correction factor $k^{\tau}{}_{eq}$ from Equation 2.33 and the equivalent shear strain amplitude $\frac{\Delta\gamma^{cr}_{eq}}{2}$ from Equation 2.34 into Equation 2.29, the ESA multiaxial fatigue damage parameter is obtained, correlating the number of cycles to failure N_f. This is given as:

$$ESA = \frac{\tau_{max}}{\tau'_f} + \frac{\Delta\gamma_{max}}{2} = \frac{\tau'_f}{G}\left(2N_f\right)^{2b'} + \gamma'_f\left(2N_f\right)^{b'+c'} \tag{2.35}$$

Notably, experimental validations in multiaxial fatigue under proportional and non-proportional loading have shown that the equivalent shear strain amplitude $\frac{\Delta\gamma^{cr}_{eq}}{2}$, as defined by Shang [39,40], is a useful and consistent fatigue damage parameter for

multiaxial analysis. The maximum normal stress $\sigma^*_{n,max}$ during the normal strain path between adjacent turning points of the maximum shear strain range on the critical plane can be determined with Equation 2.34 by corresponding ε^*_n. Furthermore, by replacing this value into Equation 2.35 a modified ESA (MESA) model for multiaxial fatigue life assessment can be proposed in Equation 2.36, and the calculation of the parameter for a counted reversal is illustrated in Fig. 2.15.

$$MESA = \left(\frac{\tau_{max}}{\tau'_f} + \frac{\sigma^*_{n,max}}{\sqrt{3}\sigma'_f} \right) \sqrt{3\varepsilon^{*2}_n + \left(\frac{\Delta\gamma_{max}}{2} \right)^2} = \frac{\tau'_f}{G} \left(2N_f \right)^{2b'} + \gamma'_f \left(2N_f \right)^{b'+c'} \quad (2.36)$$

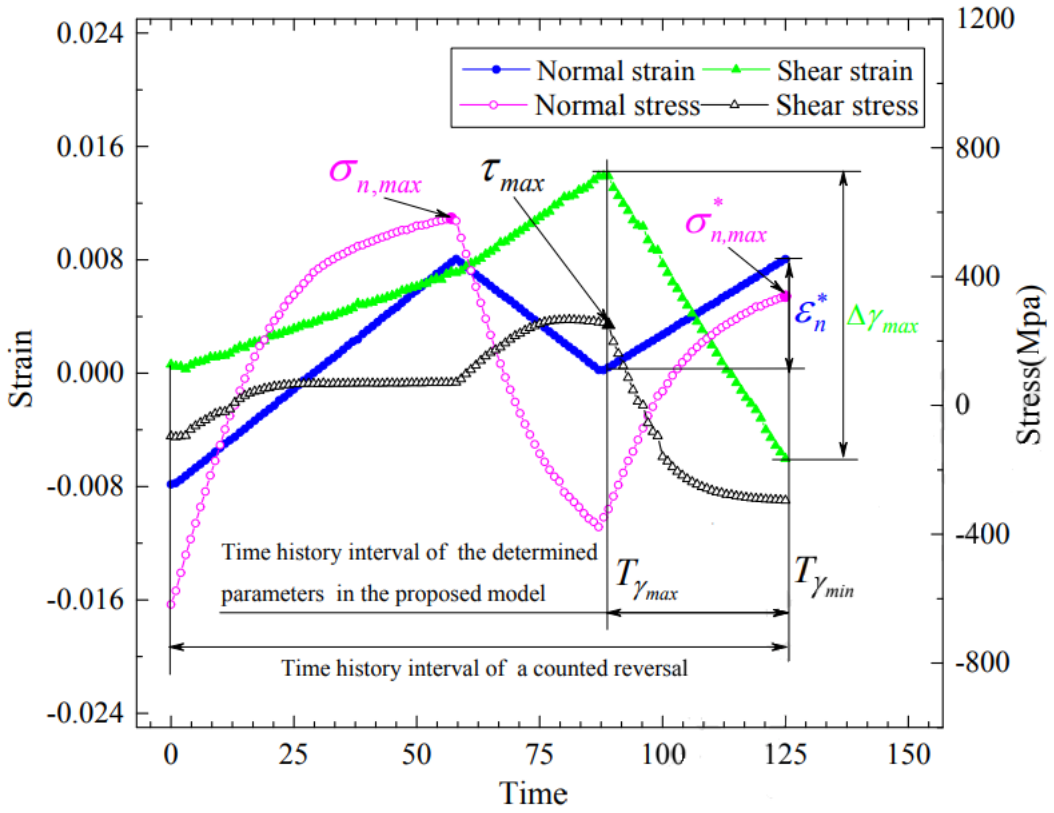

FIGURE 2.15 SCHEMATIC DIAGRAM OF PARAMETERS PRESENT IN THE MESA MODEL [38]

2.6 Multiaxial cycle counting

Engineering components such as turbines, crankshafts, pressure vessels, and transmission systems often undergo a state of multiaxial stress, with loading conditions that are variable or random. Such loads may be either proportional or non-proportional. Proportional loading occurs when the directions of the principal stresses remain constant, while non-proportional loading occurs when these directions change with time.

The comprehension of multiaxial fatigue remains a complicated issue, as the component or system is exposed to several strains or stresses simultaneously. Nevertheless, numerous studies on multiaxial fatigue have been conducted in the last fifty years and new theories or enhancements of the old ones have emerged. Despite the advancements in multiaxial fatigue, there is still a lack of consensus among the scientific community about which theories are superior [41]. In practical applications, since most components experience variations in magnitude as well as direction, uniaxial loading should also be studied as non-proportional multiaxial loading [42].

In real-life situations, the loads experienced by components are often multiaxial rather than uniaxial. The traditional von Mises model is not ideal for multiaxial loading since it performs better under proportional loading conditions. Critical plane models are better suited for multiaxial loading since they locate the plane that experiences the most damage [31]. These models offer better results than traditional ones and are widely used for multiaxial cases. An advantage of the critical plane approach is that it can be applied in both high and low cycle fatigue applications when both stress and shear terms are incorporated in its model. Additionally, the critical plane approach provides consideration on material behaviour in non-proportional loading conditions [15].

Predicting the fatigue life of a component under multiaxial loading poses several challenges. According to Wei and Dong [43], one of the challenges is the lack of a proper definition of stress/strain damage parameter, and current cycle counting methods exhibit inconsistencies. In addition, the hysteresis in multiaxial fatigue is not well defined compared to the uniaxial method [44]. In the following section, various multiaxial cycle counting techniques will be discussed.

2.6.1 Rainflow

The cycle counting method, proposed by Matsuishi and Endo [45], was originally developed as an analogy to raindrops falling on the roof of a Pagoda (a common tower in Asia). The method counts the number of cycles contained in each stress range of a loading history. To perform the counting, the loading history is rotated so that the time axis is vertical with the positive direction pointing downwards. The cycle counting then begins with the analogy of a water drop "falling off the roof." The method is defined by the following rules:

• The path of the "drop" starts at each peak and valley (on the "inside" of the path);

• When a path starting at a peak reaches the edge of the roof (valley) and falls, the fall stops if there is a peak of greater magnitude than the original peak on the opposite side of the timeline.

• When a path starting at a valley reaches the edge of the roof (peak) and falls, the fall stops if there is a valley of greater magnitude than the original valley on the opposite side of the timeline.

• If the "drop" flowing over the roof intercepts another previously considered "drop" path, the current path of the "drop" ends;

• A new path does not start until the current path has ended.

Each path is counted as half a cycle. Once the paths are identified, they are paired in twos (for each stress/strain range) to form a complete cycle until there are no more pairs left. There are other cycle counting methods that yield identical results to the original Rainflow method as long as the loading starts at the highest peak or lowest valley. When this is not the case, although different, the results are similar [46]. Some examples of similar methods are the range-pair method, the Hayes method, the range-pair-range method, the ordered overall range counting method, and the racetrack method [46].

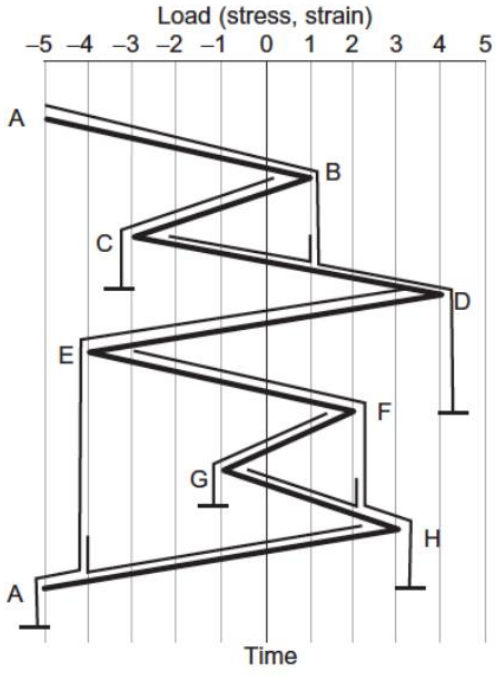

FIGURE 2.16 APPLICATION OF THE RAINFLOW METHOD TO LOAD-TIME HISTORY [47]

Many of these methods, in their original design, require prior knowledge of the complete loading, i.e., they are not applicable in monitoring situations, either because they carry out several "sweeps" or because they alter the order of occurrence of the various events that occur in a loading history. Therefore, improved algorithms are necessary to allow continuous counting, such as the one proposed by Downing and Socie [48] along with others that can be consulted in the ASTM standard for cycle counting.

2.6.2 Wang and Brown

In the 1990s, Wang and Brown developed a cycle counting technique that is applicable to both proportional and non-proportional loading [31]. This technique, known as the WB method, utilizes the equivalent stress/strain approach and combines the von Mises criterion with the Rainflow cycle counting method to perform the counting [49].

This method utilizes the von Mises criterion to assess fatigue damage indirectly. The criterion is applied to convert the complex multiaxial stress state to a uniaxial state. The equivalent strain of von Mises can be mathematically represented as:

$$\varepsilon_{eq} = \frac{1}{\sqrt{2}(1+\upsilon)}\sqrt{(\varepsilon_x-\varepsilon_y)^2+(\varepsilon_y-\varepsilon_z)^2+(\varepsilon_z-\varepsilon_x)^2+\frac{3}{2}\left[\gamma_{xy}{}^2+\gamma_{yz}{}^2+\gamma_{xz}{}^2\right]} \quad (2.37)$$

The equivalent strain, denoted by ε_{eq}, can be determined using this method. It involves the strain components ε_x, ε_y, and ε_z, as well as the shear strain components γ_{xy}, γ_{yz}, and γ_{xz}. The effective Poisson ratio, represented by υ, is the average of the elastic and plastic coefficients and is usually 0.5. This ratio is determined by using Equation 2.38.

$$A\cdot\upsilon = \frac{\upsilon^e\varepsilon^e+\upsilon^p\varepsilon^p}{\varepsilon} \quad (2.38)$$

The limitation of using the von Mises equivalent strain is that it does not distinguish between the fatigue processes in different directions. Consequently, the von Mises value always results in a positive one regardless of the applied load direction. This can lead to incorrect predictions of fatigue life. To address this limitation, Wang and Brown introduced the relative equivalent strain, which is calculated using the Equation 2.39:

$$\varepsilon_{eq} = \frac{\sqrt{\left(\Delta\varepsilon_x - \Delta\varepsilon_y\right)^2 + \left(\Delta\varepsilon_y - \Delta\varepsilon_z\right)^2 + \left(\Delta\varepsilon_z - \Delta\varepsilon_x\right)^2 + \frac{3}{2}\left[\Delta\gamma_{xy}{}^2 + \Delta\gamma_{yz}{}^2 + \Delta\gamma_{xz}{}^2\right]}}{\sqrt{2}\left(1+\upsilon\right)} \tag{2.39}$$

The process of multiaxial cycle counting with the Wang and Brown method is conducted as follows:

1. Identify the maximum von Mises strain in the loading history.
2. Reorder the loading history so that it starts with the highest von Mises strain.
3. Determine the relative von Mises strain for the entire history by using the previously selected maximum von Mises strain value. To complete the cycle, locate the peak point of the relative von Mises strain.
4. Once the highest relative von Mises strain has been identified and the previously counted cycle path has been determined, it can be considered as half a cycle. The counting process can be continued by following steps 2 through 4.

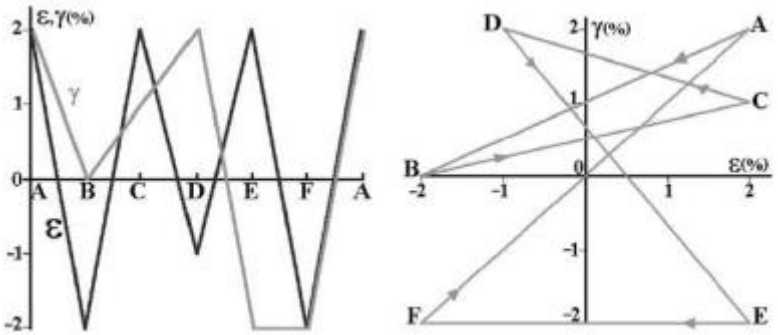

FIGURE 2.17 STRAIN HISTORY FOR A NIP LOADING AND CORRESPONDING $\gamma - \varepsilon$ DIAGRAM [50]

The WB method offers numerous advantages. Firstly, it is more effective when dealing with loading histories that are random or consist of few long blocks, as it allows for the critical plane to change with every reversal, thus maximizing the calculated damage. However, under torsional loading, the shear damage criterion may exaggerate the actual fatigue damage suffered, as noted by Wang and Brown. Another issue with this method is that it does not accurately predict the plane where the crack will occur.

According to Matus and Dominik [51], the Wang and Brown method performs the entire cycle counting process in one run, making it less time-consuming and allowing the extracted cycles to be correlated with other multiaxial criteria. However, it can only extract half-cycles and may ignore the highest stress during the loading history.

Additionally, Wei and Dong [43] observed that this method does not consider the impact of path dependency on fatigue damage.

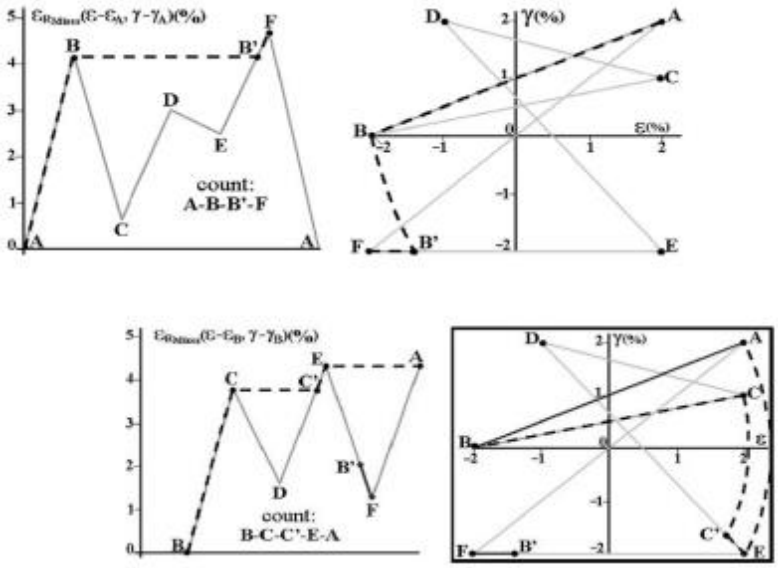

FIGURE 2.18 RAINFLOW PATH OF THE NEXT EVENT OF THE HISTORY AND CORRESPONDING $\gamma-\varepsilon$ DIAGRAM [50]

2.6.3 Bannantine and Socie

Bannantine and Socie produced a solution to address the challenge of cycle identification when determining the fatigue life in a multiaxial variable loading scenario. Their proposed approach combines the critical plane damage parameter, the Rainflow cycle counting technique, and Miner's Rule damage accumulation [52]. According to both Bannantine and Socie, the plane that undergoes the most damage is the one where fatigue damage occurs, and this can be established by using the strain approach in the variable loading history on that specific plane.

The Bannantine and Socie method involves counting cycles using the conventional Rainflow technique on the critical plane and then using Miner's rule to sum up the damage contribution for that specific plane. The critical plane where the maximum damage occurs is determined using the strain approach in the variable loading history. The process is depicted in Figure 2.19.

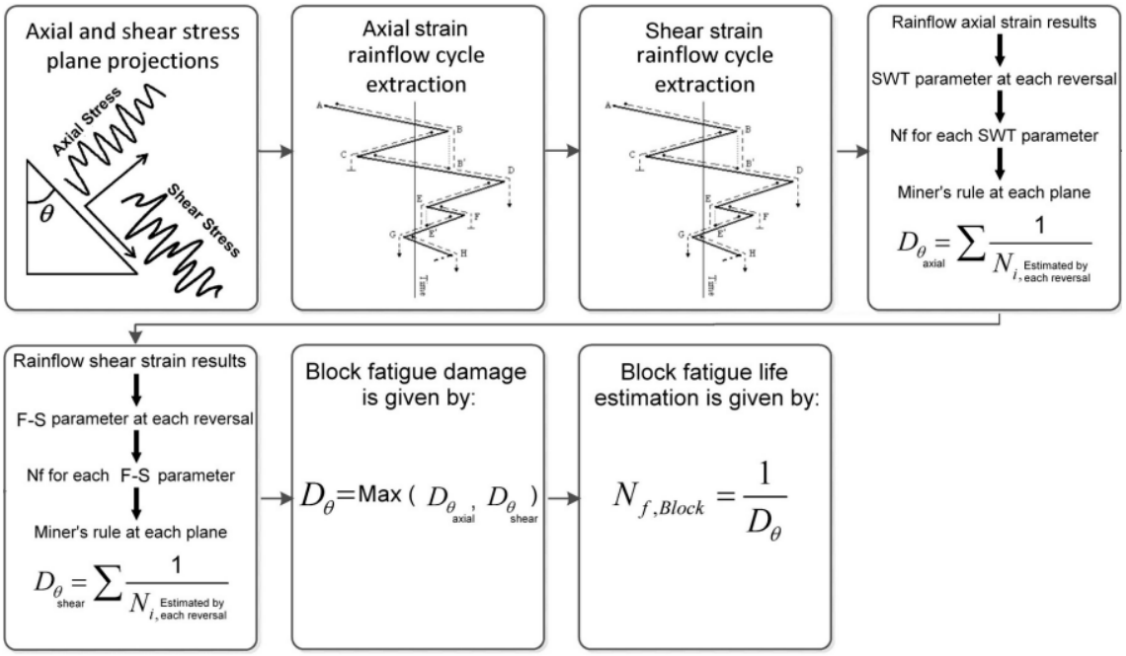

FIGURE 2.19 BANNANTINE AND SOCIE METHOD FOR MULTIAXIAL LOADING HISTORY [22]

According to Matus and Dominik [51], the BS approach has some major drawbacks. One of them is that applying the Rainflow flow methods to multiple planes makes it a very time-consuming process. Anes et al. [22] also noted another drawback of the BS approach, which is the inability to determine the amount of contribution of axial and shear loading components to the fatigue damage.

2.6.4 Virtual cycle counting

An alternative cycle counting method, known as "virtual cycle counting," was created by Anes et al. [22]. The concept of virtual cycle counting is based on the correlation between the maximum damage parameter within a block and the total damage. This approach does not analyse hysteresis curves, which is why the authors use the term "virtual" for the counting, although it is based on physical assumptions. It was developed specifically to deal with multiaxial loading with variable amplitudes.

Figure 2.20 illustrates the process of cycle counting using the virtual cycle counting technique and the estimation of fatigue life. Figure 2.18 a) displays the stress variation between axial and shear components. This stress variation is used to construct the SSF (Stress Scale Factor) time history, as depicted in Figure 2.18 b). Once the SSF time history is computed, the shear stress value corresponding to peak stress and valley stress between successive zero stress points is identified, as shown in Figure 2.18 c).

Figure 2.18 d) shows the block damage value, which is obtained using the maximum SSF value, and this block damage value is utilized to determine block fatigue life estimations, as demonstrated in Figure 2.18 e).

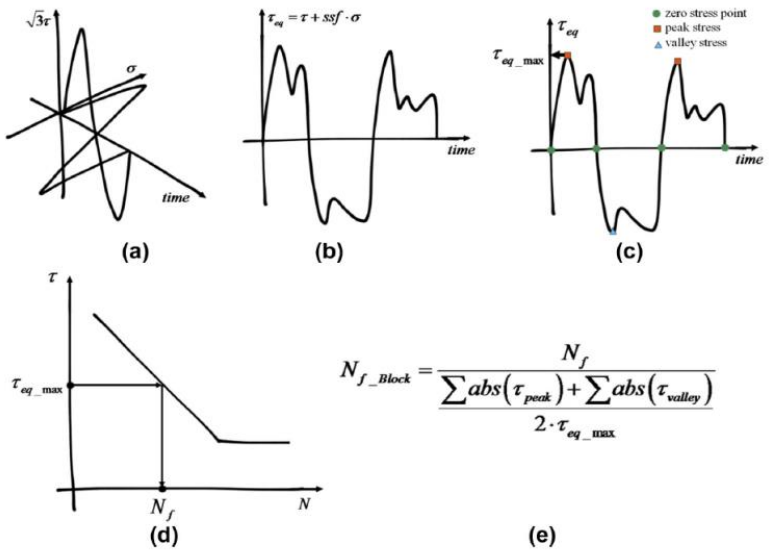

FIGURE 2.20 VIRTUAL CYCLE COUNTING METHOD AND FATIGUE LIFE ESTIMATION BLOCKS [22]

This method utilizes an SSF function, which takes into account the impact of both load magnitude and amplitude on fatigue strength and can be calculated using Equation 2.40. Cycle counting is conducted using the following equation:

$$vcc = \frac{\sum abs\left(\tau_{eq}\right)_{peak} + \sum abs\left(\tau_{eq}\right)_{valley}}{2 \cdot \left(\tau_{eq}\right)_{max,block}} \tag{2.40}$$

Where vcc represents the number of virtual cycles counted on a loading block, and τ_{eq} refers to the SSF equivalent shear stress at each peak or valley. An advantage of using virtual cycle counting is that its theory is uncomplicated and can be easily applied on similar scenarios.

2.7 Damage accumulation

It is widely recognized that components in practical applications are typically subjected to a series of unpredictable loads, making the analysis of fatigue even more challenging. It is worth noting that most of the available fatigue data are obtained under constant amplitude loading, which is rarely encountered in real-world situations. The

reason for this is that tests conducted under variable amplitude loading are costly and time-consuming.

To evaluate the damage in a material due to variable loading, a cycle counting technique is employed to identify the cycles from the loading history. Then, a damage parameter is calculated to quantify the damage caused by each cycle. Finally, the overall damage is determined by summing up the impact caused by each cycle. Many factors such as applied stress, number of cycles, temperature, frequency, moisture content, and geometric shape of the material affect the amount of damage that the material undergoes.

2.7.1 Palmgren-Miner

In 1924, Palmgren [53] introduced the concept of linear damage accumulation, but Miner is often credited with this concept due to his work on axial fatigue data for aircraft skin material, which showed good correlation between experimental data and the linear rule. However, it should be noted that most available experimental fatigue data were obtained under constant load, while in reality, most applications involve variable loading conditions, making the loading profile more complex.

The linear rule is based on assessing the contribution of each cycle to the total damage by considering the fraction of the number of cycles that lead to failure at a given stress or load level. Fatigue failure occurs when the damage parameter D equals 1. Miner's rule can be expressed by the following equation:

$$D = \sum \frac{n_i}{N_f} \tag{2.41}$$

The Equation 2.41 shows the variables used in Miner's rule:

- D represents the total damage
- ni represents the number of cycles at a certain stress/load level i
- Nf represents the number of cycles until failure considering only the load level i.

There are numerous models available in the literature for cumulative damage assessment. However, Palmgren-Miner model remains the most commonly used due to its simplicity and ease of use, and Miner's rule has demonstrated good agreement with experimental results [53]. The linear damage rule is the most frequently used in the

European automotive industry [54]. Nevertheless, there are some limitations associated with this rule, such as load-level independence, load-sequence independence, and lack of load-interaction accountability [55].

The results obtained using the Miner's rule approach only consider damage caused by stress levels above the fatigue limit. However, in practical applications, such as in industrial machines, components may experience cyclic loading below the fatigue limit that can lead to damage, as seen in Figure 2.21. According to Kondo [56], the probable reason for this discrepancy is that the Miner's rule did not consider stress levels below the fatigue limit, because traditionally, the SN curve is not established beyond 10^6 cycles, resulting in a significant decrease in cumulative damage at failure when the value of D was small.

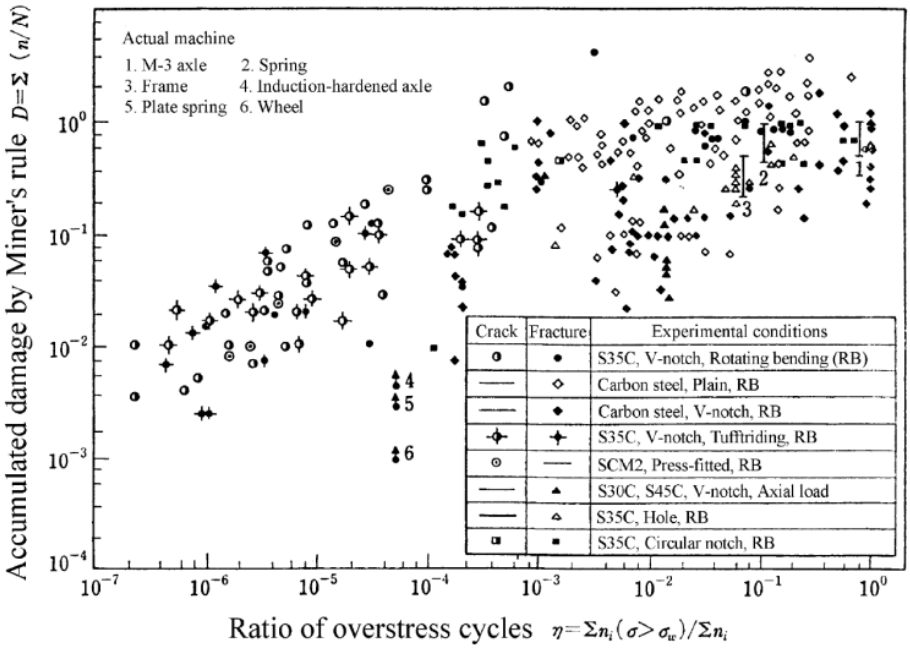

FIGURE 2.21 LINEAR CUMULATIVE DAMAGE MODEL FOR EXPERIMENTAL AND REAL-LIFE MACHINES [56]

In regard to load sequence, it has been observed that the damage sum leading to failure is greater than one for low-high tests and less than one for high-low tests [57]. This means that if there is a loading block that goes from high to low, fatigue failure would occur at a lower cumulative damage, whereas from low to high, it would occur at a higher cumulative damage.

Despite the proposal of many nonlinear cumulative damage models, linear damage rules are still the most commonly used. The disadvantages associated with linear

damage rule in estimating fatigue damage are often attributed to the use of an inappropriate damage parameter, rather than the rule itself [58]. Although the Miner Rule has many shortcomings and cannot fully capture the behaviour of materials under variable loading, its simplicity has led to its wide use in the analysis of variable loading fatigue.

2.7.2 Morrow

The Morrow rule is a nonlinear cumulative damage rule that considers the effects of load interaction. Morrow proposed that in a specimen subjected to a cycle of variable stress amplitude, the fatigue damage caused by a stress amplitude σ_i is given by the expression in Equation 2.42 [59].

$$D_{cycle} = \frac{1}{N_i} \cdot \left(\frac{\sigma_i}{\sigma_{max}} \right)^d \tag{2.42}$$

The total damage over the loading spectrum or a block can be calculated by summing up the damage from each cycle, given by the Equation 2.43:

$$D_{block} = \sum_{i=1}^{k} \frac{n_i}{N_i} \cdot \left(\frac{\sigma_i}{\sigma_{max}} \right)^d \tag{2.43}$$

Where k represents the number of cycles in the block, ni is the number of cycles executed, and Ni is the fatigue life corresponding to the applied stress in block i. The exponent d is a material constant that can be seen as indicative of its sensitivity to changes in stress amplitude [59]. This constant can be obtained using Equation 2.44.

$$d = \frac{b + c + 1}{b} \tag{2.44}$$

The variables b and c refer to the exponents of fatigue resistance and ductility, in that order.

3 . Bibliometric analysis

3.1 Analysis overview

Bibliometric analysis employs quantitative methods to investigate bibliographic materials, making it a valuable tool. The method has gained popularity for providing a concise summary of classified bibliography [60]. To ensure the relevance of the study, researchers must follow a pre-established research protocol that takes into account all potential sources of error or bias [61]. The protocol for this study includes several stages, which are outlined in Figure 3.1.

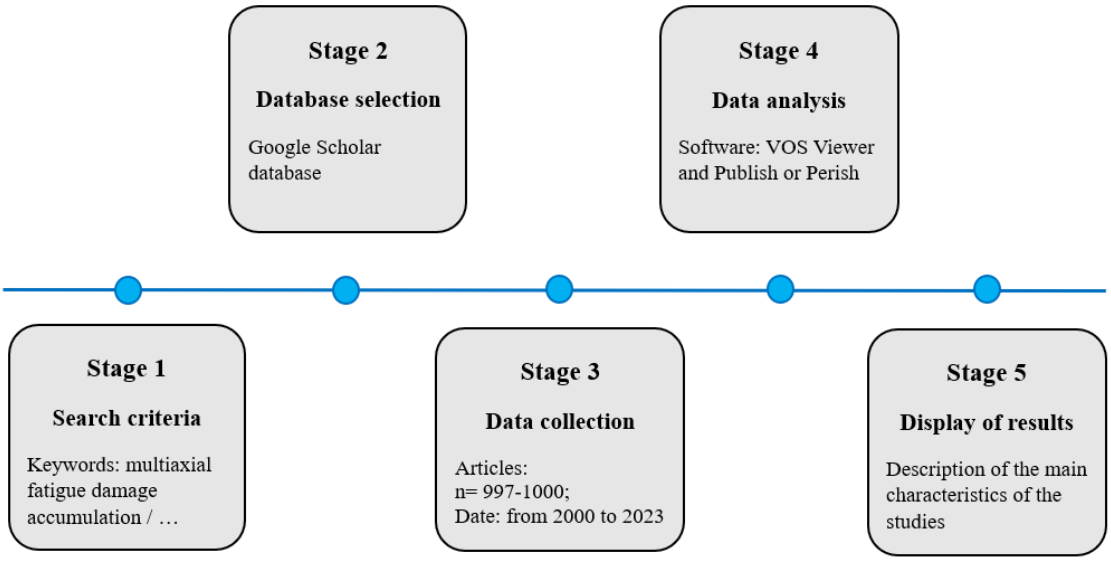

FIGURE 3.1 THE FIVE STAGES OF BIBLIOMETRIC ANALYSIS.

Moreover, prior to Stage 1, the following research questions were formulated:

- RQ1: what is the output and growth trend of publications in the selected research areas?
- RQ2: which are the most influential countries and journals that are impacting the research streams?
- RQ3: How is the connection between internationalization and multiaxial fatigue and damage accumulation being explored and studied?

3.1.1 Stage 1: *Search Criteria*

With this study relying on scientific papers that specifically investigate the subject of multiaxial fatigue and damage accumulation became its main concepts of focus. The use of keywords was introduced to ensure the study wouldn't divert away from the main research questions. Hence, numerous keyword combinations were utilized to tackle multiple sub-subjects of multiaxial fatigue, such as:

i. "multiaxial" ; "fatigue" ; "damage" ; "accumulation"
ii. "multiaxial" ; "cycle" ; "counting"
iii. "proportional" ; "nonproportional" ; "loading"
iv. "critical" ; "plane" ; "fatigue"; "models"
v. "variable" ; "amplitude" ; "loading"

All of the search results contained the specified terms either in the title, abstract, or keywords of publications.

3.1.2 Stage 2: *Database Selection*

The selected database used for the conducted study is Google Scholar. Among other reputable database sources such as Web of Science, PubMed, Scopus, Crossref and OpenAlex, Google scholar stands out as a free, useful and known database able to provide an optimal quality of journals and publications referencing the topics in question. Every publication in Google Scholar includes details such as the publication dates, authors, addresses, title, abstract, journal, references, etc. Moreover, standardized literature entries exported from the Google Scholar can be directly applied in various bibliometric analysis tools to collect said data.

3.1.3 Stage 3: *Data Collection*

The search was performed in April 2023 using Harzing's Publish or Perish software tool [62]. Collecting only research papers, as they featured the results of investigations on multiaxial fatigue and damage accumulation, the tool is used to collect a data file from publications analysed. This data collection included the period from the 2000's to present day, 2023. A fixed maximum of 1000 results for the search in Google Scholar was selected, resulting in a varied 996 to 1000 results per search. Also, in order to analyse the selected keywords, the language filter was applied excluding any

publication not written in English. Once the data was finalised, the results were exported with all available information in ".RIS" format, which was then used in the analysis.

3.1.4 Stage 4: *Data Analysis*

Following data collection, the selected articles underwent assessment through a review of the chosen subjects prior to the synthesis of data. This procedure enabled to confirm the relevance of the study overall.

For quantitative data analysis, the construction and further visualisation of bibliometric networks was used by applying VOSviewer free software. VOSviewer provides a broader view of search results by generating 2 dimensional maps based on bibliographic coupling, co-authorship, citation, co-citation, co-occurrence of keywords, authors and countries in order to visualise the relationships between them.

3.1.5 Stage 5: *Display of Results*

After the data analysis and processing, the results and quantitative evaluation of the examined phenomenon ensue and are presented in the following sections. With the addition of detailed results, visualizations of said data are provided in the analysis review section. Moreover, the discussion and conclusions on the topic follow last.

3.2 Analysis Review

3.2.1 Output and Growth Trend of Publications

To address RQ1, the output of annual publications was utilized as a metric. The number of scientific papers is an important measurement for determining the relevance and development of a specific field of research. Overall, the publications related to multiaxial fatigue and damage accumulation increased over the analysed period with a total of 1000 scientific documents being published from 2000 to 2023. The number of publications in year 2000 started off high as compared to the following years, ever so increasing since 2015 (more than 50 publications were published every year since then) to present day, with 2023 already having 23 publications documented as of April.

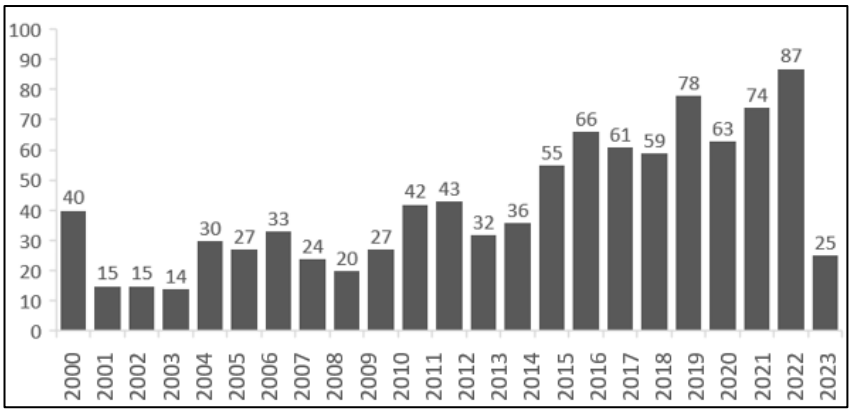

FIGURE 3.2 GROWTH TREND OF PUBLICATIONS RELATED TO: MULTIAXIAL FATIGUE DAMAGE ACCUMULATION – 2000-PRESENT DAY

The publications related to variable amplitude loading (996 were analysed over the same period) start off high in the number of publications documents, with 58 in the year 2000. Followed by a decrease of 30 papers published in the following year, it increases again and remains somewhat stable until its peak in 2008 (n=61). Followed by another decrease, 2013 sees its lowest point with having 24 publications documented, seen yet again with another rise for the following years. Every year since 2020 however, it's apparently on a steady decline going from 48 to 40 publications in 2022.

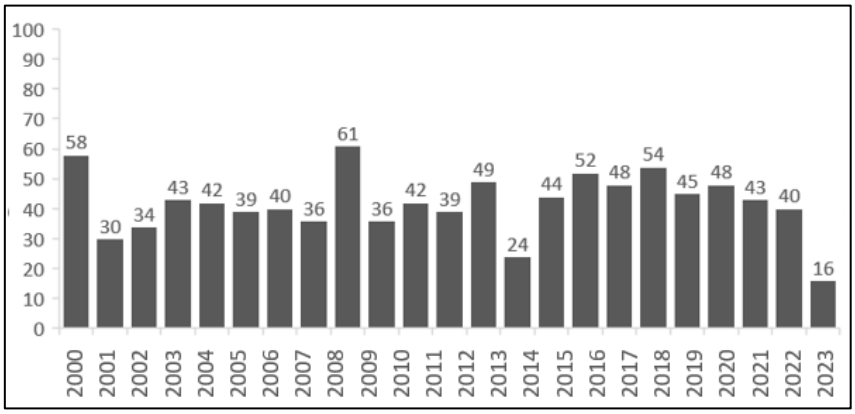

FIGURE 3.3 GROWTH TREND OF PUBLICATIONS RELATED TO: VARIABLE AMPLITUDE LOADING – 2000-PRESENT DAY

The publications related to proportional and nonproportional loading (998 were analysed over the same period) see an all-time high in publications in the year 2000 (n=74), followed by a decrease of only 31 papers published in the following year. Steadily, the number increased to 48 in 2010 and decreased again in 2012 with only 22. Ensuing came another increase reaching a peak of 69 and 68 publications in 2019 and 2022, respectively.

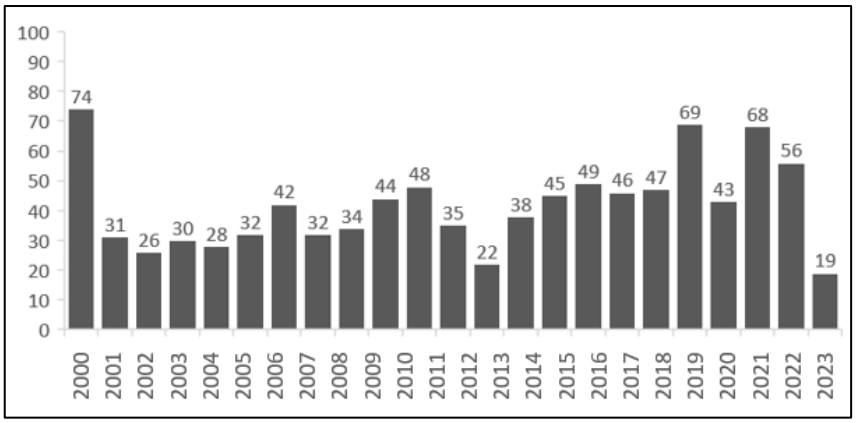

FIGURE 3.4 GROWTH TREND OF PUBLICATIONS RELATED TO: PROPORTIONAL AND NONPROPORTIONAL LOADING – 2000-PRESENT DAY

Overall, the publications related to critical plane fatigue models increased over the analysed period with a total of 997 scientific documents being published from 2000 to 2023. The number of publications in year 2000 started off at its lowest (n=31), steadily increasing every year since then to reach its peak of 88 documents published in 2022.

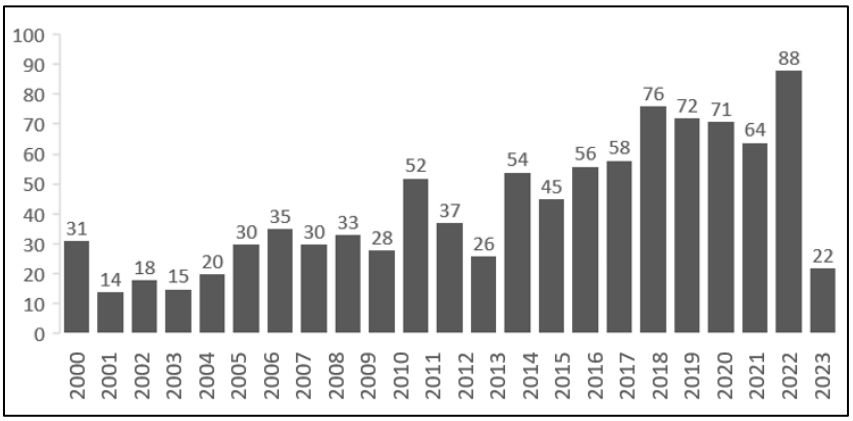

FIGURE 3.5 GROWTH TREND OF PUBLICATIONS RELATED TO: CRITICAL PLANE FATIGUE MODELS – 2000-PRESENT DAY

Finally, the publications related to multiaxial cycle counting (with a number of 1000 scientific documents analysed in the last 23 years) show a total of 32 publications documented in the year 2000, followed by a decrease to only 8 in the following year. Since 2001 however, an increase of linear proportions became apparent, reaching its high in 2022 with a total of 86 publications. Already, since the start of 2023, 29 papers have been published on the matter showing the same behaviour as previous years.

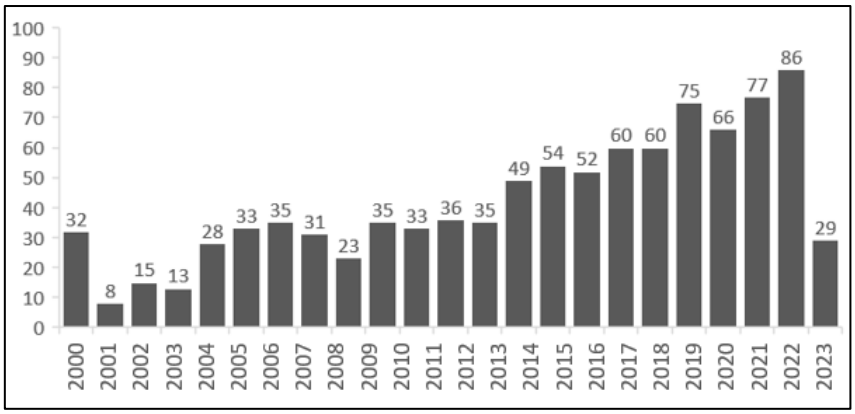

FIGURE 3.6 GROWTH TREND OF PUBLICATIONS RELATED TO: MULTIAXIAL CYCLE COUNTING – 2000-PRESENT DAY

3.2.2 The Most Cited Publications

The most cited and influential publications on every keyword mentioned in the search criteria are presented in Table 3.1.

TABLE 3.1 – THE MOST CITED PUBLICATIONS

	Title	Author(s)	Journal	Y [C] *
"Variable amplitude loading"	Metal fatigue in engineering	RI Stephens, A Fatemi, RR Stephens and HO Fuchs	Wiley-Interscience	2000 [2758]
"Proportional and nonproportional loading"				
"Critical fatigue plane models"				
"Multiaxial cycle counting"				
"Multiaxial fatigue and damage accumulation"	Fatigue damage, crack growth and life prediction	F Ellyin	Chapman & Hall	2012 [721]
	Fatigue damage modelling of fibre-reinforced composite materials	J Degrieck and W.V. Paepegem	Appl. Mech. Rev	2001 [698]
	Fatigue in composites: science and technology of the fatigue response of fibre-reinforced plastics	B Harris	Woodhead Publishing	2003 [579]
"Variable amplitude loading"	Fatigue of structures and materials	J Schijve	Springer Science	2009 [2456]
	Recommendations for fatigue design of welded joints and components	AF Hobbacher	Springer International	2016 [2016]
	A review of wind energy technologies	GMJ Herbert, S Iniyan and E Sreevalsan	Renewable and Sustainable Energy Reviews	2007 [1259]

"Proportional and nonproportional loading"	The cohesive zone model: advantages, limitations and challenges	M Elices, GV Guinea, J Gomez and J Planas	Engineering Fracture Mechanics	2002 [1247]
	Kinematic hardening model suitable for ratchetting with steady-state	M Abdel-Karim and N Ohno	International Journal of Plasticity	2000 [454]
	Life prediction of rolling contact fatigue crack initiation	JW Ringsberg	International Journal of Fatigue	2001 [378]
"Critical plane fatigue models"	Additive manufacturing of fatigue resistant materials: Challenges and opportunities	A Yadollahi and N Shamsaei	International Journal of Fatigue	2017 [687]
	A literature survey on fatigue analysis approaches for rubber	WV Mars and A Fatemi	International Journal of Fatigue	2002 [558]
	A review of rolling contact fatigue	F Sadeghi, B Jalalahmadi, TS Slack and N Raje	Journal of Tribology	2009 [554]
"Multiaxial cycle counting"	Fatigue testing and analysis: theory and practice	YL Lee, J Pan, R Hathaway and M Barkey	Elsevier	2005 [1293]
	A review of critical plane orientations in multiaxial fatigue failure criteria of metallic materials	A Karolczuk and E Macha	International Journal of Fracture	2005 [384]
	Multiaxial fatigue: An overview and some approximation models for life estimation	A Fatemi and N Shamsaei	International Journal of Fatigue	2011 [376]

* Y[C] – year published [total citations]

3.2.3 The most influential Institutions

By examining the most influential institutions affiliated with publications related with the multiple categorized keywords, it is possible to highlight the top 17 illustrated in Figures 3.7 through 3.11. Regarding the topic of multiaxial fatigue and damage accumulation, it's possible to highlight that Instituto Superior Técnico is tied for the most influential institution with Fraunhofer Institute of Structural Durability and System Reliability.

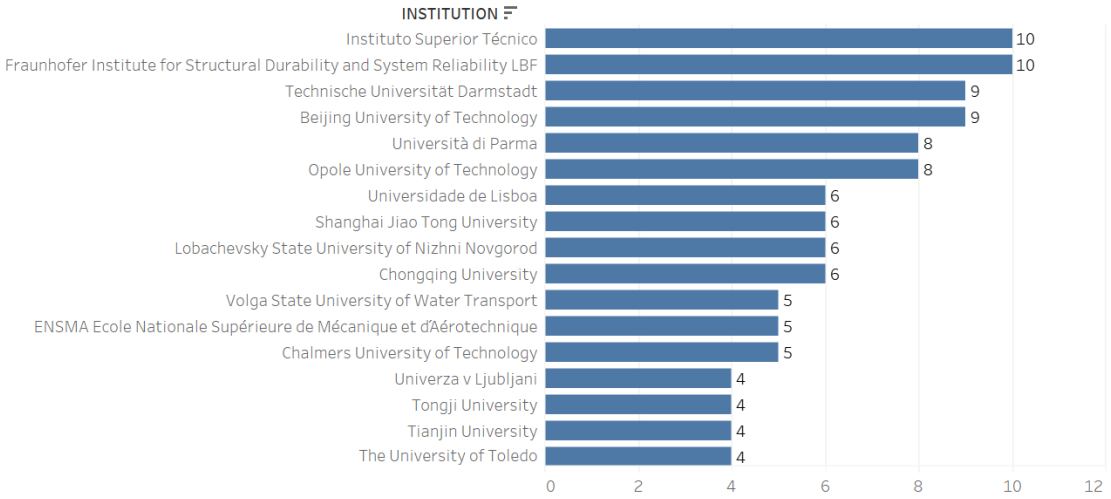

FIGURE 3.7 MOST INFLUENTIAL INSTITUTIONS UNDER PUBLICATIONS RELATED TO: MULTIAXIAL FATIGUE DAMAGE ACCUMULATION – 2000-PRESENT DAY

On the subject of variable amplitude loading, three institutions prove their dominance and knowledge over the matter. At number one, Fraunhofer Institute of Structural Durability and System Reliability managed to publish 75 scientific papers followed by the Ministry of Education of China with 73 and finally University Kebangsaan of Malaysia with 72.

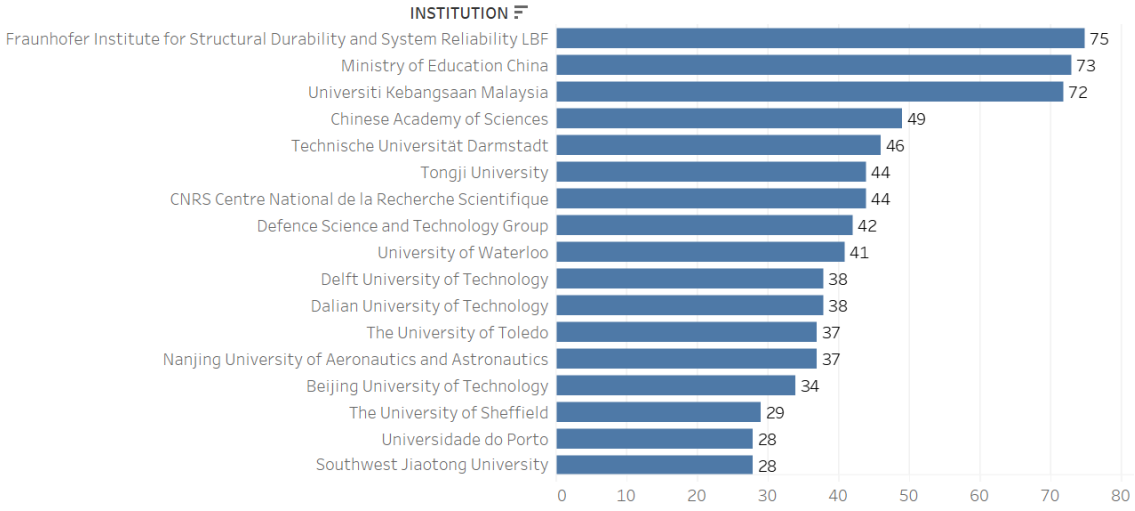

FIGURE 3.8 MOST INFLUENTIAL INSTITUTIONS UNDER PUBLICATIONS RELATED TO: VARIABLE AMPLITUDE LOADING – 2000-PRESENT DAY

Discussing the subject of proportional and nonproportional loading, Ritsumeikan University Biwako-Kusatsu Campus leads the majority of documented publications with 39. Following, Tongi University and University of Fukui have 26 and 25 publications the same time period.

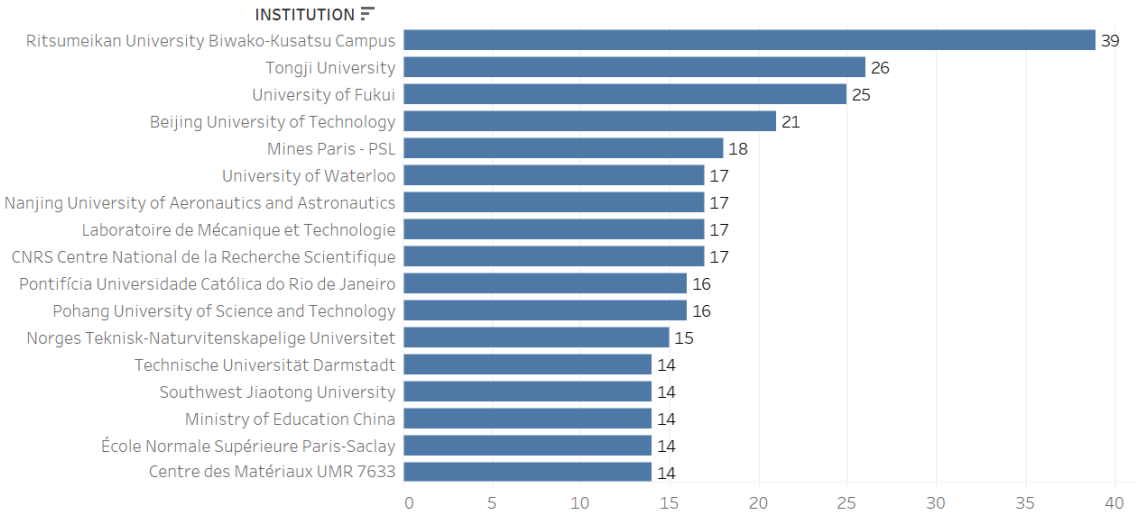

FIGURE 3.9 MOST INFLUENTIAL INSTITUTIONS UNDER PUBLICATIONS RELATED TO: PROPORTIONAL AND NONPROPORTIONAL LOADING – 2000-PRESENT DAY

Regarding the subject of critical plane fatigue models, it's possible to highlight that the Ministry of Education of China (*n*=36) has having the most influence through the last 23 years. Furthermore, the Opole and Beijing Universities of Technology follow behind with 27 and 26 scientific publications, respectively.

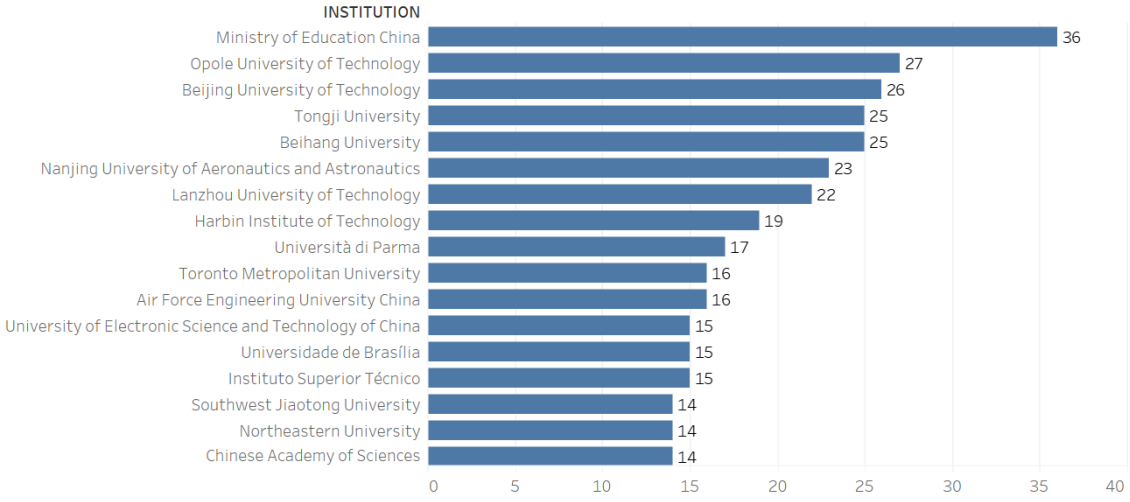

FIGURE 3.10 MOST INFLUENTIAL INSTITUTIONS UNDER PUBLICATIONS RELATED TO: CRITICAL PLANE FATIGUE MODELS – 2000-PRESENT DAY

Lastly, on the subject of multiaxial cycle counting, Beijing Institute of Technology stands at the top with a total of 14 publications since the year 2000. Right behind it, Instituto Superior Técnico (n=10) and Nanjing University of Aeronautics and Astronautics (n=9) follow with its contribution on the same subject.

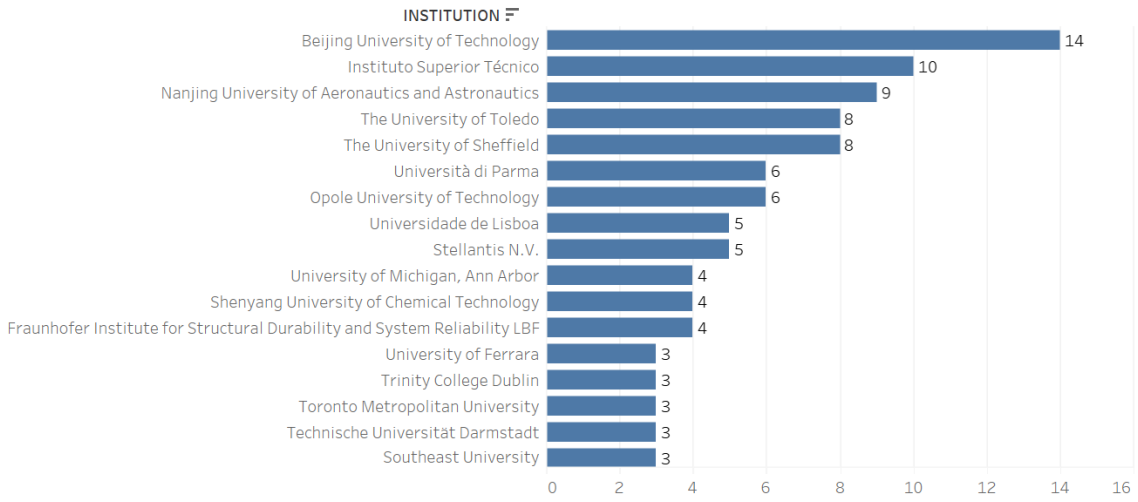

FIGURE 3.11 MOST INFLUENTIAL INSTITUTIONS UNDER PUBLICATIONS RELATED TO: MULTIAXIAL CYCLE COUNTING – 2000-PRESENT DAY

3.2.4 The most Cited Journals

Aiming to answer RQ2, the most cited and influential journals had to be analysed. The most cited and influential journals on every keyword mentioned in the search criteria are presented in Table 3.2. The most cited journal is International Journal of Fatigue with 749 documents and is cited in a total of 64516 citations with an average number of citations per document of n=31323. In second, the most cited journal is Fatigue and Fracture of Engineering Materials with 77 documents and with a total of 8780 citations, with an average citations per document of n=3800. Third, the most cited journal is Engineering Fracture Mechanics with 74 documents and with a total of 7544 citations, with an average citations per document of n=3136.

TABLE 3.2 – THE MOST CITED JOURNALS.

Journal	Documents	Citations	Avg. C. per doc.
International Journal of Fatigue	749	64516	31323
Fatigue and Fracture of Engineering Materials	77	8780	3800
Engineering Fracture Mechanics	74	7566	3136
International Journal of Plasticity	46	5504	2412
Wear	23	2596	769
International Journal of Fracture	8	11023	1488
Materials Science and Engineering	28	2141	568
Materials and Design	32	1935	491
International Journal of Mechanical Sciences	24	1644	547
Renewable and Sustainable Energy Reviews	3	1523	444
Tribology International	29	1230	463
Journal Biomech	1	1133	283

Acta Materiala	10	1182	301
Advances in Materials Science	9	1112	274
Additive Manufacturing	1	1076	269

3.2.5 Co-Citation Analysis of Authors

Co-citation analysis of authors helps determine the relatedness of authors based on the frequency they are cited together. The size of the circles represents how large the number of citations is mentioned. Meanwhile, the distance represents relatedness and cooperation between the authors while the colours represent clusters. Only the results meeting a threshold of 15 citations are shown. The results are divided by two separate analyses with some similarities although the one showed in Figure 3.12 illustrates the search dealt on the group of the following keywords: “multiaxial fatigue damage accumulation”, ”critical plane models”, “multiaxial cycle counting” and “variable amplitude loading”.

In total 15 different clusters can be identified in Figure 3.12: cluster in red (L. Susmel (*n*=100) bottom middle); cluster in green (Y. Liu (*n*=68) middle left); cluster in dark blue (A. Nielstony (*n*=107) middle right); cluster in yellow (D.G. Shang (*n*=109) far left); cluster in purple (A. Carpinteri (*n*=81) top); cluster in baby blue (C.M. Sonsino (*n*=38) far right); cluster in orange (P. Dong (*n*=77) top left); cluster in brown (L. Reis (*n*=60) middle); cluster in pink (D. Benasciutti (*n*=40) bottom middle); cluster in light red (Y. Jiang (*n*=54) middle); cluster in light green (T. Itoh (*n*=65) top middle); cluster in light blue (M.A. Meggiolaro (*n*=96) middle right); cluster in light yellow (M. Margetin (*n*=25) bottom right); cluster in light purple (T. Pejkowski (*n*=22) top right) and cluster in light blue (J.A. Araújo (*n*=19) bottom).

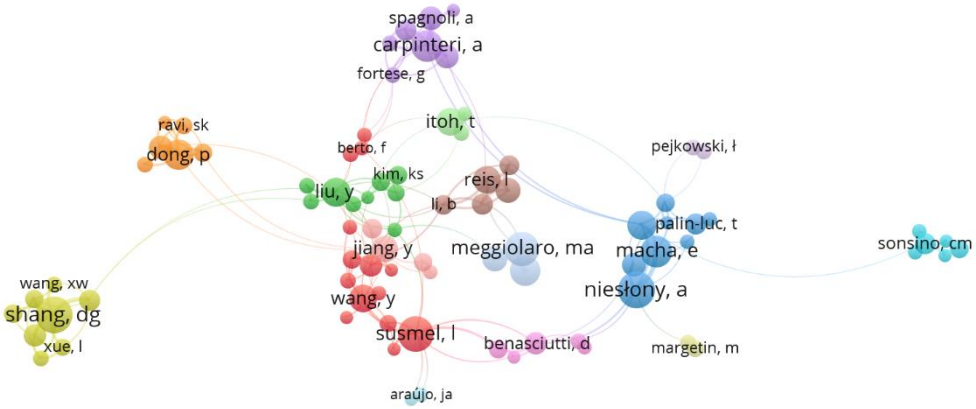

FIGURE 3.12 CO-CITATION ANALYSIS OF AUTHORS BY KEYWORDS: "MULTIAXIAL FATIGUE DAMAGE ACCUMULATION", "CRITICAL PLANE FATIGUE MODELS", "MULTIAXIAL CYCLE COUNTING", "VARIABLE AMPLITUDE LOADING" AND "PROPORTIONAL AND NONPROPORTIONAL LOADING" – 2000-PRESENT DAY

3.2.6 Authorship Analysis of Countries

To be able to accurately answer RQ2, an analysis was conducted on the most cited and influential countries regarding the subject of multiaxial fatigue and damage accumulation, as well as all other keywords introduced in the search criteria. Information on authorship reveals the importance level and consideration that countries take based on the degree of need and productive sources on said subjects (Figures 3.13 through 3.17). The colour on the map relates to the density of the number of authors shown per country, dark blue being the most heavily dense and light blue the least.

When searching for the keywords: "multiaxial", "fatigue", "damage", "accumulation", the countries that have documented this subject the most are People's Republic of China (n=44), the USA (n=33) and Germany (n=31).

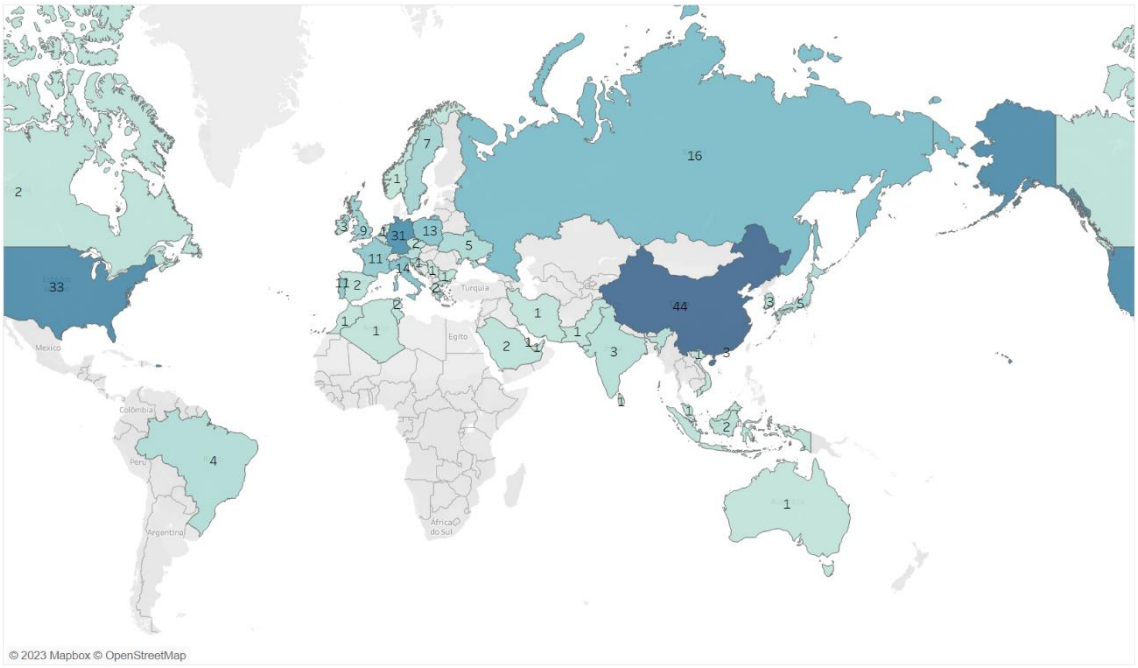

FIGURE 3.13 GEOGRAPHIC MAP OF PUBLICATIONS RELATED TO: MULTIAXIAL FATIGUE DAMAGE ACCUMULATION – 2000-PRESENT DAY

When searching for the keywords: "multiaxial", "cycle", "counting", the countries that have documented this subject the most are People's Republic of China (n=40), the USA (n=28) and Italy (n=10).

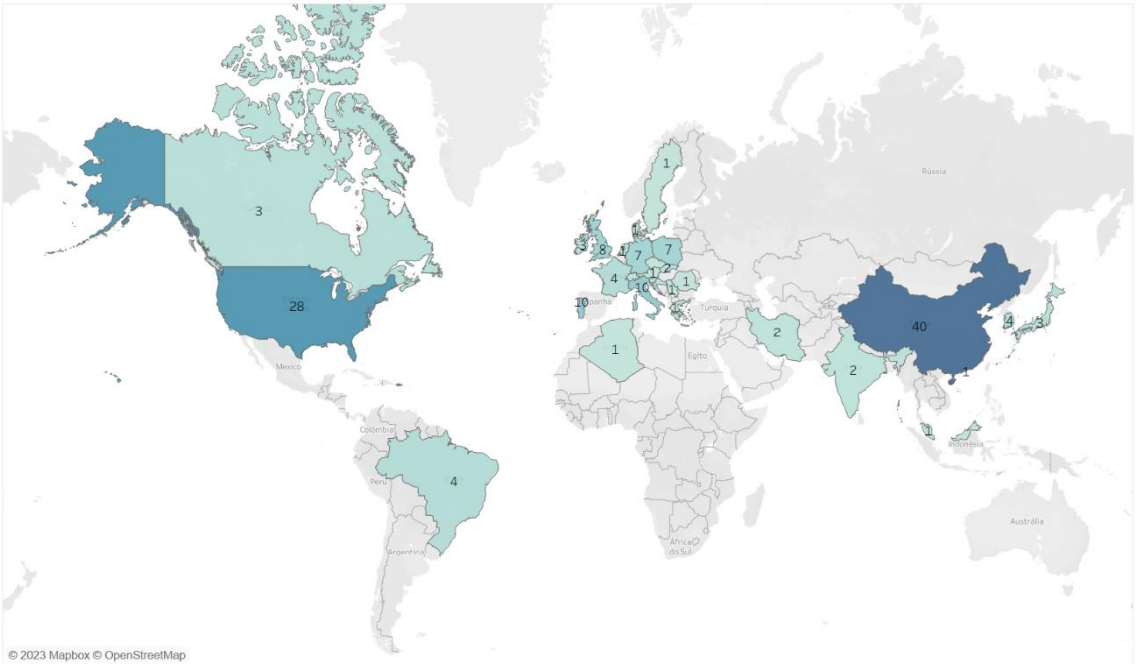

FIGURE 3.14 GEOGRAPHIC MAP OF PUBLICATIONS RELATED TO: MULTIAXIAL CYCLE COUNTING – 2000-PRESENT DAY

When searching for the keywords: “proportional”, “nonproportional”, “loading”, the countries that have documented this subject the most are People’s Republic of China (*n*=208), the USA (*n*=122) and France and Japan tied (*n*=71).

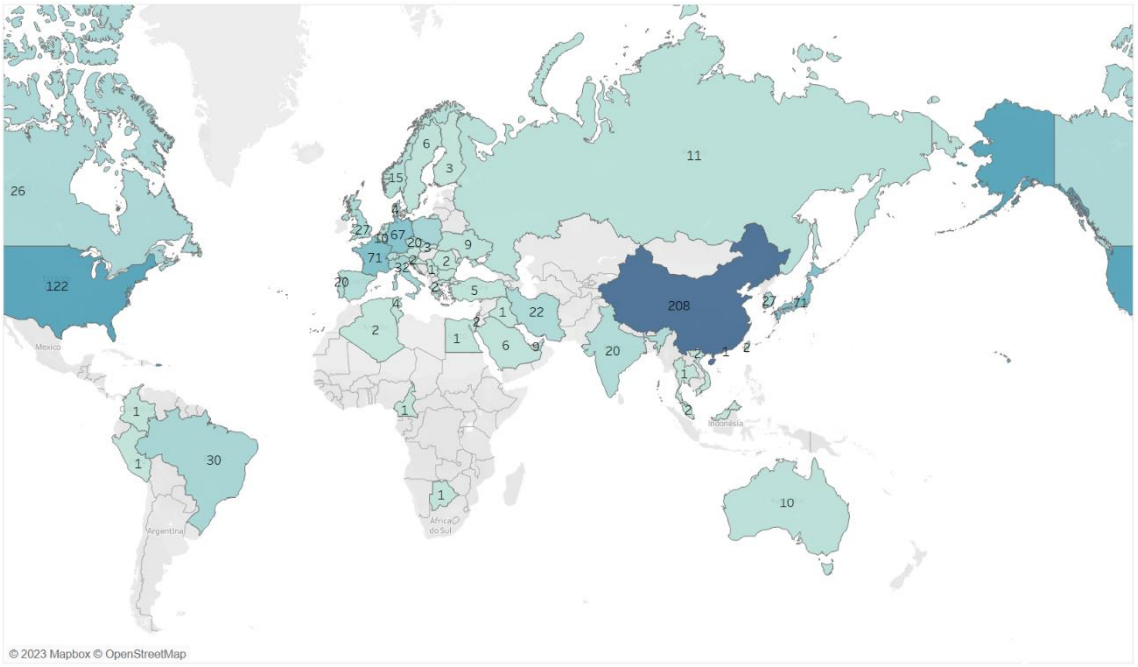

FIGURE 3.15 GEOGRAPHIC MAP OF PUBLICATIONS RELATED TO: PROPORTIONAL AND NONPROPORTIONAL LOADING – 2000-PRESENT DAY

When searching for the keywords: “critical”, “fatigue”, “plane”, “models”, the countries that have documented this subject the most are People’s Republic of China (*n*=349), the USA (*n*=149) and the United Kingdom (*n*=49).

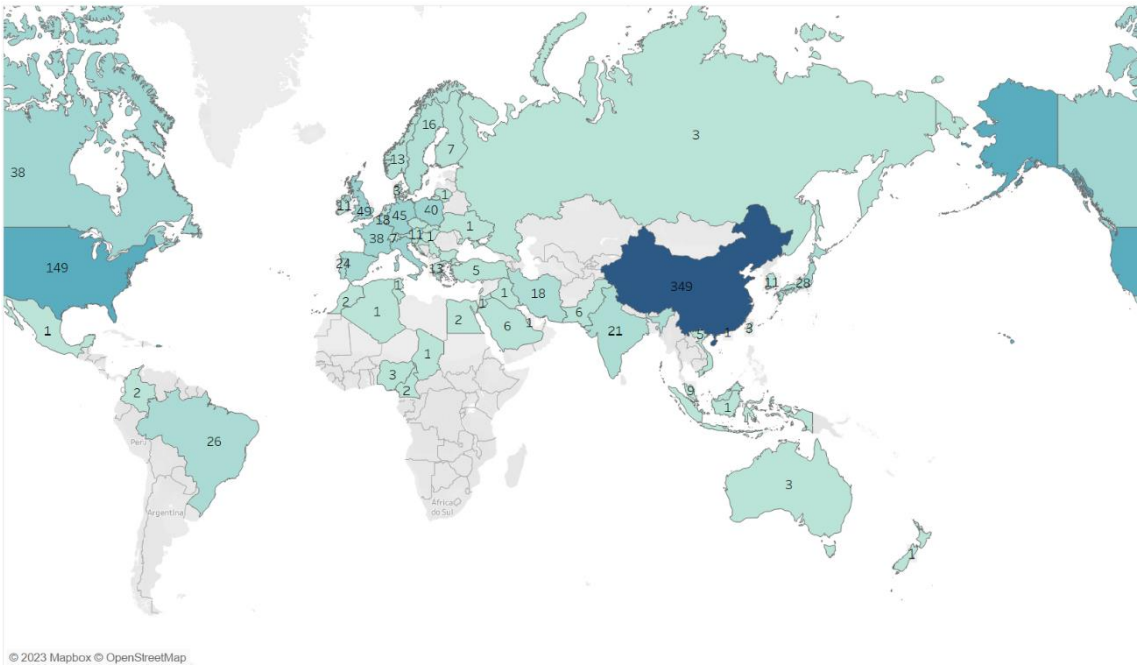

FIGURE 3.16 GEOGRAPHIC MAP OF PUBLICATIONS RELATED TO: CRITICAL PLANE FATIGUE MODELS – 2000-PRESENT DAY

When searching for the keywords: "critical", "fatigue", "plane", "models", the countries that have documented this subject the most are People's Republic of China (n=793), the USA (n=562) and Germany (n=316).

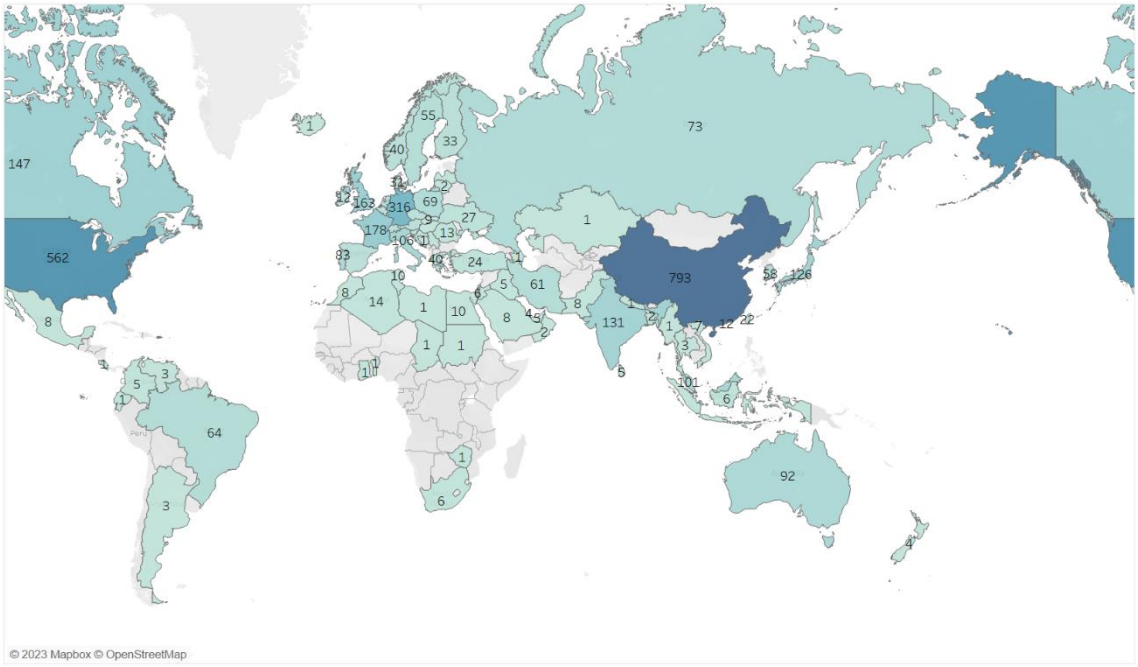

FIGURE 3.17 GEOGRAPHIC MAP OF PUBLICATIONS RELATED TO: VARIABLE AMPLITUDE LOADING – 2000-PRESENT DAY

3.2.7 Keywords

Finally, to answer the final question RQ3, an analysis was conducted on certain terms that are used in scientific documents. Co-occurrence of author's keywords analysis aims to determine the relatedness of keywords based on the number of documents in which authors share the specific keywords. Figure 3.18 illustrates the most commonly used keywords by authors below the abstract to characterize their papers. Circles' size represents the number of keywords used while the distance represents relatedness between them, and the colours represent clusters. Notably, only the results meeting a threshold of 20 times are presented. All the keywords were inserted in the software and out of 4993 documents imported, the terms analysed remained unanimous.

In total, 9 different clusters can be identified: The cluster in purple ("Counting" (n=892) middle); cluster in green ("Plane" (n=457) middle left); cluster in red ("Variable amplitude loading" (n=605) bottom left/middle); cluster in dark blue ("Multiaxial stress state" (n=104) bottom); cluster in orange ("Fatigue loading" (n=103) middle left); cluster in light blue ("Cycle counting procedure" (n=98) top left); cluster in yellow ("Process" (n=118) middle right) and the cluster in brown ("Multiaxial cycle counting (n=82) bottom middle). The most used keywords by authors below the abstracts to characterize the papers on multiaxial fatigue damage accumulation and various underlying subjects mentioned are "Counting" (n=892), "Plane" (n=457) and "Variable amplitude loading" (n=605).

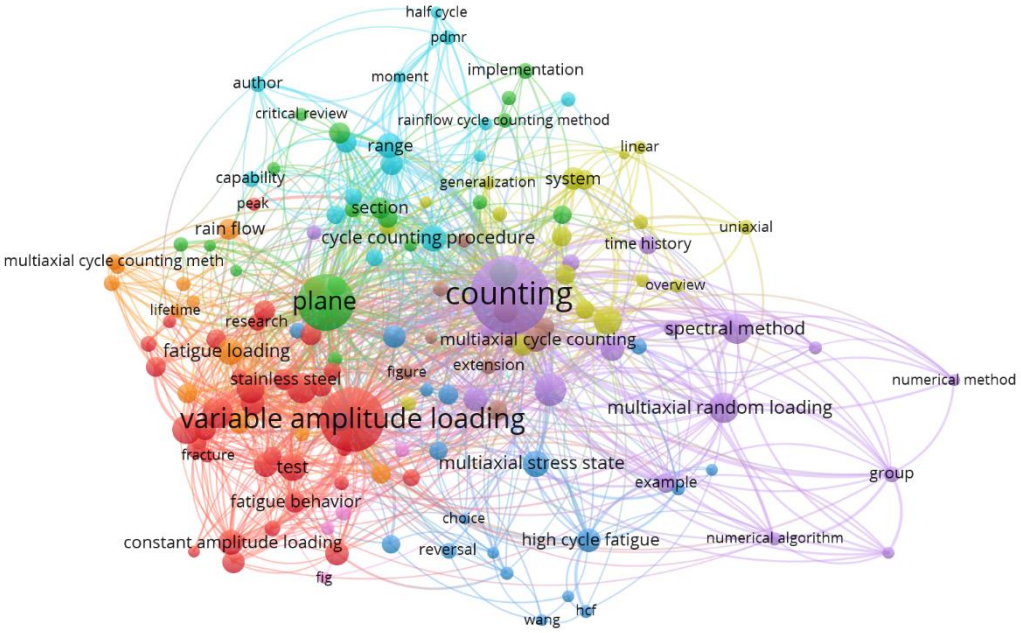

FIGURE 3.18 CO-OCCURRENCE OF AUTHOR'S KEYWORDS [2000-PRESENT DAY]

3.3 Discussion and limitations

The analysis of scientific papers on multiaxial fatigue and damage accumulation, variable amplitude loading, proportional and nonproportional loading, critical plane models and multiaxial cycle counting published from 2000 to 2023 is presented. The study includes 4991 publications and covers 13252 authors, 1883 journals, 112 countries and 1949 institutions. It's apparent that academic literature on analysed topics has been steadily increasing during the last 10 years, thus the publication output can be categorized by an exponential growth.

The bibliometric analysis provided information on the most influential and productive scholars in the research field:

- the most cited publication is by authors R. I. Stephens, A. Fatemi and R. R. Stephens and H. O. Fuchs with an average of 120.15 citations per year;
- the most cited journal is International Journal of Fatigue with a total of 64516 citations, followed by the Fatigue and Fracture of Engineering Materials journal with a total of 8780;
- the most co-cited author is L. Susmel (n = 100);

- the country with the largest publication output is the People's Republic of China with 1434 documents published across all the subjects mentioned. Other countries are sometimes linked (directly or indirectly) to one of the main countries that are publishing the most scientific documents, thus the data showed that cooperation between authors and countries is mediocre due to never really knowing for certain the author's country of origin.

The power-law distribution of the collected data lets us observe that:

- the biggest proportion of authors (65.98%) are only credited in one publication;
- a small group of authors (2.73% of all authors) published at least three papers;
- amongst the journals publishing about topics mentioned, only 7.3% of journals published more than 5 documents (from a total of 649);
- among all countries (total n = 112) publishing about topics mentioned, 44.13% countries published over 10 documents;
- a total of 798 publications (15.97% of all publications) was not (yet) cited;
- a total of 126 publications (2.52% of all publications) was cited over 200 times.

The distribution aligns with the research conducted by van Nunen et al. [63], who noted that only a small number of authors, journals, and countries make significant contributions, while a large proportion contributes significantly less. This study reveals that a small group of authors is responsible for the majority of academic literature.

By analysing the co-occurrence of author keywords, it becomes possible to differentiate four primary research domains: (1) variable amplitude loading, (2) multiaxial stress state, (3) fatigue loading, and (4) cycle counting procedure. Although each area has its own distinct research focus, the network analysis reveals that all of these main research domains are closely connected and directly linked to one another.

While bibliometric analysis addresses some of the biases often associated with expert surveys and traditional reviews, it still has certain limitations. Despite its ability to mitigate biases, this approach cannot fully replace precise content analysis and overcome its inherent limitations, as it primarily relies on quantitative analysis. This study specifically uses the number of scientific publications as its dataset, but it is challenging to comprehensively discuss all the theoretical insights presented in those articles.

Consequently, this study is confined to a quantitative method, overlooking the qualitative aspects and deeper theoretical knowledge, fundamental principles, and conclusions put forth by authors in the field of the interrelationship between multiaxial fatigue damage accumulation, variable amplitude loading, proportional and nonproportional loading, critical plane models and multiaxial cycle counting.

Another potential drawback of this study is the possibility of misleading citation analysis, where authors may reference certain publications negatively or engage in self-citations. Furthermore, the study limitations are associated with the selected timeline. If a similar study were conducted at a different time, the results would vary slightly due to the constant updating of the Google Scholar database with newer scientific documents. Additionally, significant publications may receive "delayed recognition" in the scientific literature, being cited after several years. These limitations should be considered in future studies.

4 . Case Study

A review of literature on multiaxial models and damage accumulation revealed some questions regarding the methodology of the Modified Equivalent Strain Amplitude (MESA) critical plane model and the assessment of the ability to predict fatigue life.

This chapter aims to investigate the impact of evaluating fatigue life estimates on different planes by conducting experimental tests using the MESA approach for various orientations. The study also compares the results with the other several critical plane approaches in order to fully visualize the scope of the impact present.

The primary objective of this study is to explore and discuss the reasons for the limited accuracy of critical plane models when estimating fatigue life. Experimental data related to the critical planes of high strength steel 42CrMo4 was collected from literature, and the MESA method was utilized to determine the crack initiation plane from different orientations and estimate fatigue life. The research revealed that the crack initiation plane differs when employing various implemented models, which accounts for the inadequate performance of critical plane models. These models assume a constant damage scale between normal and shear stresses, whereas, in reality, this scale varies with the evaluation plane, which is confirmed by the findings of this research.

4.1 Materials and methods

The material employed in this research was the high strength steel 42CrMo4, and its mechanical properties, both in unmodulated and cyclic loading conditions, are presented in Table 4.2. These properties were obtained by adhering to the standards of ASTM E8 and ASTM E606 [28]. This steel is commonly used in the production of various automotive parts, such as vehicle axles, steering components, crankshafts, and hot forging components. The chemical composition of 42CrMo4 can be found in Table 4.1.

TABLE 4.1 – 42CRMO4 CHEMICAL COMPOSITION [16]

Element	C	Si	Mn	Cr	P	Ni	Cu	Mo	S
Weight (%)	0.39	0.17	0.77	1.1	0.025	0.3	0.21	0.16	0.02

TABLE 4.2 – MONOTONIC AND CYCLIC MECHANICAL PROPERTIES OF 42CRMO4 [28]

	42CrMo4
Microstructure type	bcc
Poisson's ratio	0.3
Density (Kg/m^3)	7830
Hardness (HV)	362
Tensile strength (MPa)	1100
Yield strength (MPa)	980
Young's modulus(GPa)	206
Elongation (%)	16
σ'_f *Fatigue strength coeficient (MPa)*	1154
b *Fatigue strength exponent*	-0.061
ε'_f *Fatigue ductility coefficient*	0.180
c *Fatigue ductility exponent*	-0.53

Ten loading blocks were analysed and tested to compare the accumulated damage criteria discussed in previous sections. The normal and shear stress time history evolution of the loading blocks is depicted in Figure 4.1.

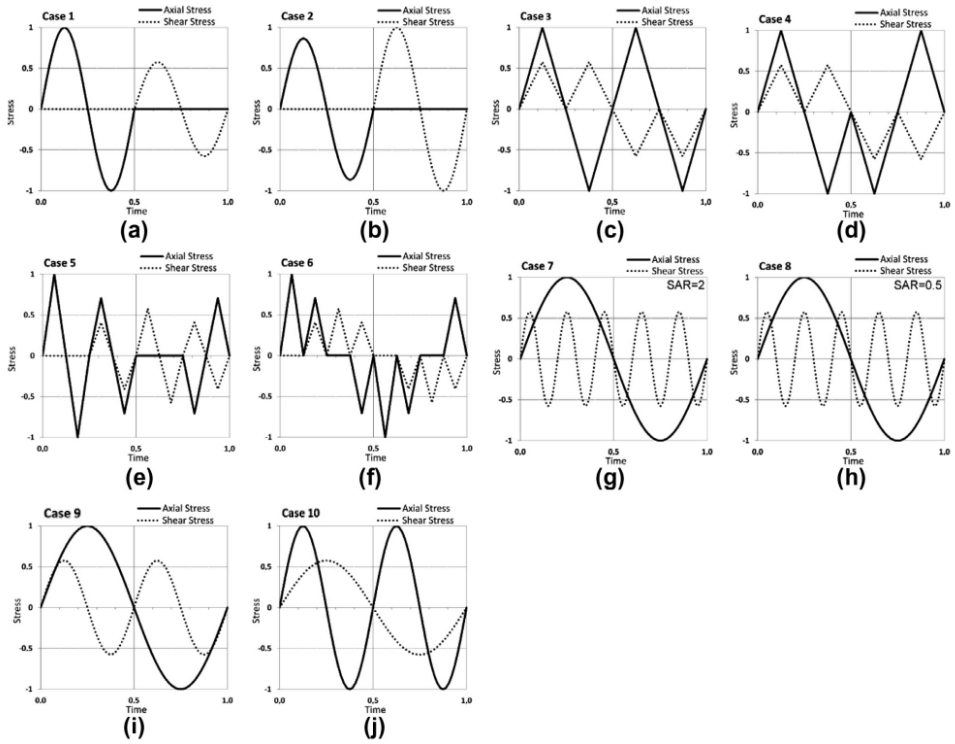

FIGURE 4.1 NORMAL AND SHEAR STRESS TIME EVOLUTION OF THE SELECTED LOADING BLOCKS [22]

4.2 Determination of MESA parameter for each reversal

Under axial-torsion multiaxial loading conditions, the stress and strain of the specimen on the plane angled $\theta°$ with the axial direction, can be expressed as [38]:

$$\varepsilon_\theta = \frac{1-\upsilon}{2}\varepsilon_x + \frac{1-\upsilon}{2}\varepsilon_x \cos(2\theta) + \frac{\gamma_{xy}}{2}\sin(2\theta) \tag{4.1}$$

$$\gamma_\theta = (1-\upsilon)\varepsilon_x \sin(2\theta) - \gamma_{xy}\cos(2\theta) \tag{4.2}$$

$$\sigma_\theta = \frac{\sigma_x}{2} + \frac{\sigma_x}{2}\cos(2\theta) + \tau_{xy}\sin(2\theta) \tag{4.3}$$

$$\tau_\theta = \frac{\sigma_x}{2}\sin(2\theta) - \tau_{xy}\cos(2\theta) \tag{4.4}$$

The procedure involves the processing of stress and strain parameters for each counted reversal to determine the maximum shear strain range plane. This is represented by the following steps:

1) Calculate the shear strain for each data point at angles ranging from 0 to 90 degrees using Equation 4.2, with a step length of 1 degree.

2) Determine the shear strain range for each angle and identify the angle (θ) and corresponding maximum shear strain range $(\Delta\gamma_{max})$ that define the maximum shear strain range plane.

3) Compute the normal strain ranges and corresponding stress ranges $(\Delta\varepsilon \; and \; \theta)$ for the 90° + θ plane and identify the critical plane orientation based on the larger normal strain range (θ_{cr})

4) Locate the two adjacent turning points on the critical plane for the maximum shear strain range and mark them as $Tmin_\gamma$ and $Tmax_\gamma$.

5) Calculate the normal strain excursion $(\Delta\varepsilon^*)$ and the maximum normal stress $(\sigma^*_{n,max})$ between the two turning points on the critical plane using Equations 4.1 and 4.3, respectively.

6) Determine the maximum shear stress (τ_{max}) on the critical plane using Equation 4.4.

7) Repeat steps 1) to 6) until all counted reversals have been processed.

4.3 Critical plane evaluation

In order to calculate the damage parameter and determine their corresponding plane orientations, the formulation of each critical plane model discussed in section 2.5.7 were utilized. The results in this study were evaluated from various plane orientations ranging from -90° to 90°. The critical plane, defined as the plane experiencing the highest level of damage, was then identified. In this evaluation, four comparative critical plane models, namely SWT, Brown-Miller, Fatemi-Socie and Liu, were considered, with the primary normal and shear stress values for all cases, presented in Table 4.4.

The MESA results conducted in this study were evaluated in all same conditions listed previously for all cases. In order to run the analysis, the MESA values for each loading path were estimated and presented in Figures 4.2 to 4.6.

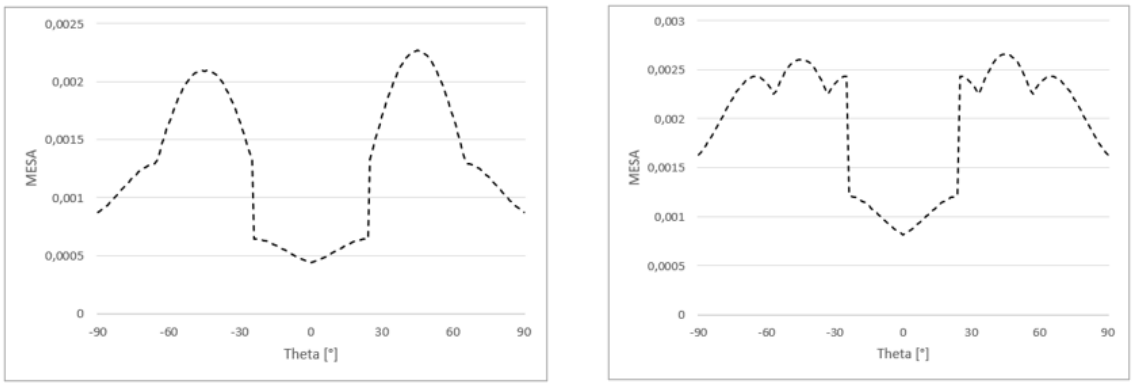

A) **B)**

FIGURE 4.2 MESA DAMAGE PARAMETER PROGRESSION THROUGH ALL PLANE ORIENTATIONS: A) CASE 1 (LEFT) AND B) CASE 2 (RIGHT)

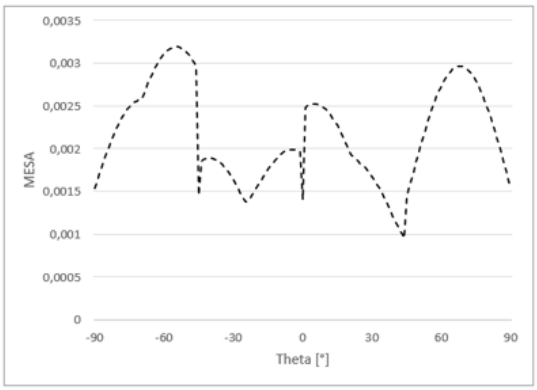

A)

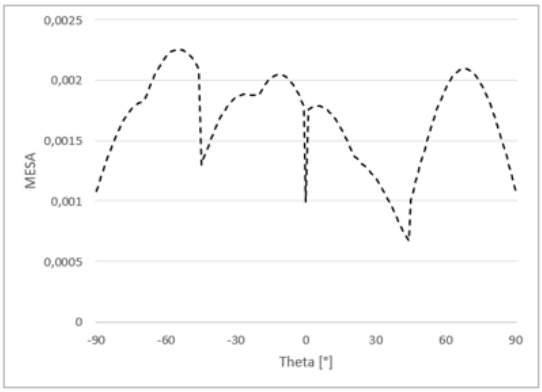

B)

FIGURE 4.3 MESA DAMAGE PARAMETER PROGRESSION THROUGH ALL PLANE ORIENTATIONS: A) CASE 3 (LEFT) AND B) CASE 4 (RIGHT)

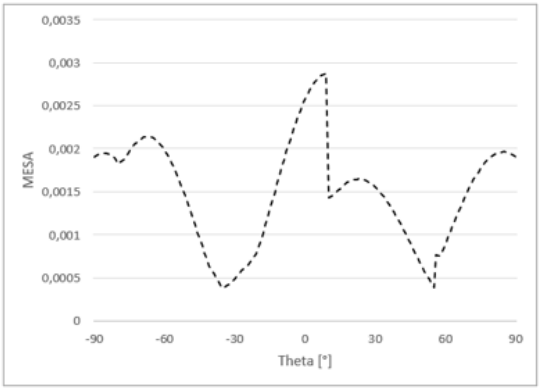

A)

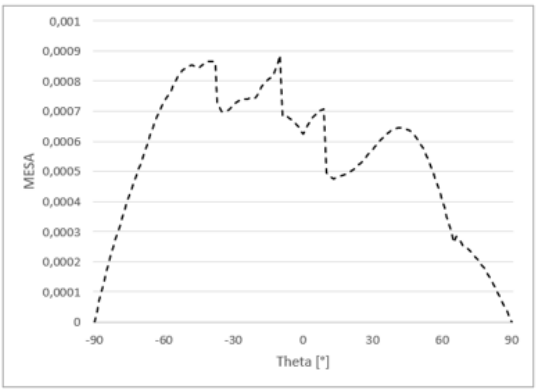

B)

FIGURE 4.4 MESA DAMAGE PARAMETER PROGRESSION THROUGH ALL PLANE ORIENTATIONS: A) CASE 5 (LEFT) AND B) CASE 6 (RIGHT)

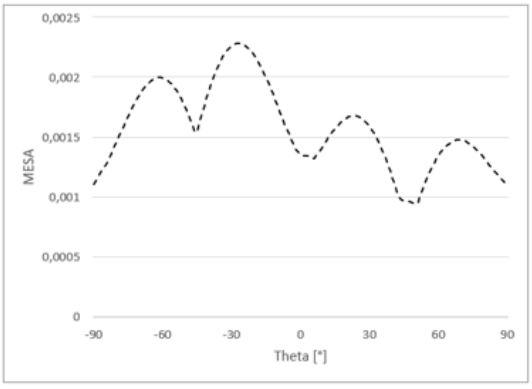

A)

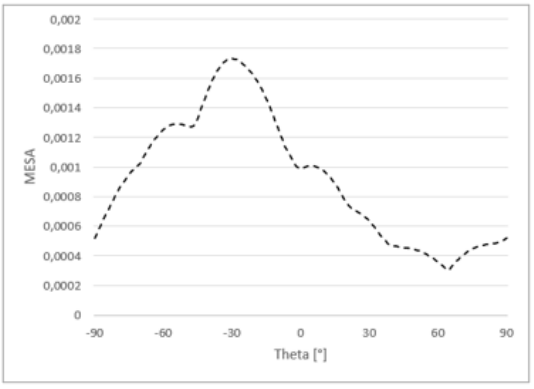

B)

FIGURE 4.5 MESA DAMAGE PARAMETER PROGRESSION THROUGH ALL PLANE ORIENTATIONS: A) CASE 7 (LEFT) AND B) CASE 8 (RIGHT)

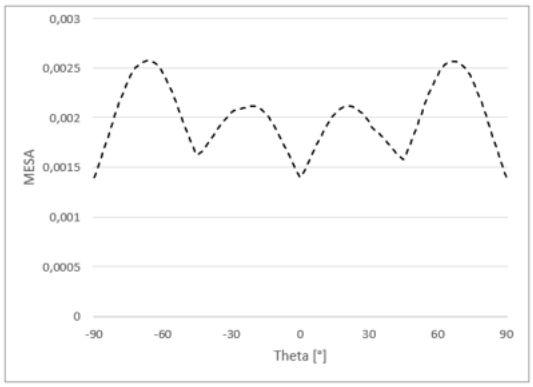

A)

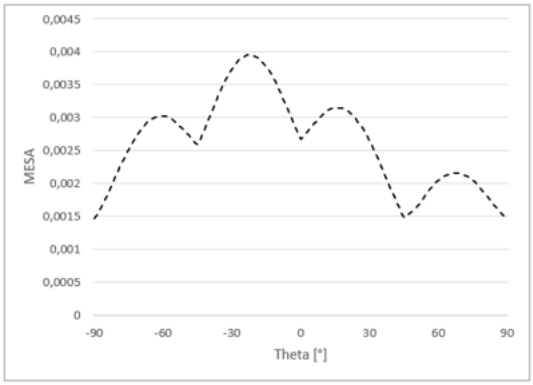

B)

FIGURE 4.6 MESA DAMAGE PARAMETER PROGRESSION THROUGH ALL PLANE ORIENTATIONS: A) CASE 9 (LEFT) AND B) CASE 10 (RIGHT)

Table 4.3 summarizes the critical plane estimations and critical plane experimental results from loading cases 1 through 10.

TABLE 4.3 – CRITICAL PLANE ESTIMATIONS AND EXPERIMENTAL RESULTS

Case	SWT (°)	F-Socie (°)	B-Miller	Liu	MESA (°)	Experiment (°)
1	0	0	±90; 0	0	45	-5
2	±45	0	±90; 0	±45	45	0
3	±25	±21	±22; ±68	±27	-55	29
4	±25	±21	±22; ±68	±28	-55	31
5	0	0	±90; 0	5	9	0
6	-7	31	-55; 35	-14	-10	-22
7	41	6	-13; 77	-34	-27	-19
8	23	9	-79; 11	-37	-30	-6
9	±26	±18	±20; ±70	±24	-67	-18
10	±24	±22	±22; ±68	±21	-22	-23

Case 1 is a sequential loading where a sinusoidal axial load is followed by a sinusoidal shear load $\sqrt{3}$ times less than the axial one. Considering the critical plane estimation calculated without accumulated damage approach, the SWT, F-Socie, Brown-Miller and Liu critical plane estimations were 0° which are in close accordance with the experimental result -5°. The MESA approach however drew poor results identifying the critical plane at 45°.

Case 2 is a sequential loading block like the loading in case 1 with the particularity that the shear stress amplitude is now greater than the axial one. The SWT, Liu and MESA critical plane estimation is ±45° whereas in F-Socie and Brown-Miller identify the critical plane as 0°, in accordance with the experimental results.

Case 3, which is composed of several proportional loading branches, with different sequential loading paths is shown to have its experimental critical plane situated at 29°. SWT results show that the greatest accumulated damage occurs at ±25°, F-Socie at ±21°, Brown-Miller at ±22° and Liu at ±27° which are fairly accurate with the experimental critical plane results. Meanwhile, the MESA approach shows the greatest damage occurred at -55° which greatly differs from the 25°.

Case 4 loading block is similar to the loading in case 3 but with a different loading sequence. Experimental results of loading case 4 show the crack initiation plane occurs at 31°. The critical plane estimations without accumulative damage approach were ±25° in SWT, ±21° in F-Socie, ±22° in Brown-Miller and ±28° in Liu. Alike case 3, the MESA approach presents the same value of -55°. From the results, it can be concluded that the loading sequence change between cases 3 and 4 do not affect the critical plane estimation and experimental crack initiation direction.

Case 5 loading block is composed of several proportional loading branches with different stress amplitude ratios (SAR). Experimental results show that crack initiation plane occurs at 0°. Critical plane results obtained without a damage accumulation approach estimates the critical plane direction at 0° in SWT, F-Socie and Brown-Miller criteria. However, Liu and MESA show slightly close results with 5° and 9° respectively.

Case 6 is similar to Case 5. The difference between them is related to the load sequence. Estimations for the critical plane directions were -7° for SWT, 31° for F-Socie, -55°/35° for Brown-Miller, -14° for Liu and -10° for MESA. These results show significant variation from the experimental critical plane identified which was -22°.

Cases 7 and 8 are asynchronous loading blocks, where the shear stress frequency is five times greater than the axial one. The difference between these two loading blocks is based on the stress amplitude ratio (SAR) between shear and axial stress components. The block's SAR was 2 for Case 7 and 0.5 for Case 8. In loading case 8 the axial stress amplitude is greater than the shear stress amplitude, i.e. axial damage predominates over the shear one. In Case 7 the opposite occurs, i.e. the shear damage predominates over the

axial one. In this case, the shear stress amplitude is twice the axial one. Experimental results show -19° and -6° for crack initiation directions in Cases 7 and 8, respectively. Critical plane estimations without using a damage accumulation criterion were, in Case 7, 41° in SWT, 6° in F-Socie, -13°/77° in Brown-Miller, -34° in Liu and -27° in MESA criteria. Moreover, in Case 8, the critical plane estimations were 23° for SWT, 9° for F-Socie, -79°/11° for Brown-Miller, -37° for Liu and -30° for MESA.

Lastly, loading cases 9 and 10 loading blocks are asynchronous loadings where the shear stress frequency is twice the axial one in Case 9 and in Case 10 the axial stress frequency is twice the shear one. Regarding Case 9, critical plane estimations without an accumulative damage approach were ±26° in SWT, ±18° in F–Socie, ±20° in Brown-Miller, ±24° in Liu which are the same or in very close proximity of the experimental result obtained for the critical plane, -18°. The MESA approach however shows a big variation when compared to this measured value with -67°. Conversely, Case 10 identifies the experimental critical plane orientation as being -23°. This goes in accordance with all approaches used with SWT identifying it as ±24, F-Socie and Brown-Miller with ±22, Liu with ±21 and MESA with -23°.

Upon comparing the estimated critical plane angles with the experimental results for all 10 cases, it is evident from Table 5 that the MESA approach yields a poor prediction for the critical plane orientation. Since the dominant failure mechanism in 42CrMo4 is shear stress-induced nucleation and crack growth, it is anticipated that the Fatemi-Socie and Brown-Miller models, which emphasize shear stress, perform well. Among the critical plane models examined, both Fatemi-Socie and Brown-Miller approaches demonstrate superior predictive capability, followed by Liu, SWT and lastly MESA with the poorest predictive capability.

4.3.1 S-N results and correlation

Table 4.4 displays the outcomes of the fatigue life experiments for the chosen loading blocks. The labels "Normal" and "Shear" in Table 6 correspond to the maximum stress values in the axial and shear loading channels, respectively. The parameter N_f represents the number of cycles until failure, and (ro) indicates a run-out test, which translates to interrupting the test when the specimen reached one million cycles, as there is a high probability of the specimen having infinite life under those conditions.

TABLE 4.4 – 42CRMO4 FATIGUE LIFE RESULTS

	Normal	Shear	N_f						
			Brown-Miller	F-Socie	SWT	Liu I	Liu II	MESA	Experiment
Case 1	610	352	1335	1339	51692	3257	23180	7412	24722
	600	346	1389	1466	62194	3665	28683	8941	30058
	570	329	1572	1958	113673	5374	57009	16466	58703
	520	300	1971	3384	371812	11447	212270	54494	176793
	495	286	2231	4617	736743	17948	445403	108788	265955
	480	277	2412	5641	1147619	24187	714366	170007	271243
	445	257	2932	9421	3545106	53633	2338295	529995	892629
	420	243	3414	14213	8713503	104886	5876846	1299585	1000000 (ro)
Case 2	375	433	1189	882	5428284	3607	44900	10242	121014
	360	416	1309	1070	10123667	4849	78184	16607	337186
	345	398	1454	1331	20301252	6850	146493	28938	518622
	305	352	1965	2544	145249545	20233	939079	159309	1000000 (ro)
Case 3	450	260	1280	1622	117075	12055	197901	32805	21485
	440	254	1351	1840	154337	14765	276508	44265	32374
	435	251	1388	1964	178239	16412	328349	51692	41060
	415	240	1556	2583	331460	25882	673550	99771	128000
	405	234	1651	2990	462568	33208	983166	141780	181991
	395	228	1756	3483	655878	43292	1453747	204612	427877
Case 4	420	243	1511	2407	282491	22978	560165	84178	34807
	415	240	1556	2583	330123	25882	673550	99751	53246
	410	237	1602	2777	390892	29261	812463	118679	86669
	400	231	1702	3224	549657	37837	1193580	169991	115474
	395	228	1756	3483	656010	43292	1453747	204613	119252
	380	219	1932	4439	1143850	66592	2679286	365367	231943
	370	214	2065	5269	1692047	90879	4096214	548630	282332
Case 5	552	318	1701	2360	169468	6922	89242	18568	26509
	540	312	1795	2689	224420	8288	122202	24519	82293
	520	300	1971	3384	371512	11447	212270	40213	461232
	490	283	2289	4930	852105	19774	520148	91333	733273
Case 6	520	300	4393	11806	930690	312059	3271817	69897709	36102
	493	285	5095	17443	2044266	650466	7677839	163371117	76297
	487	281	5274	19115	2456829	774001	9349158	203129039	90993
	466	270	5979	26733	4802293	1468010	19044174	401190973	117530
	441	255	7020	41165	11344408	3357925	46575554	1007872074	464214
Case 7	194	388	1759	1832	3947666	7314	1242431	8247	35003
	184	368	2005	2426	8981621	11447	2863705	15401	47934
	175	350	2274	3199	19648626	18097	6378451	29023	79496
	160	321	2840	5284	79268912	43516	25778290	95132	133058
	143	287	3820	10609	487133150	161836	159341289	499667	1000000 (ro)
Case 8	479	240	4127	9292	13178059	703803	178960152	33844	4088
	463	232	4530	11879	22414330	1146558	311387635	53415	10719
	434	217	5454	19534	63992386	3093166	918539730	135537	37031
	399	200	6914	37240	246332897	10974027	3535958376	464506	99052
	347	173	10711	123224	2442679945	110000857	37017576228	4356013	558219
Case 9	470	271	1541	2465	439432	18353	261303	41426	38487
	465	269	1582	2625	509057	20334	306773	47859	52836
	455	263	1668	2989	690350	25175	426304	64504	86000
	440	254	1811	3667	1117457	35492	712974	103440	127693
	430	248	1917	4232	1573115	45383	1018752	144134	265312
	420	248	2033	4914	2234035	58886	1472380	203589	803827
Case 10	510	294	1309	1634	78008	6791	99365	1906	12116
	480	277	1515	2315	163229	11301	240725	3122	41466
	460	266	1681	2986	283562	16619	457466	5263	93247
	440	254	1875	3932	519306	25554	907450	8683	200489
	435	251	1929	4227	606880	28680	1084316	9930	421814
	430	248	1985	4551	714037	32297	1299251	11401	692953

Figures 4.7 through 4.18 illustrate the correlation between theoretical estimations for the criteria utilized and experimental results. The comparison is made for SWT, Fatemi-Socie, Brown-Miller, Liu I and II, and MESA criteria.

Upon further analysis of Figures 4.7 to 4.18, it is evident that the MESA approach produces significantly better results for the estimating fatigue life than other critical plane criteria, even despite having some results exceed the boundary line in cases 2, 6, 9 and 10. This may be due to SWT, Fatemi-Socie, Brown-Miller and Liu approaches not being necessarily developed with the purpose of analysing variable amplitude loading defined by loading blocks, which have different properties such as having different directions over time. Seeing as these critical plane models are not equipped to handle the variations that are imbued in these variable amplitude loadings, the correlation between theoretical estimations and experimental results are justifiably skewed and/or poor.

However, the MESA critical plane approach was indeed able to achieve satisfactory results above the rest. Being a proposed critical plane model, it isn't traditionally expected to have a great performance while evaluating fatigue life prediction. Nonetheless, most of the points illustrated in Figures 4.7 and 4.8 are shown within the boundary lines in all reviewed cases with a fatigue life factor of 3. This may be due to a damage accumulation capability that the rest of the models don't have incorporated.

Both the Brown-Miller and Fatemi-Socie models exhibit a strikingly similar estimation of fatigue life, with both yielding overly conservative results when compared to the experimental data. This indicates that both models generate a higher damage parameter than anticipated, resulting in an inaccurate assessment of the damage incurred by the variable amplitude loading block.

In contrast, the SWT model yields non-conservative results by predicting an infinite fatigue life, despite the observed failure in the experimental fatigue life. This discrepancy can be attributed to the model producing a smaller damage parameter than expected, leading to an inaccurate evaluation of the damage experienced by the variable amplitude loading block.

Finally, among the models discussed excluding MESA, Liu I and Liu II demonstrate superior results. However, Liu II outperforms Liu I due to its emphasis on

shear stress, whereas Liu I, which focuses on normal stress-based criteria, yields fewer results within the specified bounds.

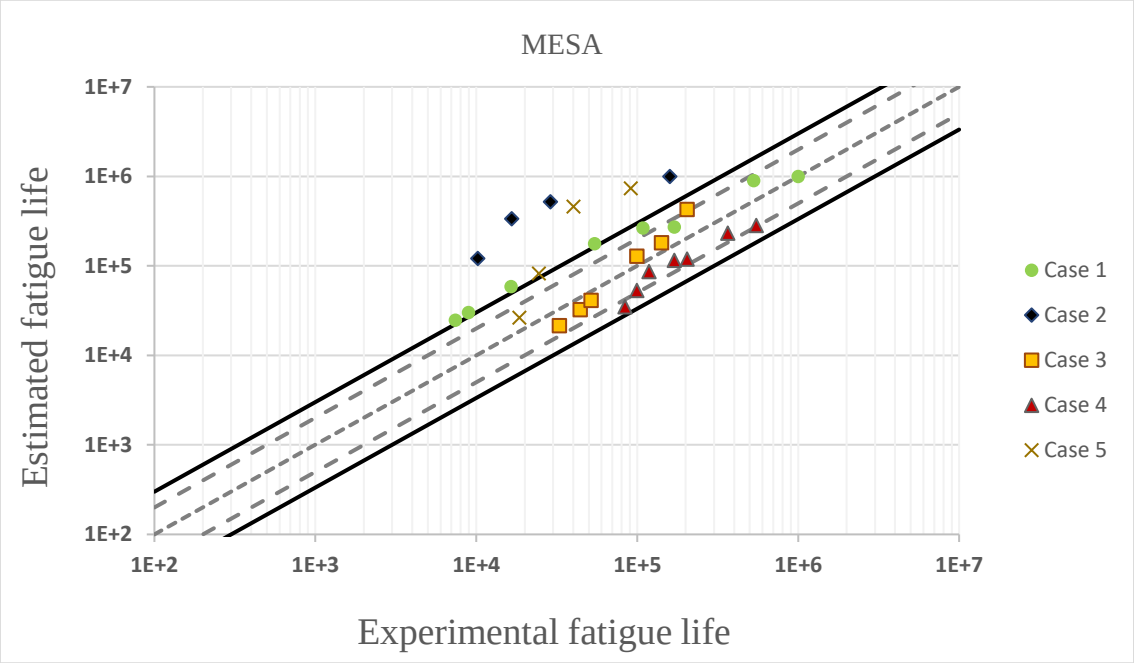

FIGURE 4.7 MESA FATIGUE LIFE CORRELATION BETWEEN EXPERIMENTAL FATIGUE AND ESTIMATED FATIGUE (CASE 1 TO CASE 5)

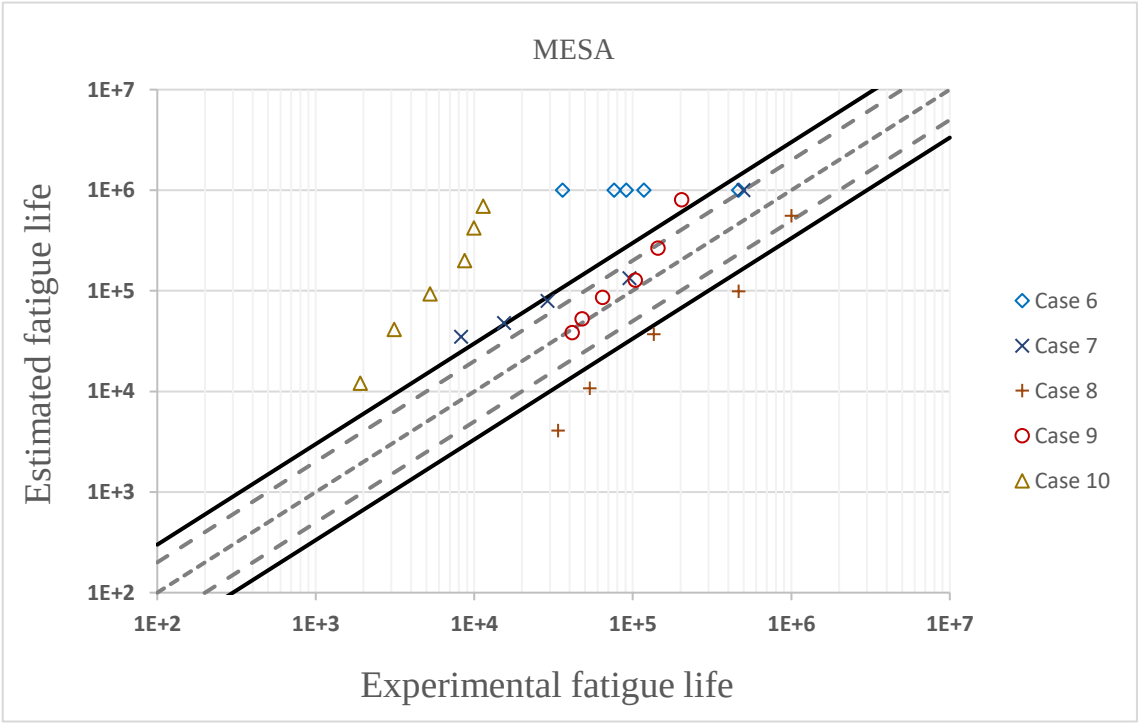

FIGURE 4.8 MESA FATIGUE LIFE CORRELATION BETWEEN EXPERIMENTAL FATIGUE AND ESTIMATED FATIGUE (CASE 6 TO CASE 10)

FIGURE 4.9 BROWN-MILLER FATIGUE LIFE CORRELATION BETWEEN EXPERIMENTAL FATIGUE AND ESTIMATED FATIGUE (CASE 1 TO CASE 5)

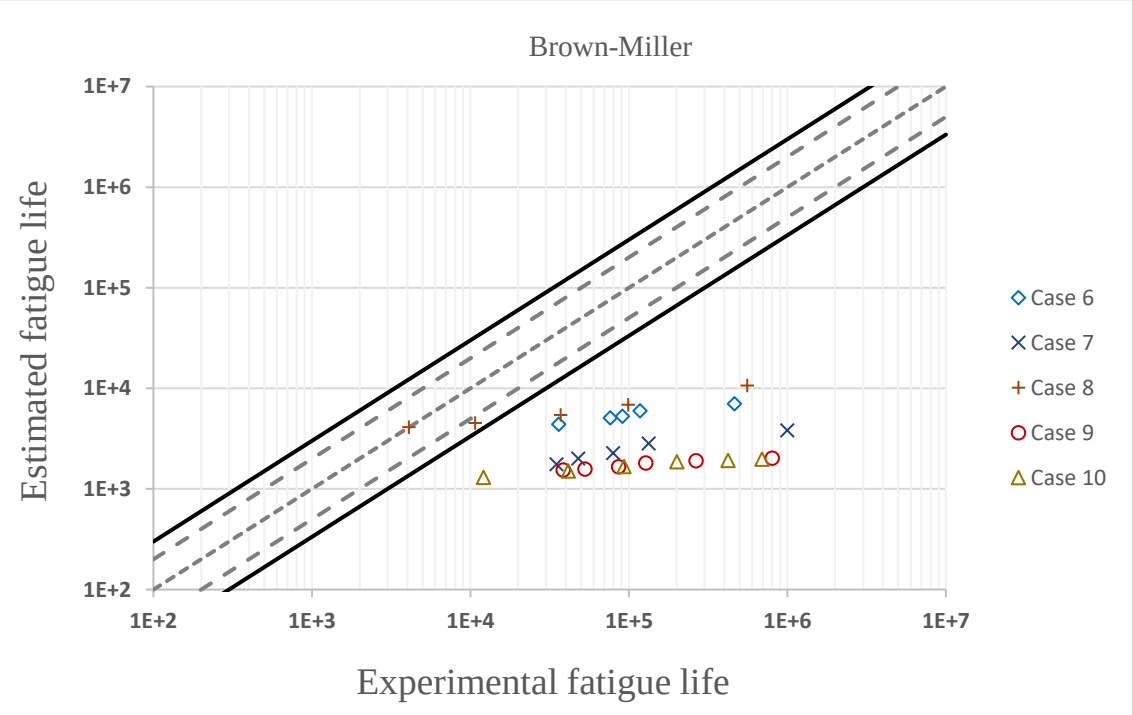

FIGURE 4.10 BROWN-MILLER FATIGUE LIFE CORRELATION BETWEEN EXPERIMENTAL FATIGUE AND ESTIMATED FATIGUE (CASE 6 TO CASE 10)

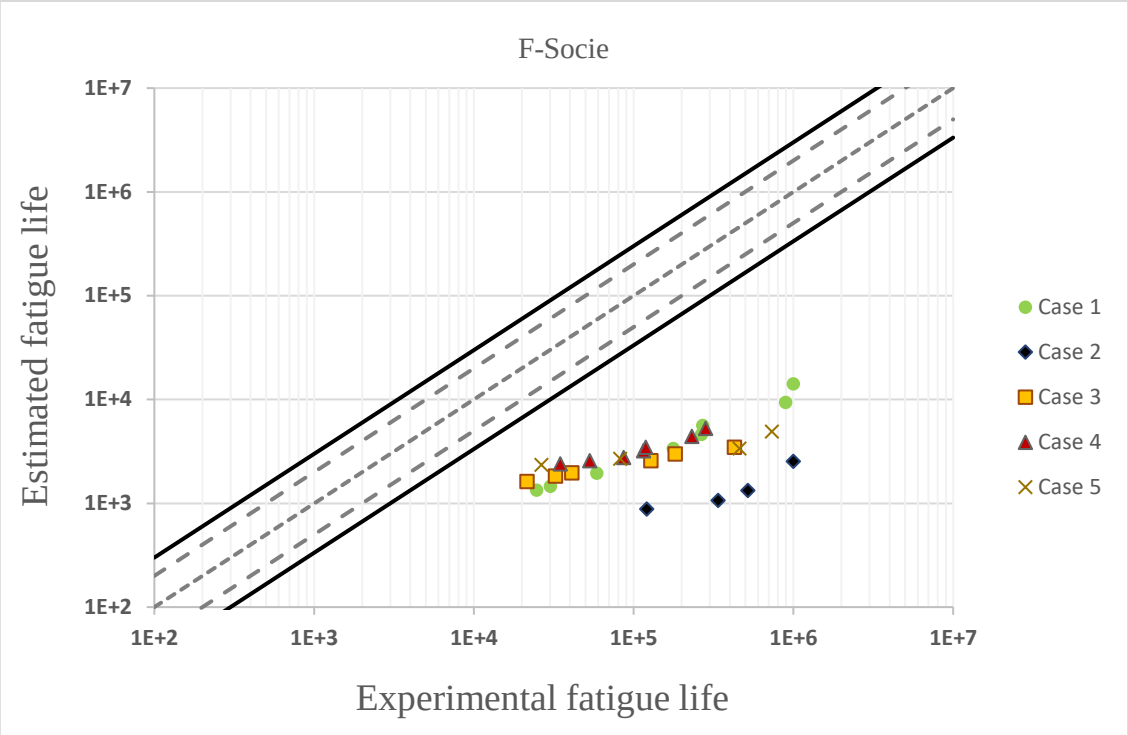

FIGURE 4.11 F-SOCIE FATIGUE LIFE CORRELATION BETWEEN EXPERIMENTAL FATIGUE AND ESTIMATED FATIGUE (CASE 1 TO CASE 5)

FIGURE 4.12 F-SOCIE FATIGUE LIFE CORRELATION BETWEEN EXPERIMENTAL FATIGUE AND ESTIMATED FATIGUE (CASE 6 TO CASE 10)

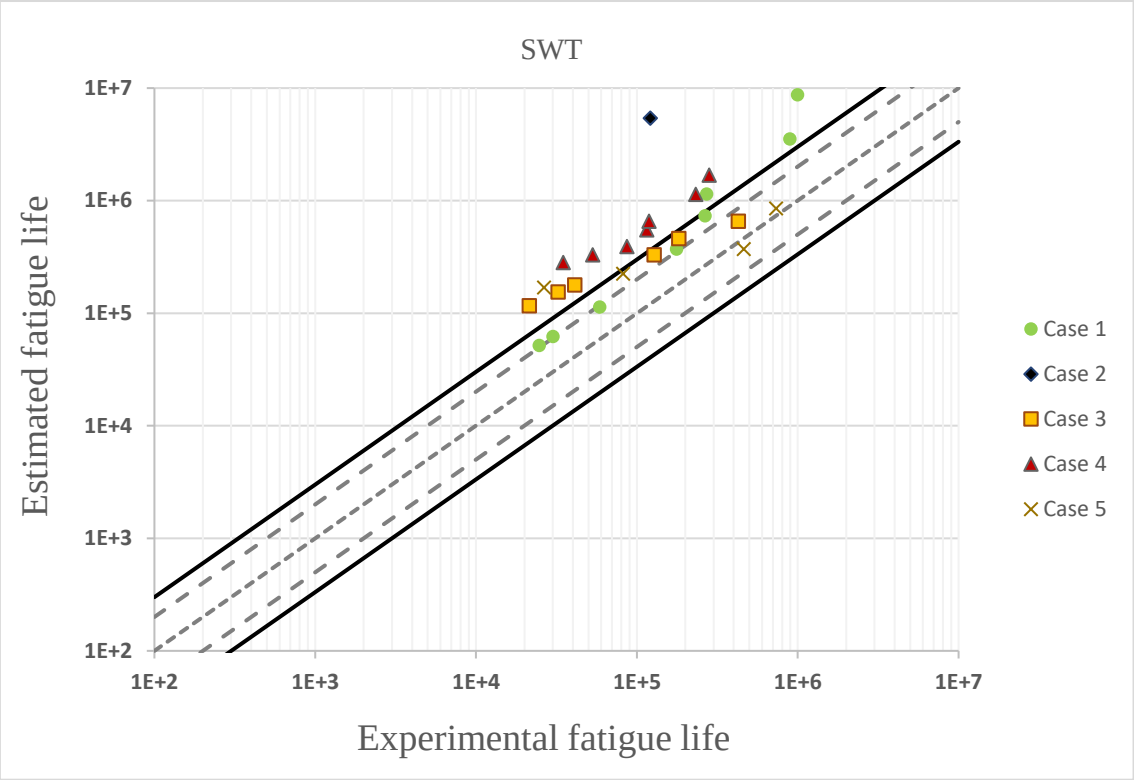

FIGURE 4.13 SWT FATIGUE LIFE CORRELATION BETWEEN EXPERIMENTAL FATIGUE AND ESTIMATED FATIGUE (CASE 1 TO CASE 5)

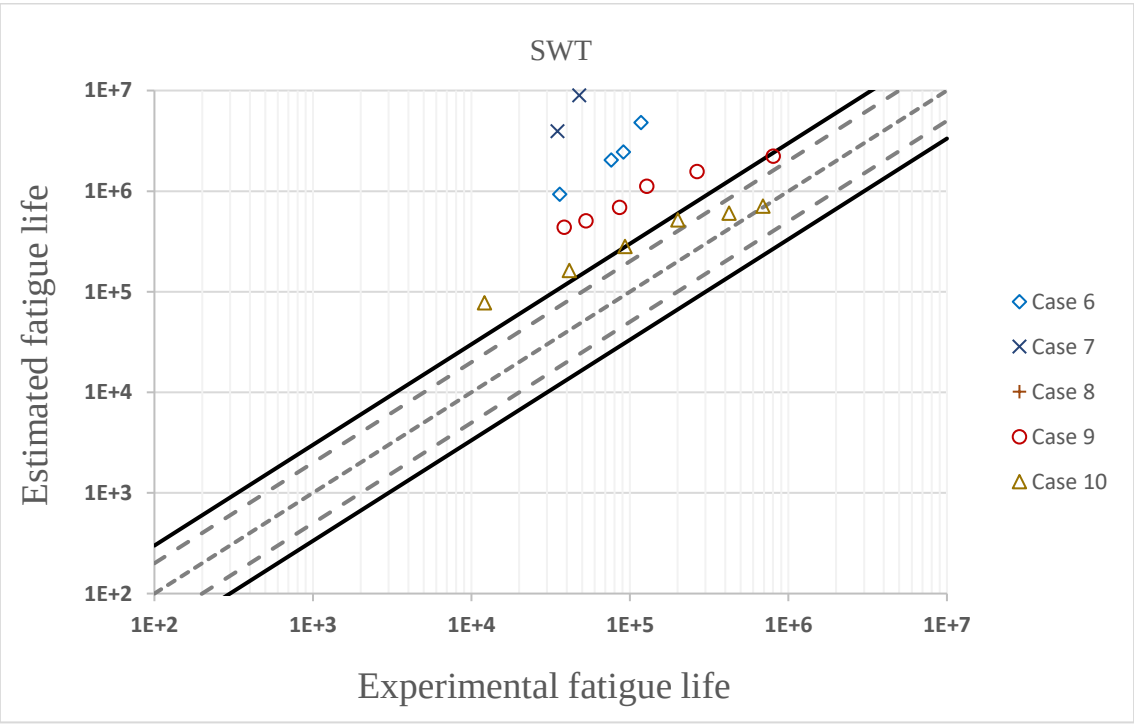

FIGURE 4.14 SWT FATIGUE LIFE CORRELATION BETWEEN EXPERIMENTAL FATIGUE AND ESTIMATED FATIGUE (CASE 6 TO CASE 10)

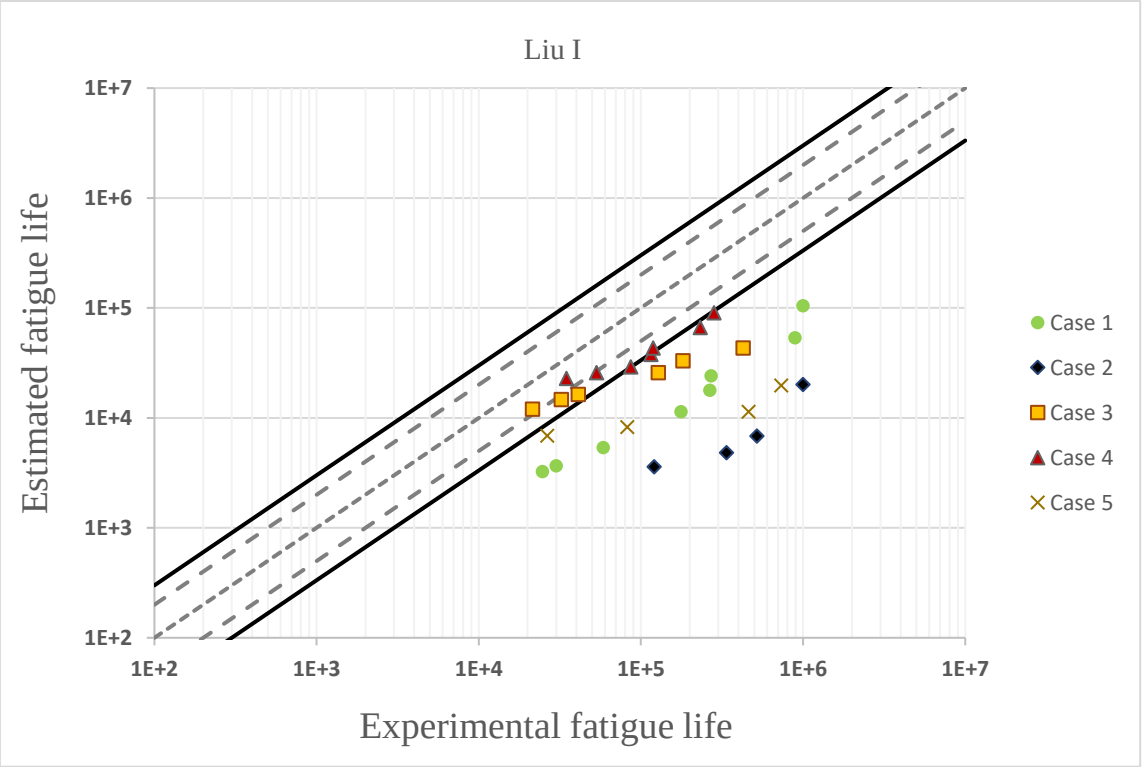

FIGURE 4.15 LIU I FATIGUE LIFE CORRELATION BETWEEN EXPERIMENTAL FATIGUE AND ESTIMATED FATIGUE (CASE 1 TO CASE 5)

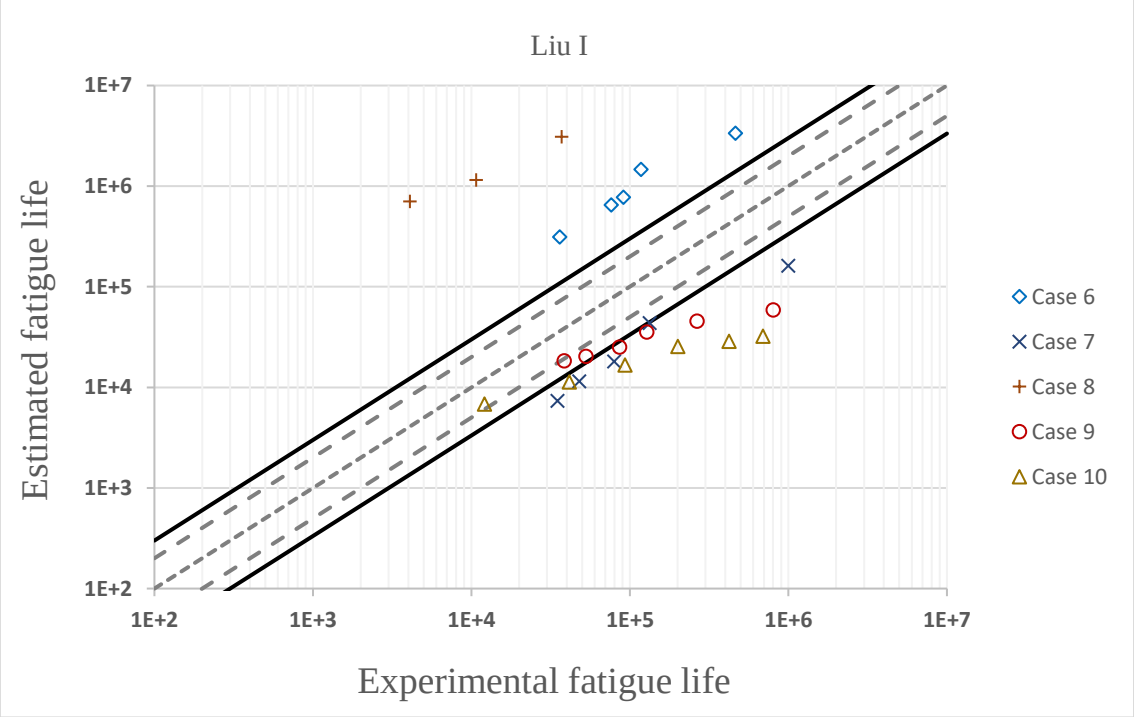

FIGURE 4.16 LIU I FATIGUE LIFE CORRELATION BETWEEN EXPERIMENTAL FATIGUE AND ESTIMATED FATIGUE (CASE 6 TO CASE 10)

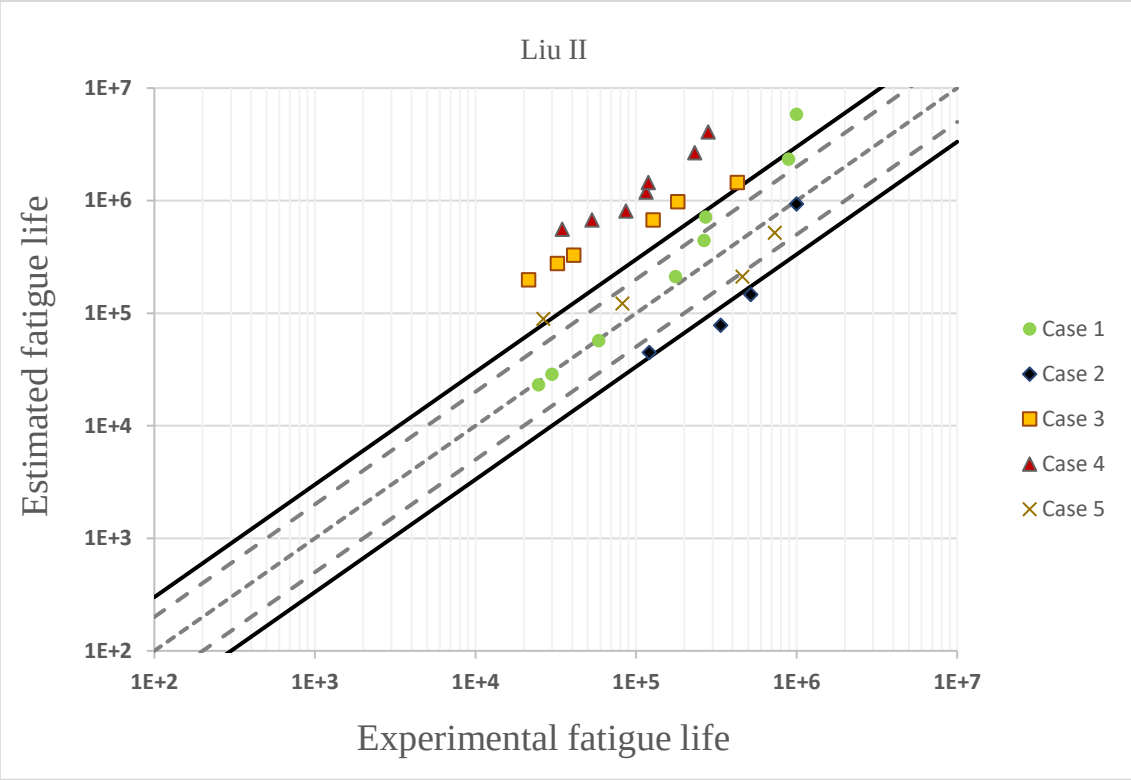

FIGURE 4.17 LIU II FATIGUE LIFE CORRELATION BETWEEN EXPERIMENTAL FATIGUE AND ESTIMATED FATIGUE (CASE 1 TO CASE 5)

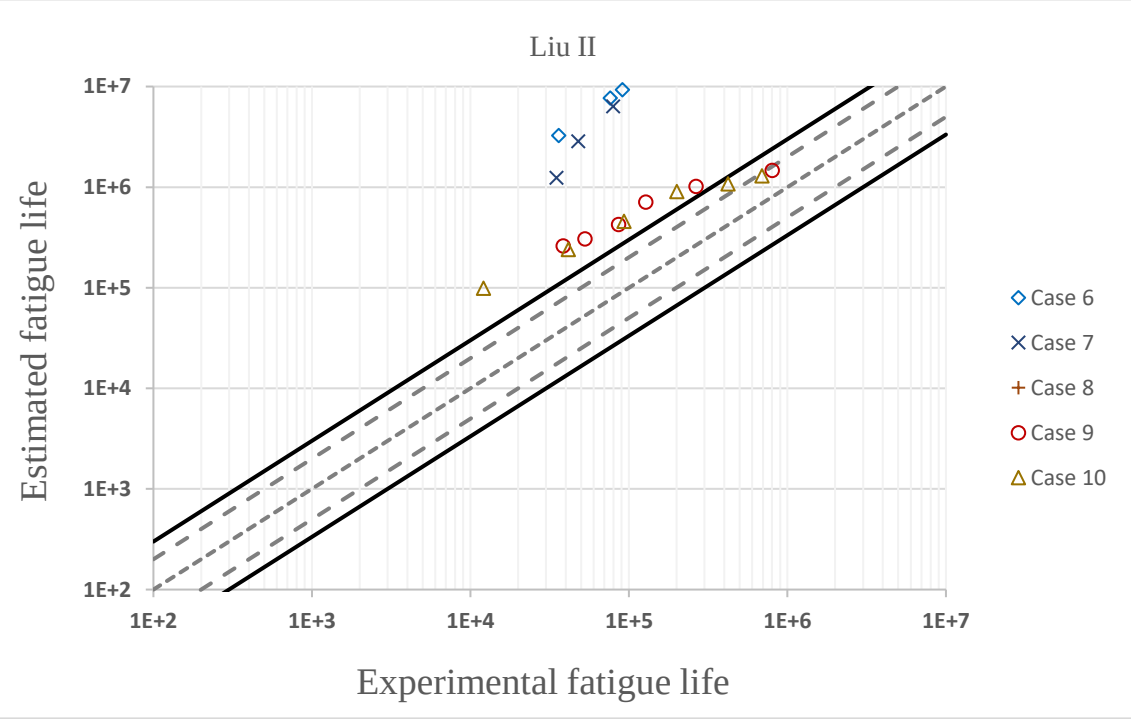

FIGURE 4.18 LIU II FATIGUE LIFE CORRELATION BETWEEN EXPERIMENTAL FATIGUE AND ESTIMATED FATIGUE (CASE 6 TO CASE 10)

5 . Conclusions and future work

This dissertation involved conducting a comprehensive review of multiaxial fatigue literature. The review encompassed fundamental concepts of fatigue, critical plane models, cycle counting methods, and well-known linear and nonlinear damage accumulation methods. Within the literature review, particular emphasis was placed on exploring the Modified Equivalent Strain Amplitude (MESA) approach. Subsequently, various analyses were conducted on bibliography regarding subjects such as multiaxial fatigue and damage accumulation, multiaxial cycle counting, proportional and nonproportional loading, variable amplitude loading and critical plane models for the purpose of better understanding the current significance this subject area. Not only does this analysis provide a clear picture of rising interest in knowledge related to fatigue development and causes but also encourages the engineering community to tackle these subjects in a much more informed manner.

Based on the findings presented in Chapter 3, several conclusions can be drawn:

- The country with the largest publication output is the People's Republic of China with 1434 documents published across all the subjects mentioned, followed by the USA and Germany. Other countries are sometimes linked (directly or indirectly) to one of the main countries that are publishing the most scientific documents, thus the data showed that cooperation between authors and countries is mediocre due to never really knowing for certain the author's country of origin. Interestingly, Portugal consistently emerges as a significant contributor in publications related to the topic of fatigue, ranking amongst the top 15 countries in terms of publishing and researching in this field.
- There has been an exponential growth trend in publications related to investigating fracture and fatigue mechanics and its intricacies in the last twenty-three years, most likely due to product innovation and trying to reduce the probability of failure of components or assemblies. From either a preventive or corrective maintenance standpoint, both stand to gain significant benefit from a deeper understanding of the subject.
- Although the majority of authors, approximately 68%, have only been credited in a single publication, more than 10 scientific papers on topics like multiaxial

fatigue and damage accumulation methods have been published by 49 countries. This represents nearly half of the countries involved in researching these subjects, indicating a wide range of nationalities contributing to the field.

However, there are potential drawbacks of this study that can lead to minimally skewed results like the possibility of misleading citation analysis, where authors may cite certain publications negatively or engage in self-citations. Furthermore, the study limitations are associated with the selected timeline. If a similar study were conducted at a different time, the results would vary slightly due to the constant updating of the Google Scholar database with newer scientific documents. Additionally, significant publications may receive "delayed recognition" in the scientific literature, being cited after several years. These limitations should be considered in future studies.

While evaluating the impact of fatigue life estimates on different planes by conducting experimental tests on several loading blocks for various orientations it is possible to draw the following conclusions based on the contents of Chapter 4:

- Based on the investigation carried out regarding the implementation of the MESA critical plane model, it can be inferred that contrary to initial expectations, the model demonstrates relatively unsatisfactory performance in estimating the crack initiation plane. However, it exhibits excellent accuracy in predicting fatigue life compared to the other analysed critical plane models, especially without the application of cycle counting methods.
- Failing to employ cycle counting techniques, account for accumulated damage while ignoring the loading trajectory and traditional models leads to the inaccurate estimation of infinite fatigue life instead of the anticipated finite life, evidenced in most cases.
- The MESA critical plane model can be deemed well-suited for practical use in mechanical design and the development of crucial mechanical components. It enables precise estimation of fatigue life and facilitates a more accurate determination of the necessary safety factor for component operation.

Due to variations in the loading trajectory, different outcomes of fatigue life are determined, emphasizing how insufficient the sole consideration of the amplitude in multiaxial fatigue really is. With the exception of MESA, the remaining critical plane models addressed were designed for application with constant amplitudes in both the

normal and shear stress components. These models do not account for the varying damage that occurs, emphasizing the necessity of extracting cycles from the loading block and conducting individual analysis to achieve a more thorough comprehension.

5.1 Future work

Furthermore, it was observed while calculating the damage parameters of SWT, Liu I, and Liu II models, that utilizing the Young's modulus in GPa instead of MPa yielded improved results. To investigate further, it is suggested further exploration on whether the original model offers any recommendations regarding this modification. From a scientific standpoint, it is reasonable for the Young's modulus to be of a similar magnitude as σ_f' , considering the latter is measured in MPa. The book "Multiaxial Fatigue" by F. Socie [15] does not provide any indications in this regard, making it worthwhile to conduct a study to confirm if this is an isolated occurrence or if there might be a misinterpretation of the formula by the author.

To calculate the fatigue life for each model, parameter estimates were derived from various formulas. While some parameters were sourced from existing literature, others had to be approximated, leading to possible deviations. This limitation holds substantial importance for future experiments, as it carries the potential to significantly influence and modify the obtained results.

Lastly, an additional aspect to consider is that by validating the Excel method, the automation of this approach can be facilitated allowing for the seamless implementation of the entire methodology or algorithm in Excel, Python, or Matlab scripts. Automating this approach will expedite the process of acquiring the damage surface for various orientations, enabling the quick identification of the plane with the highest or lowest damage.

References

[1] Dowling NE. Mechanical behavior of materials: engineering methods for deformation, fracture, and fatigue. 4th ed. Boston: Pearson; 2013.

[2] Callister WD, Rethwisch DG. Fundamentals of materials science and engineering: an integrated approach. 5th edition. Hoboken, NJ: John Wiley & Sons, Inc.; 2019.

[3] Campbell G, Lahey R. A survey of serious aircraft accidents involving fatigue fracture. International Journal of Fatigue 1984;6:25–30. https://doi.org/10.1016/0142-1123(84)90005-7.

[4] Rossmanith HP. George Rankin Irwin-The Father of Fracture Mechanics 1907-1998. Fragblast 1998;2:123–41. https://doi.org/10.1080/13855149809408882.

[5] Lampman SR, editor. ASM handbook. Volume 19: Fatigue and fracture / Steven R. Lampman, technical editor [und 6 weitere]. Materials Park, OH: ASM International; 1996.

[6] Hillmansen S, Smith R. Assessing fatigue crack growth in railway axles. 11th International Conference on Fracture 2005, ICF11 2005;8.

[7] Smith RA. Fatigue of railway axles: A classic problem revisited. European Structural Integrity Society, vol. 26, Elsevier; 2000, p. 173–81. https://doi.org/10.1016/S1566-1369(00)80049-7.

[8] Railway Axle n.d. https://en.wikipedia.org/wiki/Versailles_rail_accident (accessed April 6, 2023).

[9] Fuchs HO, Stephens RI, Saunders H. Metal Fatigue in Engineering (1980). Journal of Engineering Materials and Technology 1981;103:346–346. https://doi.org/10.1115/1.3225026.

[10] VI. The fracture of metals under repeated alternations of stress. Phil Trans R Soc Lond A 1903;200:241–50. https://doi.org/10.1098/rsta.1903.0006.

[11] O. H. Basquin. The exponencial law of endurence tests. vol. 10, pp. 625–630. American Society of Testing Materials; 1910.

[12] Zenner H. Multiaxial fatigue–methods, hypotheses and applications. Materials Testing 2005. https://doi.org/10.3139/120.100655.

[13] Lee Y-L, editor. Fatigue testing and analysis: theory and practice. Amsterdam ; Boston: Elsevier Butterworth-Heinemann; 2005.

[14] Schijve J. Fatigue of Structures and Materials. Dordrecht: Springer Netherlands Springer e-books; 2009.

[15] Socie DF, Marquis G. Multiaxial Fatigue. Warrendale, PA, EUA: Society of Automotive Engineers; 2000.

[16] Anes V, Reis L, Li B, Fonte M, Freitas MD. New approach for analysis of complex multiaxial loading paths. International Journal of … 2014.

[17] Cui W. A state-of-the-art review on fatigue life prediction methods for metal structures. Journal of Marine Science and Technology 2002;7:43–56. https://doi.org/10.1007/s007730200012.

[18] Meyers MA, Chawla KK. Mechanical Behavior of Materials n.d https://www.cambridge.org/9780521866750.

[19] Paul SK. Prediction of non-proportional cyclic hardening and multiaxial fatigue life for FCC and BCC metals under constant amplitude of strain cycling. Materials Science and Engineering: A 2016;656:111–9. https://doi.org/10.1016/j.msea.2016.01.029.
[20] Borodii M, Shukaev S. Additional cyclic strain hardening and its relation to material structure, mechanical characteristics, and lifetime. International Journal of Fatigue 2007;29:1184–91. https://doi.org/10.1016/j.ijfatigue.2006.06.014.
[21] Anes V, Reis L, Li B, De Freitas M. New approach to evaluate non-proportionality in multiaxial loading conditions: NON-PROPORTIONALITY IN MULTIAXIAL FATIGUE. Fatigue Fract Engng Mater Struct 2014;37:1338–54. https://doi.org/10.1111/ffe.12192.
[22] Anes V, Reis L, Li B, de Freitas M. New cycle counting method for multiaxial fatigue. International Journal of Fatigue 2014;67:78–94. https://doi.org/10.1016/j.ijfatigue.2014.02.010.
[23] Xia T, Yao W. Comparative research on the accumulative damage rules under multiaxial block loading spectrum for 2024-T4 aluminum alloy. International Journal of Fatigue 2013;48:257–65. https://doi.org/10.1016/j.ijfatigue.2012.11.004.
[24] Susmel L, Tovo R, Lazzarin P. The mean stress effect on the high-cycle fatigue strength from a multiaxial fatigue point of view. International Journal of Fatigue 2005;27:928–43. https://doi.org/10.1016/j.ijfatigue.2004.11.012.
[25] Shamsaei N, Fatemi A. Small fatigue crack growth under multiaxial stresses. International Journal of Fatigue 2014;58:126–35. https://doi.org/10.1016/j.ijfatigue.2013.02.002.
[26] Wang CH, Miller KJ. THE EFFECT OF MEAN SHEAR STRESS ON TORSIONAL FATIGUE BEHAVIOUR. Fat Frac Eng Mat Struct 1991;14:293–307. https://doi.org/10.1111/j.1460-2695.1991.tb00659.x.
[27] Macha, Sonsino. Energy criteria of multiaxial fatigue failure. Fat Frac Eng Mat Struct 1999;22:1053–70. https://doi.org/10.1046/j.1460-2695.1999.00220.x.
[28] Anes V, Reis L, Li B, Freitas M. Crack path evaluation on HC and BCC microstructures under multiaxial cyclic loading. International Journal of Fatigue 2014;58:102–13. https://doi.org/10.1016/j.ijfatigue.2013.03.014.
[29] Findley WN. A Theory for the Effect of Mean Stress on Fatigue of Metals Under Combined Torsion and Axial Load or Bending. Journal of Engineering for Industry 1959;81:301–5. https://doi.org/10.1115/1.4008327.
[30] Brown MW, Miller KJ. A Theory for Fatigue Failure under Multiaxial Stress-Strain Conditions. Proceedings of the Institution of Mechanical Engineers 1973;187:745–55. https://doi.org/10.1243/PIME_PROC_1973_187_069_02.
[31] Shamsaei N, Fatemi A, Socie DF. Multiaxial fatigue evaluation using discriminating strain paths. International Journal of Fatigue 2011;33:597–609. https://doi.org/10.1016/j.ijfatigue.2010.11.002.
[32] Lieb K, Horstman R, Peters K, Enright C, Meltzer R, Bruce Vieth M, et al. Multiaxial Fatigue: A Survey of the State of the Art. J Test Eval 1981;9:165. https://doi.org/10.1520/JTE11553J.

[33] Zamrik SY, Frishmuth RE. The effects of out-of-phase biaxial-strain cycling on low-cycle fatigue: Experimental investigation shows a particular phase effect on crack growth and failure mode in the selected low-cycle-fatigue range. Experimental Mechanics 1973;13:204–8. https://doi.org/10.1007/BF02322654.
[34] Fatemi A, Socie DF. A CRITICAL PLANE APPROACH TO MULTIAXIAL FATIGUE DAMAGE INCLUDING OUT-OF-PHASE LOADING. Fat Frac Eng Mat Struct 1988;11:149–65. https://doi.org/10.1111/j.1460-2695.1988.tb01169.x.
[35] Socie DF, Shield TW. Mean Stress Effects in Biaxial Fatigue of Inconel 718. Journal of Engineering Materials and Technology 1984;106:227–32. https://doi.org/10.1115/1.3225707.
[36] Smith RN, Watson P, Topper T. A Stress-Strain Parameter for Fatigue Metals. Journal of Materials, Vol 5 1970:767–78.
[37] Liu K. A Method Based on Virtual Strain-Energy Parameters for Multiaxial Fatigue Life Prediction. In: McDowell D, Ellis J, editors. Advances in Multiaxial Fatigue, 100 Barr Harbor Drive, PO Box C700, West Conshohocken, PA 19428-2959: ASTM International; 1993, p. 67-67–18. https://doi.org/10.1520/STP24796S.
[38] Xue L, Shang D, Li D, Li L, Liu X, ... Equivalent energy-based critical plane fatigue damage parameter for multiaxial LCF under variable amplitude loading. International Journal of … 2020.
[39] Shang D, Sun G, Deng J, Yan C. Multiaxial fatigue damage parameter and life prediction for medium-carbon steel based on the critical plane approach. International Journal of Fatigue 2007.
[40] Chen H, Shang D, Tian Y, Liu J. Comparison of multiaxial fatigue damage models under variable amplitude loading. Journal of Mechanical Science and … 2012. https://doi.org/10.1007/s12206-012-0872-y.
[41] Bannantine JA, Comer JJ, Handrock JL. Fundamentals of metal fatigue analysis. Englewood Cliffs, N.J: Prentice Hall: 1990.
[42] Papuga J. Mapping of fatigue damages. Program Shell of FE-Calculation, CTU, Prague 2005.
[43] Wei Z, Dong P. A generalized cycle counting criterion for arbitrary multi-axial fatigue loading conditions. The Journal of Strain Analysis for Engineering Design 2014;49:325–41. https://doi.org/10.1177/0309324713515465.
[44] Langlais T. Multiaxial cycle counting for critical plane methods. International Journal of Fatigue 2003;25:641–7. https://doi.org/10.1016/S0142-1123(02)00148-2.
[45] Lalanne C. Mechanical Vibration & Shock: Fatigue Damage Volume IV. Hoboken, NJ, EUA: John Wiley & Sons Inc.; 2001.
[46] E08 Committee. Practices for Cycle Counting in Fatigue Analysis. ASTM International; n.d. https://doi.org/10.1520/E1049-85R17.
[47] Lee Y-L, Barkey ME, Kang H-T. Metal fatigue analysis handbook: practical problem-solving techniques for computer-aided engineering. Waltham, MA: Butterworth-Heinemann; 2012.

[48] Downing S, Socie D. Simple rainflow counting algorithms. International Journal of Fatigue 1982;4:31–40. https://doi.org/10.1016/0142-1123(82)90018-4.
[49] Wang CH, Brown MW. Life Prediction Techniques for Variable Amplitude Multiaxial Fatigue—Part 1: Theories. Journal of Engineering Materials and Technology 1996;118:367–70. https://doi.org/10.1115/1.2806821.
[50] Meggiolaro M, Castro J de. An improved multiaxial rainflow algorithm for non-proportional stress or strain histories–Part II: The Modified Wang–Brown method. International Journal of Fatigue 2012.
[51] Margetin M, Biro D. Performance of chosen multiaxial cycle counting method under non-proportional multiaxial variable loading. MATEC Web of Conferences 2018.
[52] Bannantine JA, Socie DF. A variable amplitude multiaxial fatigue life prediction method 1989.
[53] Miner MA. Cumulative Damage in Fatigue. Journal of Applied Mechanics 1945;12:A159–64. https://doi.org/10.1115/1.4009458.
[54] Schoenborn S, Kaufmann H, Sonsino CM, Heim R. Cumulative Damage of High-strength Cast Iron Alloys for Automotive Applications. Procedia Engineering 2015;101:440–9. https://doi.org/10.1016/j.proeng.2015.02.053.
[55] Fatemi A, Yang L. Cumulative fatigue damage and life prediction theories: a survey of the state of the art for homogeneous materials. International Journal of Fatigue 1998;20:9–34. https://doi.org/10.1016/S0142-1123(97)00081-9.
[56] Kondo Y. Fatigue under variable amplitude loading, in Comprehensive Structural Integrity, Elsevier, 2003. doi: 10.1016/B0-08-043749-4/04029-5.
[57] Hwang W, Han KS. Cumulative Damage Models and Multi-Stress Fatigue Life Prediction. Journal of Composite Materials 1986;20:125–53. https://doi.org/10.1177/002199838602000202.
[58] Fatemi A, Shamsaei N. Multiaxial fatigue: An overview and some approximation models for life estimation. International Journal of Fatigue 2011.
[59] Lv Z, Huang H-Z, Zhu S-P, Gao H, Zuo F. A modified nonlinear fatigue damage accumulation model. International Journal of Damage Mechanics 2015;24:168–81. https://doi.org/10.1177/1056789514524075.
[60] Cancino C, Merigó JM, Coronado F, Dessouky Y, Dessouky M. Forty years of Computers & Industrial Engineering: A bibliometric analysis. Computers & Industrial Engineering 2017;113:614–29. https://doi.org/10.1016/j.cie.2017.08.033.
[61] Pedro E, Leitão J, Alves H. Back to the future of intellectual capital research: a systematic literature review. MD 2018;56:2502–83. https://doi.org/10.1108/MD-08-2017-0807.
[62] Harzing's Publish or Perish n.d. https://harzing.com/resources/publish-or-perish (accessed July 6, 2023).
[63] Van Nunen K, Li J, Reniers G, Ponnet K. Bibliometric analysis of safety culture research. Safety Science 2018;108:248–58. https://doi.org/10.1016/j.ssci.2017.08.011.